FACULTY OF ENGINEERING
AND ARCHITECTURE

Flexible Operation of Power-to-Hydrogen and Electrical Loads to Provide Grid Support

Akbar Dadkhah

Doctoral dissertation submitted to obtain the academic degree of
Doctor of Electromechanical Engineering

Supervisors
Prof. Lieven Vandevelde, PhD - Dimitar Bozalakov, PhD
Department of Electromechanical, Systems and Metal Engineering
Faculty of Engineering and Architecture, Ghent University

December 2022

GHENT
UNIVERSITY

FACULTY OF ENGINEERING AND ARCHITECTURE

Flexible Operation of Power-to-Hydrogen and Electrical Loads to Provide Grid Support

Akbar Dadkhah

Doctoral dissertation submitted to obtain the academic degree of
Doctor of Electromechanical Engineering

Supervisors

Prof. Lieven Vandevelde, PhD - Dimitar Bozalakov, PhD

Department of Electromechanical, Systems and Metal Engineering
Faculty of Engineering and Architecture, Ghent University

December 2022

GHENT UNIVERSITY

ISBN 978-94-6355-655-2
NUR 959
Wettelijk depot: D/2022/10.500/96

Members of the Examination Board

Chair

Prof. Em. Hendrik Van Landeghem, PhD, Ghent University

Other members entitled to vote

Prof. Emmanuel De Jaeger, PhD, Université catholique de Louvain
Prof. Jeroen De Kooning, PhD, Ghent University
Prof. Chris Develder, PhD, Ghent University
Prof. Amin Hajizadeh, PhD, Aalborg University, Denmark

Supervisors

Prof. Lieven Vandevelde, PhD, Ghent University
Dimitar Bozalakov, PhD, Ghent University

Acknowledgements

This work covers most of the research carried out for 3 years, 3 months and 9 days. While it has been a life-changing adventure, it would not have been finished without the support of people whom I want to thank.

First, I would like to express my appreciation to my thesis promoters, prof. Lieven Vandevelde and dr. Dimitar Bozalakov. Lieven, thank you for trusting me and allowing me to work on different challenging projects. Your insights have made this an inspiring experience. Dimitar, thanks for being a supportive supervisor. I am grateful for our friendly chats at the end of the meetings and your help in my academic efforts. I would like to, especially thank prof. Greet Van Eetvelde, whose support and encouragement have been invaluable throughout the final year of my PhD.

I am also grateful to the defence committee: prof. Emmanuel De Jaeger, prof. Amin Hajizadeh, prof. Chris Develder, prof. Jeroen De Kooning, and the chairman, prof. Hendrik Van Landeghem. Thank you for reviewing this thesis and for providing recommendations.

Special gratitude to prof. Jeroen De Kooning for the discussions we had in the past years. Jeroen, thanks for all the advice on modelling, your help with the publications, and just for being *een toffe pee*.

Thanks to my colleagues from EELAB and my office mates (Cyril, Daan, Dominique, Francisco, Jens, Joannes, Narender, Samie and Siavash). I am deeply indebted to Arash & Nezmin for their unconditional support during this journey. Nienke, special thanks to you for translating my summary into Dutch! Still soon, but I cannot wait to attend your defence. I also extend my appreciation to the administrative and technical personnel, Ingrid, Marilyn, Tony, and Vincent.

I would be remiss in not mentioning my parents, brother and sister. Thank you for all the support throughout these years. Last but not least, I wish to thank my wife, who has stood by me and created peace of mind. Sahar, I will now clear all the papers off the tables as promised!

Ghent, Aug 2022
Akbar Dadkhah

Table of Contents

List of Figures

List of Tables

Samenvatting

Ten gevolge van de dringende klimaatproblematiek zijn ambitieuze plannen opgezet in de voorbije decennia ter ondersteuning van de uitbouw van hernieuwbare energiebronnen in de energiebevoorrading en de diversificatie van de energiebevoorrading door het financieren van groene technologieën waaronder waterstofproductie. In de energiesector is de transitie naar voornamelijk hernieuwbare energiebronnen deel van het traject voor het bereiken van verlaagde broeikasgasemissies. In België is een aanzienlijk deel van de elektriciteitsproductie reeds afkomstig van hernieuwbare energiebronnen. De traditionele elektrische energienetten zijn destijds niet ontworpen voor dit hoge aandeel aan intermitterende energiestromen. Hierdoor veroorzaakt de toenemende integratie van dergelijke variabele, hernieuwbare energiebronnen in het energiesysteem stress bij de conventionele productie-eenheden, die cruciaal zijn voor het in balans houden van het energienet. Om deze stress op te vangen, vereist het energiesysteem een toegenomen hoeveelheid flexibiliteit.

De eerste mogelijkheid tot flexibiliteit volgt uit de werking van productie-eenheden. Netbeheerders en de energiemarkt geven signalen aan de producenten over wanneer hoeveel elektriciteit geproduceerd dient te worden ten gevolge van wijzigingen in consumptie. Deze aanbod-volgt-vraag redenering in de energiesector is historisch gegroeid, maar ondervindt moeilijkheden door het toenemende aandeel aan variabele productie-eenheden. De energiemarkt en markt voor systeemdiensten hebben reeds een transformatie ondergaan de voorbije decennia, in de hoop zo een gelijk speelveld te creëren voor alle technologieën en partijen die kunnen bijdragen en voordeel halen uit hun flexibiliteit. Het alternatief voor flexibiliteit bij elektriciteitsproductie is flexibiliteit van de vraagzijde door gebruik te maken van opslag en vraagsturing.

Dit werk geeft in de eerste plaats een overzicht van het valoriseren van elektrische flexibiliteit op zowel een impliciete als expliciete wijze. Impliciete flexibiliteit is de reactie van een marktspeler op een prijssignaal, terwijl expliciete flexibiliteit het doel is van de markt voor systeemdien-

sten. Deze laatstgenoemde bespreekt hoeveelheden vanvermogen en energie met derde partijen, dikwijls de netbeheerders, die dan op hun beurt verschillende flexibiliteitsmethodes kunnen activeren in tijden van nood. In deze context kunnen elektrische belastingen, waaronder ook recente technologieën zoals energie-naar-waterstof-systemen (power-to-hydrogen), die naast een afname in broeikasgasemissies ook kunnen bijdragen tot het balanceren van het energienet. Waterstof als indirecte energieopslag via energie-naar-waterstof kan ook een aantrekkelijke oplossing bieden voor langdurige opslag dankzij haar grootschalige opslagpotentieel. Waterstofproductie en -opslag in energie-naar-waterstof installaties zijn echter energie-intensieve processen en de techno-economische haalbaarheid van dergelijke systemen is nog niet bewezen bij een combinatie van verschillende inkomstenbronnen. Hierdoor is investeren in dergelijke faciliteiten onzeker en risicovol. Bijgevolg dienen nieuwe strategieën deze uitdagingen aan te gaan en tegelijkertijd de CO_2-emissies van verschillende sectoren te reduceren. Bovendien dient niet alleen het effect van flexibiliteitsvoorziening bij de investering in energie-naar-waterstof-systemen deel te zijn van het onderzoek, maar ook de impact van het voorzien van flexibiliteit door elektriciteitsconsumenten in het algemeen en hun rationaliteit in de werking van het energiesysteem.

Om deze aspecten te onderzoeken heeft dit proefschrift de intentie om de techno-economische haalbaarheid van het balanceren van het energienet door middel van energie-naar-waterstof-systemen te bekijken, rekening houdend met de impact op de werking van flexibiliteit aangeboden door reactieve consumenten en hun rationaliteit op het energiesysteem. Deze doelen in acht genomen werden verschillende optimalisatiealgoritmes en -modellen ontwikkeld: een eerste studie is de flexibele werking van een energie-naar-waterstof-installatie. Een optimalisatiealgoritme dient om de impact van het voorzien van frequentiecontroldiensten op het ontwerp en de werking van een waterstof tankstation te onderzoeken. Het voorgestelde techno-economische model berekent de totale jaarlijkse winst, investerings- en werkingskosten in rekening genomen en over verschillende inkomstenbronnen zoals de mobiliteit, aardgasmarkt en de markt voor systeemdiensten. Resultaten van deze studie tonen aan dat het valoriseren van flexibiliteit, de prijzen op de energiemarkt en beperkingen in primaire reserves in acht genomen, winstgevend is, zeker ten opzichte van het werken aan een constante belasting.

Terwijl in eerste onderzoeksonderwerp het voorzien van frequentiebegrenzingreserves bij energie-naar-waterstof-installaties geanalyseerd wordt

op vlak van investerings- en operationele strategieën, dienen de gevolgen van het ondersteunen van de netbeheerders met behulp van frequentiegerelateerde systeemdiensten, zoals frequentieherstel via automatische en manuele activering, nog onderzocht te worden. Bijgevolg is het tweede onderzoeksonderwerp de flexibele werking van een energie-naar-waterstof-installatie om zo verschillende frequentiegerelateerde systeemdiensten aan te bieden, rekening houdend met de onzekere vraag naar en productiecapaciteit van waterstof en de energieprijzen. Een probabilistische optimalisatiemethode dient om een optimale grootte en flexibele werking van het energie-naar-waterstof-systeem te bepalen. Het onderzochte testsysteem is gelinkt met een elektriciteits-, gas- en industrieel waterstofnetwerk dat waterstof aanlevert aan de mobiliteitssector. Verschillende strategieën voor het aanbieden van frequentiegerelateerde systeemdiensten, i.e., frequentiebegrenzing, frequentieherstel via automatische activering en frequentieherstel via manuele activering, bepalen de wijzigingen in vraag naar elektriciteit, winst en uiteindelijke break-evenprijs voor waterstof. Het ontwikkelde model regelt de werkingspunten van de verschillende subcomponenten op basis van de elektriciteitsprijs, vraag naar waterstof, frequentie van het energienet en signalen van de netbeheerders.

De bevindingen tonen aan dat de eerste twee voorgestelde strategieën het voorzien van frequentiegerelateerde systeemdiensten via energie-naar-waterstof-faciliteiten mogelijk maakt met winstmaximalisatie. Resultaten van de simulaties tonen aan dat de economische winst kan vergroten door deelname van de installatie in dergelijke markten voor systeemdiensten terwijl het een stabiele werking voorziet voor het waterstoftankstation.

Zoals hierboven reeds vermeld, wordt bij de eerste twee strategieën de rol van grootschalige responsieve elektrolysers in het aanbieden van frequentiegerelateerde systeemdiensten onderzocht terwijl de potentiële impact op vlak van investeringen en operationele kenmerken worden bekeken vanuit het perspectief van de elektriciteitsconsument. Echter dient ook de rol van vraagsturing en deze potentiële impact op de betrouwbaarheid van het energiesysteem bekeken te worden. Uit responsieve belastingen kan men de grootste waarde halen via slimme planning. Hierbij wijzigt de vraag van dergelijke flexibele belastingen om zo de kost voor zowel consumenten als systeembeheerders te verlagen, een hoger aandeel aan hernieuwbare energiebronnen te accommoderen en de nadelige impact van nieuwe strategieën en technologieën op het energiesysteem te beperken.

In deze context is het derde onderwerp het onderzoek naar de rol van verschillende vraagsturende strategieën op de betrouwbaarheid van het

energiesysteem terwijl de operationele kosten zich tot een minimum beperken. Verschillende beperkingen, waaronder deze van het transmissienet, productie-eenheden, vraagsturende programma's en systeemveiligheid, worden hierbij in rekening genomen. De voorgestelde methodologie introduceert vraagsturende modellen op basis van de elasticiteit van de prijs van elektriciteit, rekening houdend met consumentencomfort en het niveau van flexibiliteit. De verkregen resultaten tonen aan dat met een degelijke uitrol van vraaggestuurde regelingen en de optimale benutting van actuele prijzen en stimulansen, de operationele kosten verlagen terwijl de betrouwbaarheid van het systeem blijft behouden.

Kort samengevat, dit proefschrift stelt verschillende operationele en ontwerpstrategieën voor om de integratie van energie-naar-waterstof en elektrisch reactieve belastingen in het energienet te faciliteren. De resultaten tonen de significantie van de strategieën aan in een optimale deelname in de energiemarkt, markt voor systeemdiensten en vraaggestuurde programma's. De voorgestelde methodes maken het mogelijk bij te dragen tot het stroomnet van de toekomst met hoge aandelen aan hernieuwbare energiebronnen.

Kernwoorden: *Betrouwbaarheid, consumentencomfort, consumentengedrag, elektrolyse, flexibiliteit, frequentiecontrole, optimale capaciteit, optimale planning, productieplanning, systeemdiensten, techno-economische analyse, vraagsturing, waterstof.*

Summary

Following the urgency of climate change issues, ambitious plans have been set out in the past decade to boost the share of renewables in the energy mix and diversify the energy supply by financing green technologies such as hydrogen production facilities. In the electricity sector, shifting towards primarily renewable power production is among the solutions to decrease greenhouse gas emissions. In Belgium, for example, a large part of the electricity is already being generated by non-dispatchable renewable sources. However, the classical power grids are not designed to accommodate such a high level of intermittent power. Hence, the increasing integration of non-dispatchable renewable energy resources into power systems increases the stress on conventional generation plants, which have the responsibility of grid balancing. Then, power systems need enhanced flexibility to relieve this pressure.

The first option for flexibility is looking at the operation of the generation side. Grid operators or the market send signals to the supply side when and how much electricity to produce following the changes in consumption on the demand side. This supply-follows-demand relation in the electricity sector has been present historically but is being disrupted due to the increasing share of non-dispatchable generation. The energy and ancillary service markets have experienced a massive transformation over the past decades, facilitating a level playing opportunity for all technologies and various parties to benefit from their flexibility. Thus, the alternative for generation-side flexibility is the flexibility of the demand side by using storage or demand response schemes.

Therefore, this work first gives an overview of the options to valorise electrical flexibility in implicit and explicit ways. Implicit flexibility is the reaction of a market party to price signals, while explicit flexibility is procured via the ancillary services market. For the latter, volumes of power and energy are contracted with a third party, often the transmission system operator, which then activates different flexibility options in case of system needs. In this context, electrical loads, including novel technologies

such as power-to-hydrogen systems, are not only able to help reduce greenhouse gas emissions, but can also support the power system operators to balance the power grid. The inclusion of hydrogen for indirect energy storage via power-to-hydrogen might also be attractive for long-term storage due to its large-scale energy storage potential. However, hydrogen production and storage in power-to-hydrogen facilities are energy-intensive, and the techno-economic viability of such systems is not clear yet when various sources of income are combined. That is why investment in such plants is uncertain and risky. Therefore, new strategies are needed to handle these challenges and accelerate the fast reduction of CO_2 emissions in various sectors. Moreover, not only the effect of flexibility provision on the investment in power-to-hydrogen systems, but the impact of providing flexibility by electricity consumers in general and their rationality on the operation of power systems also need to be examined.

In order to consider these aspects, this dissertation intends to examine the techno-economic feasibility of grid balancing with power-to-hydrogen systems, together with the operational impact of the flexibility of responsive consumers on power systems. Taking into account the above-mentioned goals, several optimisation algorithms and models are developed:

First, the flexible operation of a power-to-hydrogen facility is studied. An optimisation algorithm is proposed to investigate the impacts of providing the Frequency Containment Reserve (FCR) on the design and operation of a hydrogen refuelling station. The proposed techno-economic model calculates the total annual profits, considering investment and operational costs and different revenue streams from the mobility, natural gas and ancillary service markets. Results show that valorising flexibility, considering the energy market prices and primary reserve constraints, is profitable, especially compared to working at a flat load.

While the first research topic analyses the effects of providing FCR on the investment and operational strategies in power-to-hydrogen facilities, the consequences of supporting the transmission system operator with other frequency ancillary services, including automatic Frequency Restoration Reserve (aFRR) and manual Frequency Restoration Reserve (mFRR), still need to be studied. Thus, the second research topic investigates the flexible operation of a power-to-hydrogen plant to provide various frequency ancillary services considering the uncertainty of hydrogen demand and capacity and energy prices. A probabilistic optimisation method is suggested to address the challenges of optimal sizing and the flexible operation of the power-to-hydrogen system. The examined test system is coupled with

electricity, natural gas, and industrial hydrogen networks while delivering hydrogen to the mobility sector. Various scheduling strategies for different frequency ancillary services, i.e., the Frequency Containment Reserve, automatic Frequency Restoration reserve, and manual Frequency Restoration reserve, are compared in terms of electricity demand adjustment, the influence on profits and the final hydrogen break-even price. The developed model regulates the setpoints of different subcomponents based on electricity prices, hydrogen demand, grid frequency and signals from the transmission system operator.

The findings show that the first two proposed strategies enable the power-to-hydrogen plants to provide different frequency ancillary services while maximising the total annual profits. The simulation results reveal that the economic profits can be increased following participation in the ancillary service markets while fulfilling its operation specifications and considering the stable operation of the hydrogen refuelling station.

As mentioned above, the first two strategies explore the role of large responsive electrolysers to provide frequency ancillary services while looking at the potential effects on the investment and operational aspects from the electricity consumers point of view. However, the role of demand response programs and potential impacts on the reliability of power systems still must be considered. It is critical to draw the most value from scheduling responsive loads through so-called smart dispatch. Smart scheduling implies flexibly modifying the consumption of flexible loads to reduce costs for consumers and power system operators, accommodating higher levels of renewables and minimising the adverse impact of new strategies and technologies on the power system.

In this context, the third topic is to analyse the role of different demand response strategies in assuring power systems reliability while minimising operating costs. Several constraints, including those related to the transmission system, generation units, demand response programs and system security, are taken into account. The proposed methodology introduces demand response models based on the price elasticity of demand, considering consumers comfort and flexibility levels. Obtained results demonstrate that with proper deployment of demand response schemes and optimal design of real-time prices and incentives, the operating costs will decrease while the security of the system is guaranteed.

In summary, various operating and design strategies are proposed in this thesis to facilitate the integration of power-to-hydrogen technology and electrical responsive loads into the power grid. The results show the signif-

icance of the formulated strategies for optimal participation in the energy and ancillary markets and demand response programs. The proposed methods are able to contribute to the evolution of the future grid under the high penetration levels of renewables.

Keywords: *Ancillary services, customers behaviour, customers comfort, demand response, electrolysis, flexibility, frequency control, hydrogen, optimal scheduling, reliability, size optimisation, techno-economic analysis, unit commitment.*

Abbreviations

A

ACE	Area control error
AEL	Alkaline electrolyser
aFRR	automatic Frequency Restoration Reserve

B

BESS	Battery energy storage systems
BRP	Balancing responsible party
BSP	Balancing service provider

C

CCGT	Combined cycle gas turbines
CAPEX	Capital expenditure
CDI	Consumption delay index
CWI	Consumption way index

D

DER	Distributed energy resources

DRP	Demand response program
DSR	Demand side response

E

EDNS	Expected demand not served
EDRP	Emergency demand response program
ENTSO-E	European association for the cooperation of TSOs for electricity
ESS	Energy storage systems
EU	European Union
EV	Electric vehicles

F

FAS	Frequency ancillary services
FCEV	Fuel cell electric vehicle
FCR	Frequency containment reserve
FOR	Forced outage rate

G

GC	Grid costs
GHG	Greenhouse gas
GR	Gas grid revenue
GT	Gas turbine

H

HRS	Hydrogen refuelling station

I

IBDRP	Incentive-based demand response program
IEA	International Energy Agency
IGCC	International Grid Control Cooperation
IGDT	Information gap decision theory

L

LRC	Long-range consumer
LFC	Load–frequency control

M

MC	Mixed consumer
mFRR	manual Frequency Restoration Reserve
MILP	Mixed-integer linear programming
MINLP	Mixed-integer nonlinear programming

N

NPC	Net present cost
NRV	Net regulation volume

O

OPEX	Operating expenditure

P

PBDRP	Price-based demand response program
PEM	Price elasticity matrix
PEMEL	Polymer electrolyte membrane electrolyser
PHES	Pumped hydroelectric energy storage
PI	Payment index
PMILP	Probabilistic mixed-integer linear programming
$P2H_2$	Power to hydrogen
PV	Photovoltaic

R

RES	Renewable energy sources
RoCoF	Rate of change of frequency
RT	Real-time
RTS	Reliability test system

S

SCUC	Security-constrained unit commitment
SI	System imbalance
SOC	State of charge
SOEC	Solid oxide electrolyser cell
SRC	Short-range consumer

T

TAC	Total annual costs
TAP	Total annual profits

TAR	Total annual revenues
TOU	Time-of-use
TSO	Transmission system operator

U

UC	Unit commitment

V

VoLL	Value of lost load

1 Introduction

This chapter introduces the research presented in this dissertation. With this introduction, the author intends to give a general overview of the presented research in this work. Section 1.1 provides the context in which this research is embedded. Section 1.2 allows the readers to understand the objectives and challenges followed by the main assumptions and outline of this thesis in Sections 1.3 and 1.4, respectively.

1.1 Context

The shift to renewable energy sources (RES) in the electrical power, heating, and transportation sectors has gained lots of attention and is happening quickly to minimise global warming aftermaths. According to the *Fit for 55* program, the European Union (EU) aimed to raise the renewable energy share by at least 40% and lower greenhouse gas (GHG) emissions by at least 55% by 2030 compared to 1990 levels. However, in light of the war in Ukraine and the energy supply crisis, the European Commission adopted a package of proposals, referred to as the *RePowerEU* plan, which increases the EU target of renewables in the energy mix to at least 45% by 2030.

While reducing GHG emissions, such a large-scale deployment of intermittent RES puts the balanced operation and frequency stability of power systems at risk. Therefore, novel flexibility options, including new tech-

nologies and operating strategies are necessary for the reliable operation of energy systems, particularly electrical power systems. Energy storage systems (ESS), curtailment of available renewable energy and demand side response can be part of the solution to guarantee the reliability of power systems. Among various storage options, hydrogen is one of the most promising choices to support the integration of RES into power systems. Emerging forms of clean hydrogen produced based on renewable energy will be a game changer in long-term and economy-wide decarbonisation.

As a feedstock, hydrogen can be used in main industrial processes, including the production of chemicals, iron, and steel. As a fuel, hydrogen can be used in fuel cells in the transportation sector and as a low-carbon way to supply high-temperature heat needed for industrial processes. Moreover, hydrogen can act as an energy buffer and help balance the power system year-round [1]. During times of high wind and solar supply, excess renewable energy can produce green hydrogen for long-term energy storage. The stored hydrogen will then provide a clean energy source to meet demand by being converted to electricity when renewable supplies are low. Not only in the long-term, but also in shorter time scales could the timing of the hydrogen production be adjustable to the variations of the electricity and hydrogen prices. In addition to a longer period for energy storage, hydrogen-based systems allow lower capital costs compared to batteries [1]. Given the mentioned benefits, hydrogen can play a fundamental role in future power systems to provide flexibility, allowing higher integration of RES and accelerating the reduction of GHG emissions.

Next to ESS, improved flexibility of consumers on the demand side is another solution to accommodate increased penetration of variable energy sources in power systems. Next to the continuous evolution in electricity generation, an extreme shift is happening in the European energy sector and related principles. Electricity and ancillary service markets are opened up, letting both energy producers and consumers benefit from the new mechanisms. These situations allow the demand side to provide flexibility in various shapes. For example, by supplying frequency ancillary services (FAS) and price- and emergency-based demand response programs (DRP) in case of contingency events, electricity consumers help transmission system operators (TSOs) to improve the reliability of power systems and minimise the operating cost. However, changing load patterns of residential, commercial and industrial users to provide flexibility is not only valuable to grid operators but also lets the responsive consumers minimise their electricity bills and/or earn financial incentives by adjusting their energy consumption. These mutual benefits are exactly what this thesis intends to cover in the following chapters.

1.2 Objectives

From data collection to engineering analyses, this thesis offers different methods to enable responsive electricity consumers to reduce their operating costs and maximise their total profits, considering investment strategies.

As mentioned earlier, the accommodation of more fluctuating renewable power demands the more active participation of consumers in DRPs and the provision of ancillary services. In this context, power-to-hydrogen ($P2H_2$) systems, equipped with MW-scale electrolysers, are able to provide new balancing services to the grid operators. This is achieved by their energy storage potential and manageable electricity consumption capabilities. While technically beneficial to the grid, the impact of flexibility provision by electrolysers on the design and operation of the $P2H_2$ plant must be taken into account. That is why a large part of this work is dedicated to investigating the potential profits for $P2H_2$ systems that provide FAS. Considering the TSO point of view, the role of generation-side flexibility and price-based and emergency-based DRPs in power systems reliability and operating cost reduction will be examined. Thus, the main goals of this research are to analyse the feasibility of $P2H_2$ systems to balance the electrical grid and investigate the role of DRPs in power systems reliability under different constraints. This overall goal can be split into the following sub-objectives:

- Analysing the techno-economic viability of the flexible operation of $P2H_2$ systems and assessing the cost/value of hydrogen production;
- Identifying the design requirements of a $P2H_2$ plant and developing the essential algorithms to convince investors about the necessity of financing the $P2H_2$ conversion;
- Examining the impact of supply- and demand-side flexibility and consumers preferences on the reliable operation of power systems.

Given the above-mentioned objectives, the techno-economic challenges need to be addressed to assure the cost-efficient contribution of responsive loads in the FAS market and DRPs. Normally, electrolysers are scheduled to run constantly at their nominal capacities or variable levels based on hydrogen demand. Hence, the flexible operation of a $P2H_2$ plant, as a FAS provider, is usually not considered in the system design. Moreover, the operation of electrolysers, storage facilities and compressors is subject to strict constraints concerning components size, operating ranges, injection

capacities, etc. Ȧny proposed solution should define to which extent the hydrogen system has to be redesigned to make the plant available for grid services while at the same time satisfying the hydrogen demand. So, how to size different subcomponents remains to be answered. The offered models should also give a clear response on what the consequences of the possible redesign for the investment and operation costs of the plant are and to which extent the revenues from grid services will compensate these extra costs. So, in addition to technical constraints, a suitable investment and scheduling scheme is needed for the flexible operation of hydrogen systems to satisfy grid service requirements while maximising profits. This will solve one of the most influential barriers to convincing investors to financially support the $P2H_2$ systems and equip them with demand response (DR) capabilities.

Moreover, as given in the objectives, customers behaviour and comfort as fundamental principles must be included in the optimal scheduling of demand units to improve the reliability of power systems and efficiency of DRPs. Thus, an accurate model of DR still should be developed considering customer behaviour and the effect of customers preferences on the power systems operation.

Given the raised challenges, several investment and scheduling approaches are suggested in this work to determine the capability of responsive loads, especially the $P2H_2$ plants benefiting from the flexibility markets. Two investment models are offered and implemented to estimate the size of required electrolysers, storage facilities, and compressors in an HRS under different FAS constraints. A hydrogen cost metric is included in the models to express the value of hydrogen in an energy market. While the first two optimisation models are developed based on the specific case of an HRS, they are deemed expandable to other industrial sectors. An overview of the flexible operation of electrolysers in various FAS with a focus on the European and Belgian markets shows today and future opportunities.

Next to proposing optimisation algorithms for hydrogen systems, a novel operational optimisation model, comprising various DRPs and consumer preferences, is developed to analyse the impact of the flexibility of not electrolysers but the flexible generators and loads in general on the stable and reliable operation of power systems. A pricing algorithm is developed to find the optimal electricity prices and incentives to guarantee network reliability and customers comfort, while minimising system operation costs in the presence of uncertainties.

1.3 Scope and main assumptions

Deterministic optimisation models are often used in this research to provide answers for the objectives outlined before. Except Chapter 5, perfect foresight of future events, like the magnitude of hourly hydrogen demand and electricity prices, is assumed, neglecting uncertainty. Although there is no perfect foresight in real-world scenarios, using such a procedure has the advantage of delivering transparent results. As stated before, two different types of optimisation models are developed; two combined investment/operational models and an only-operational model. For the investment models, an optimisation horizon of 1 year with hourly time steps is considered (Chapters 4 and 5). The operational model, which includes more technical details of a power system, is employed with an optimisation horizon of 24 hourly time steps (Chapter 6). It is worth mentioning that Chapters 4 and 5 focus mainly on the role of electrolysers and do not include a detailed discussion of the possible flexibility that could be offered by hydrogen-fuelled gas turbines or fuel cells. More detail about the assumptions will be presented in Chapters 4-6.

1.4 Thesis outline

This dissertation is organised as follows:

Chapter 2 *Energy transition and need for flexibility*
Chapter 2 gives an overview of the current policy and incentives supporting the energy transition globally and the potential consequences. It summarises the plans and actual implementations regarding the increasing share of RES in the energy mix. The challenges and consequences of deploying large-scale renewable energy plants will be discussed together with the flexibility needs and potential solutions to facilitate the integration of a high share of renewables in the power systems.

Chapter 3 *Grid balancing and role of hydrogen*
Chapter 3 describes the flexibility in power systems. The grid balancing principle is explained as applied in Europe with a focus on the Belgian electricity system. Frequency ancillary services (FAS) and price-based DRPs, with them linked to explicit and implicit flexibility options, are discussed. Chapter 3 ends with an overview and the role of hydrogen and DRPs in a secure power grid.

Chapter 4 *Operation & investment plans of P2H$_2$ systems providing FCR*

Chapters 2 and 3 discussed the need for flexibility and the possible role of hydrogen systems in providing FAS by electrolysers. As electrolysers are energy-intensive systems with favourable dynamic properties, they are particularly suitable for frequency support services. In this context, Chapter 4 evaluates the effect of FCR provision by large-scale electrolysers on the optimal planning and operation of P2H$_2$ systems. First, a system investment model is presented, which determines the cost-optimal system design to serve a given hydrogen demand under different grid constraints. Next, an analysis expands the optimisation of the hydrogen production and storage scheduling by considering the FAS provision and injection of hydrogen to the mobility sector and natural gas (NG) grid. At last, the impact of FCR provision on the hydrogen break-even price and total annual profits (TAP) is studied. This chapter includes elements from [2].

Chapter 5 *Opportunities for P2H$_2$ systems to provide FAS*
Chapter 5 studied the flexible operation of electrolysers for the FCR provision. However, other FAS, such as aFRR and mFRR needs to be analysed as well. Moreover, electrolysers provide an essential source of hydrogen for different sectors. Hence, Chapter 5 aims to expand the analysis presented in Chapter 4 by including different FAS in the optimisation problem, considering the optimal design for the P2H$_2$ system capacity and deviations in both the hydrogen demand and price profiles of FAS. These topics are brought together in Chapter 5 in which novel investment and operation strategies are presented for an extended P2H$_2$ system supplying various sectors with hydrogen. This chapter is based on [3, 4].

Chapter 6 *Flexible supply- & demand-sides in a reliable power system*
Chapters 4 and 5 respectively studied the flexible operation of the demand side provided by specific loads, in this case, electrolysers, to support the grid frequency. Chapter 6 introduces a novel strategy for the daily operation of the whole power transmission system. This model analyses the impact of DRPs, provided not by a single load such as an electrolyser but via aggregated loads connected to different nodes and voltage levels, on the secure operation of power systems. This chapter includes elements from [5].

Chapter 7 *Conclusions and perspectives*
Chapter 7 summarises and concludes the research and provides a view of potential future works.

References

[1] J. B. Von Colbe, J. Ares, J. Barale, M. Baricco, C. Buckley, G. Capurso, N. Gallandat, D. Grant, M. N. Guzik, I. Jacob, et al. *Application of hydrides in hydrogen storage and compression: Achievements, outlook and perspectives*. International Journal of Hydrogen Energy, 44(15):7780–7808, 2019.

[2] A. Dadkhah, D. Bozalakov, J. D. M. De Kooning, and L. Vandevelde. *On the optimal planning of a hydrogen refuelling station participating in the electricity and balancing markets*. International Journal of Hydrogen Energy, 46(2):1488–1500, 2021.

[3] A. Dadkhah, D. Bozalakov, J. D. M. De Kooning, and L. Vandevelde. *Techno-Economic Analysis and Optimal Operation of a Hydrogen Refueling Station Providing Frequency Ancillary Services*. IEEE Transactions on Industry Applications, 58(4):5171–5183, 2022.

[4] A. Dadkhah, D. Bozalakov, J. D. M. De Kooning, and L. Vandevelde. *Optimal Sizing and Economic Analysis of a Hydrogen Refuelling Station Providing Frequency Containment Reserve*. In 2020 IEEE International Conference on Environment and Electrical Engineering and 2020 IEEE Industrial and Commercial Power Systems Europe (EEEIC/I&CPS Europe), 2020.

[5] A. Dadkhah, N. Bayati, M. Shafie-khah, L. Vandevelde, and J. Catalão. *Optimal price-based and emergency demand response programs considering consumers preferences*. International Journal of Electrical Power & Energy Systems, 138:107890, 2022.

2

Energy transition & need for flexibility

This chapter gives an overview of the current policy and incentives supporting the energy transition around the world and the potential consequences. Section 2.1 summarises the plans and actual implementations regarding the increasing share of RES in the energy mix. The challenges and consequences of deploying large-scale RE plants will be discussed in Section 2.2. Afterwards, the flexibility needs and potential solutions to facilitate the integration of a high share of renewables in power systems will be introduced in Sections 2.3 and 2.4, respectively. This chapter will be concluded in Section 2.5.

2.1 Increasing share of renewables

The global warming caused by a rise in greenhouse gasses (GHG) emissions has pushed countries to take action. The Paris Agreement was put into effect in 2016 to decrease emissions with the goal of climate neutrality by 2050 [1, 2]. Energy use in different sectors has been at the heart of this shift by delivering huge emission reductions. However, since most of the energy demand was still covered by fossil fuels, emissions from the energy sector and industry recovered from the dip in 2020 to reach their highest annual level in 2021, 36.3 Gt [3].

In response, the commitments put into effect as a result of the Paris agreement toward a massive transition from fossil fuels to renewable energy sources (RES) were renewed in 2021 in Glasgow. Such a transition towards low carbon energy strategies has triggered a large installation of renewables in the past decade. Even with rising commodity prices and manufacturing costs for photovoltaic (PV) panels, PV capacity additions have increased in 2021 to set an annual record of almost 160 GWp. Back then in 2021, PV accounted for 60% of all renewable capacity expansions, with nearly 1100 GWp becoming functional. Global onshore wind expansions got an exceptional level of almost 110 GWp, and by 2026 are foreseen to be almost 25% higher than in the 2015-2020 period. Global offshore wind capacity proliferation is expected to reach 134 GWp by 2026, thanks to quick development in markets outside Europe and China [4]. Fig. 2.1 shows how the share of renewables in the electricity mix has evolved in the past decades.

2.1.1 Renewables on a European level

On a European level, the EU has decided to reduce their GHG emission by 55% by 2030 compared to levels in 1990. The EU intends to obtain 40% of their final energy consumption from RES and enhance the energy efficiency by 32.5% [6]. The war in Ukraine has emphasised the need for RES to end the dependency of the EU on fossil fuels, which can be used as economic and political leverage. Now, according to the REPowerEU plan, the EU Commission has proposed to revise the 2030 target of the EU for renewables from the current 40% to 45%. The REPowerEU Plan will boost the total RE generation capacities to 1,236 GW by 2030, compared to the 1,067 GW envisaged under the Fit for 55 plan.

As part of the REPowerEU, the EU Solar Energy Strategy seeks to bring online over 320 GWp of additional installed solar PV by 2025, and almost 600 GWp new installations by 2030 [7]. The EU energy plan is also proposing to double the wind capacity. Recently, North Sea countries – Germany, Belgium, the Netherlands, and Denmark – initiated a joint project to expand offshore wind capacity tenfold to help the security of energy supply in the region. Fig. 2.2 shows how wind and solar power generation has evolved in Europe over the last decade.

All pathways to move toward a cleaner energy system entail a crucial role for the electrical power system in decreasing GHG emissions. The numbers show a significant increase in global electricity consumption over the past decades. The 25,027 TWh consumption of 2019 is expected to rise by 30% until 2040 [3], which necessitates more decarbonisation efforts and a faster shift to renewables in the electrical power sector. Moreover,

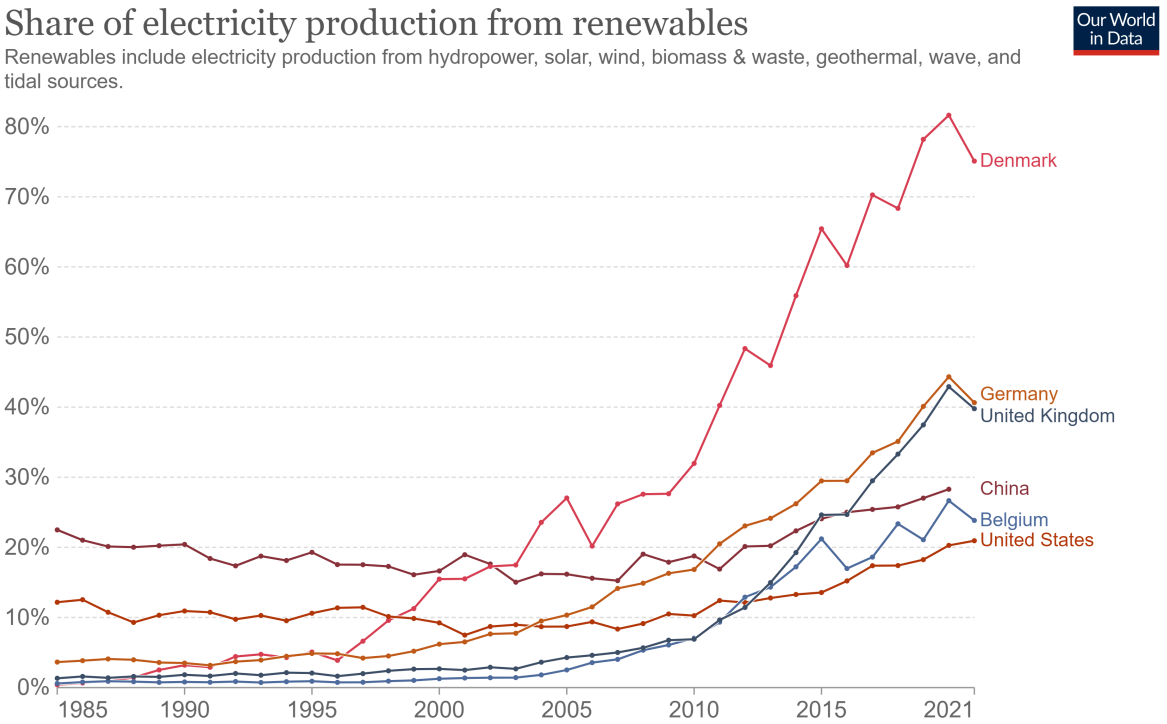

Figure 2.1: Share of renewables in different countries in the global electricity mix [5]

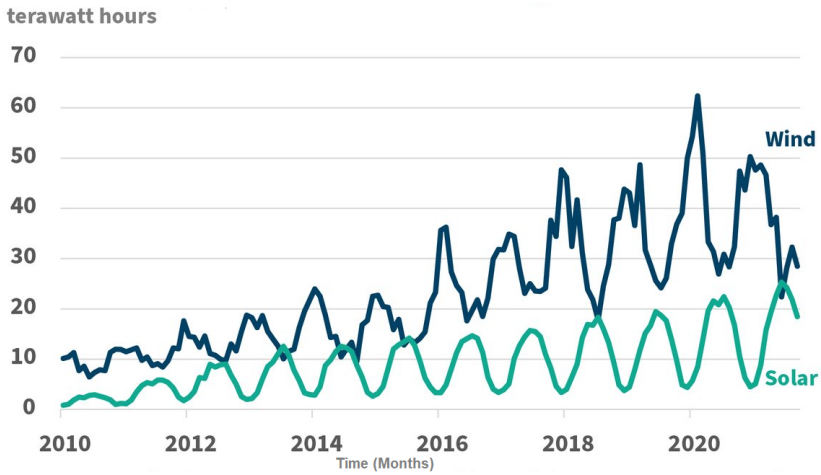

Figure 2.2: Wind and solar generation in Europe (TWh-monthly) [8]

the needed removal of GHG emissions for heating and in the transportation sector probably causes a move from fossil-fuelled heating to electric heat pumps and from fossil fuel-supplied to electricity and hydrogen-powered vehicles. This makes the role of the electrical power system even more decisive in the transition toward sustainable energy provision.

Depending on the transition path, RES shares in the European electrical power sector are planned to grow up to 64-97% by 2050 [9]. The "solar rooftop initiative" presented by the European Commission will mandate the installation of solar panels on new public and commercial buildings by 2027 and residential buildings by 2029. It is expected that rooftop PV could supply almost 25% of the electricity consumption in the EU.

2.1.2 Renewables on a Belgian level

On a country level, from 2011 to 2019, energy-related CO_2 emissions declined by only 3.5 million tonnes to reach 90 million tonnes [10]. It is notable that 71% of all energy in Belgium is supplied by fossil fuels, where industry and transport are the most considerable consumers. Thus, more assertive policies are required to decrease fossil fuel reliance and accelerate emissions reductions in Belgium. Under the EU Renewable Energy Directive, Belgium has set out targets for renewables in energy consumption, electricity generation, heating, and transport (Fig. 2.3). These targets have intended to support the goals of EU to achieve a 20% and 40% share of RE in final energy consumption by 2020 and 2030, respectively [11].

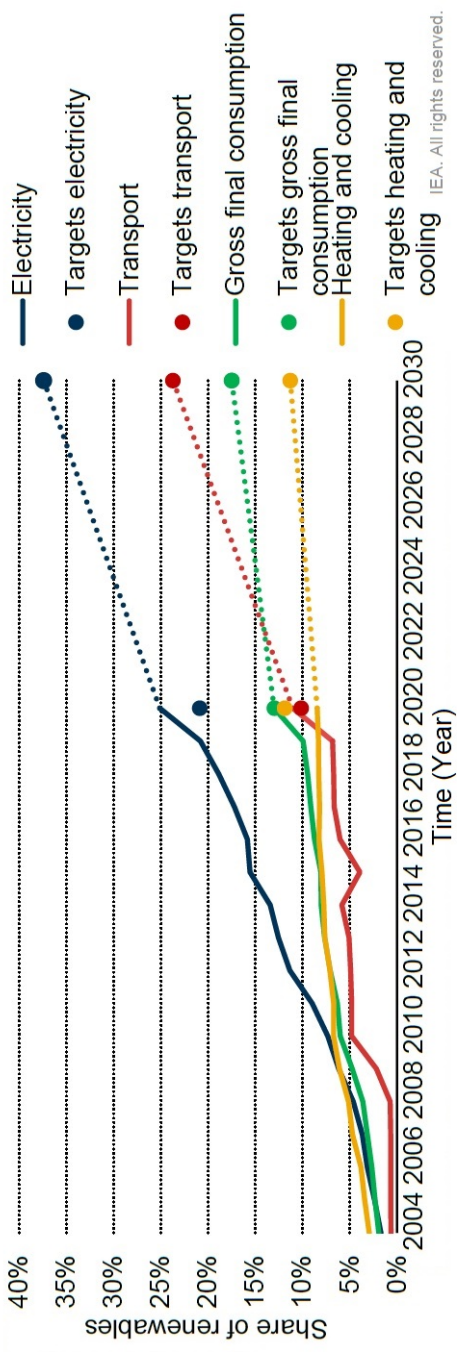

Figure 2.3: Targets for renewables in final consumption, electricity generation, heating and cooling, and transport in Belgium [10]

Belgium has made progress on these goals. The use of oil and solid fossil fuels has declined enormously (over the last decade -82.4% and -57.8%, respectively) in favour of renewables. From 2010 to 2020, the share of RE in the total final energy consumption doubled in Belgium, from 6% to 12%, caused by a boost in renewable electricity production, mainly from wind and solar PV (Fig. 2.4). In 2020, renewables supplied 25% of electricity production, 8% of heating and cooling demand, and 11% of transport consumption [10]. It is planned that 1.5 and 5.7 million EVs will be on the roads in Belgium by 2030 and 2050, respectively [12]. This will further impose a demand for electricity, which must come from RES.

Coming to the electricity system, the policy of the Belgian federal government is focused on boosting the share of renewables and cross-border interconnection capacity, a secure phase-out of nuclear power plants, and improving the competitiveness of the electricity markets. In 2021, nuclear energy covered a 52.4% of the electricity generation mix in Belgium [13]. However, the federal government had a plan to phase out most nuclear electricity production by 2025. In light of the war in Ukraine and objectives to decrease fossil fuel dependency, the federal government decided in March 2022 to extend 2 GW of nuclear capacity by 2035 [10].

Renewable electricity generation in Belgium shows an increase from 5.4 TWh to 23.4 TWh (Fig. 2.5) from 2010 to 2020. This has been mainly driven by expanded wind generation, which grew from 1.4% to 14.4% of total electricity generation, and grown solar PV generation, which increased from 0.6% to 5.8% of total electricity production [10]. Specifically for offshore wind, Belgium had 2.23 GW installed in 2020, 2.26 GW in 2021 and plans for 5.7 GW by 2030 [10, 14, 15]. Hydropower plays a limited role in electricity generation in Belgium, and with almost no growth since 2000, covered only 0.3% of electricity production in 2020.

On the one hand, there is a decrease in conventional thermal power generation. On the other hand, there is an increase in renewable electricity generation capacity, mainly solar and wind. Thus, power production from what has been called a “controllable” energy source will reduce in the coming years and replace solar and wind energy. This shift to green electricity will bring consequences for the power systems, which will be discussed in the next section.

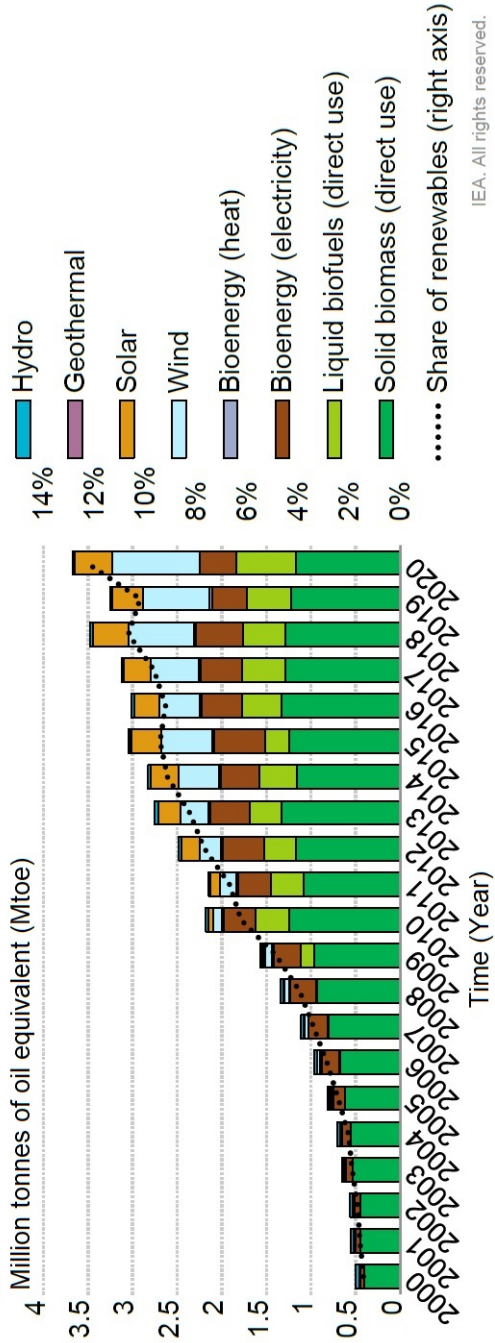

Figure 2.4: Share of renewables in the total final energy consumption in Belgium [10]

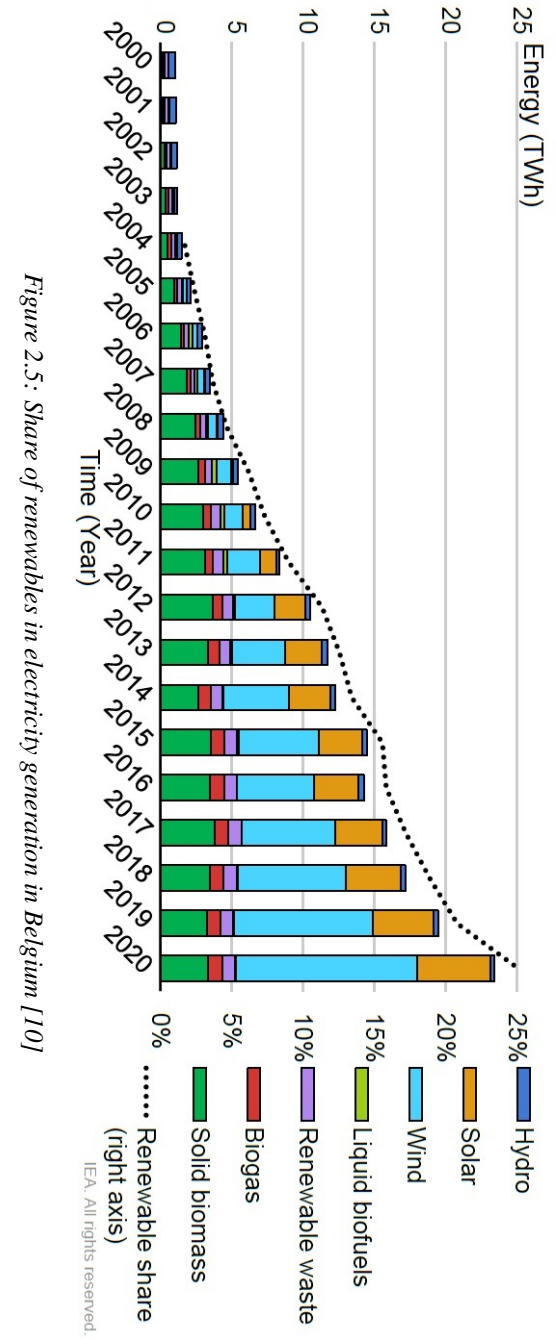

Figure 2.5: Share of renewables in electricity generation in Belgium [10]

2.2 Challenges

The energy systems of many countries have been able to adapt to rising shares of RES, and this transition is supported to continue. However, this trend poses substantial challenges to the existing systems due to the problem of coping with the variability of RES when these plants dominate production portfolios. For example, solar and wind power are intermittent and highly dependent on weather conditions. While solar fluctuates on a diurnal and seasonal scale, the wind is much more variable on a weekly basis. Wind also shows a seasonal component, which could be complementary to solar infeed with a winter peak and summer valley. Thus, the challenge here will be the storage of energy at the time of energy surplus or meeting electricity demand when there is no or lack of wind or sun. This imbalance between electricity generation and consumption will radically raise the complexity of the power system reliability [16, 17]. More specifically, the most notable challenges can broadly be grouped into several categories described below.

2.2.1 Frequency Stability

To have a good understanding of frequency stability issues, first, we have to introduce inertia as one of the most vital parameters in the operation of power systems. In power systems, inertia is defined as the kinetic energy stored in large rotating machines. This energy can stabilise the grid when a contingency happens due to generator tripping, sudden change in generation or sudden change in load value. Conventionally, the inertia has been provided by spinning generators, i.e., nuclear, hydroelectric, and fossil-fuelled power plants. However, RE power plants and converter-interfaced energy storage systems are isolated from the grid and connected to the system through voltage-sourced converters. Therefore, after the replacement of a large conventional power generation facility with renewable power plants, directly-connected inertia will decrease.

A lower level of inertia impacts system operation and its balance margin. Since inertia level determines the rate of frequency change after a disturbance, decreased inertia results in faster frequency dynamics [18]. This could, in case of a negative imbalance when mechanical driving power is less than electrical load, even cause critical situations such as a frequency nadir[1] lower than 49 Hz that activates under frequency load shedding [19]. Large power deviations cause the malfunctioning of devices, which eventually can initiate system-wide severe disturbances or even blackouts. An

[1]The frequency nadir is defined as the minimum value of frequency reached during the transient period.

example is a disturbance on November 4, 2006, caused by the tripping of several high-voltage lines, which started in Northern Germany. Consequently, the European grid was split into three separate areas (West, North-East and South-East), with significant power imbalances. Those power imbalances induced a severe frequency divergence where over 10 million users in Belgium, France, Germany, Italy, and Spain lost power or were influenced by the incident [20]. As another example, on January 8, 2021, the failure of a substation in Croatia triggered an increase in frequency in south-east Europe and a corresponding frequency drop in the north-west (see Fig. 2.6). Such a drop will normally result in widespread blackouts if not fixed within a few seconds. In that case, the immediate ramping up of generation from flexible hydropower and gas peaking plants, as well as load shedding in France and Italy, contained the frequency and prevented another huge blackout. Thus, for the safe function of the power system, the frequency cannot differ too much from the reference value. More details on the frequency stability will be given in Section 3.2.

2.2.2 Voltage Stability

In addition to the effect on rotating inertia, power system strength will also be reduced as a result of the increased penetration of renewables. This may result in more voltage disturbances [22]. System strength indicates the local dynamic performance of a power system in response to a voltage disorder. Practically, system strength is measured through short-circuit power as the fault current contributed by all production units [23]. Even though RES contribute to the fault current, their ability is limited compared to conventional generators. Thus, increased penetration levels of renewables may compromise voltage stability due to the decrease in system strength.

2.2.3 Network congestion

The shift from a classic to a renewables-based power system will affect the power flows both at the transmission and the distribution levels [24]. In addition to bidirectional energy flows, large amounts of power from small-scale RES will be injected into distribution systems. This, together with a growth in demand caused by the electrification of transport and heat sectors, will further boost congestion in distribution grids. Regarding transmission systems, the proliferation of large-scale renewable energy plants, particularly wind, has increased the congestion issues.

For example, in June 2022, the Dutch TSO (TenneT) formally reported that in the provinces of Limburg and North Brabant there will be a tempo-

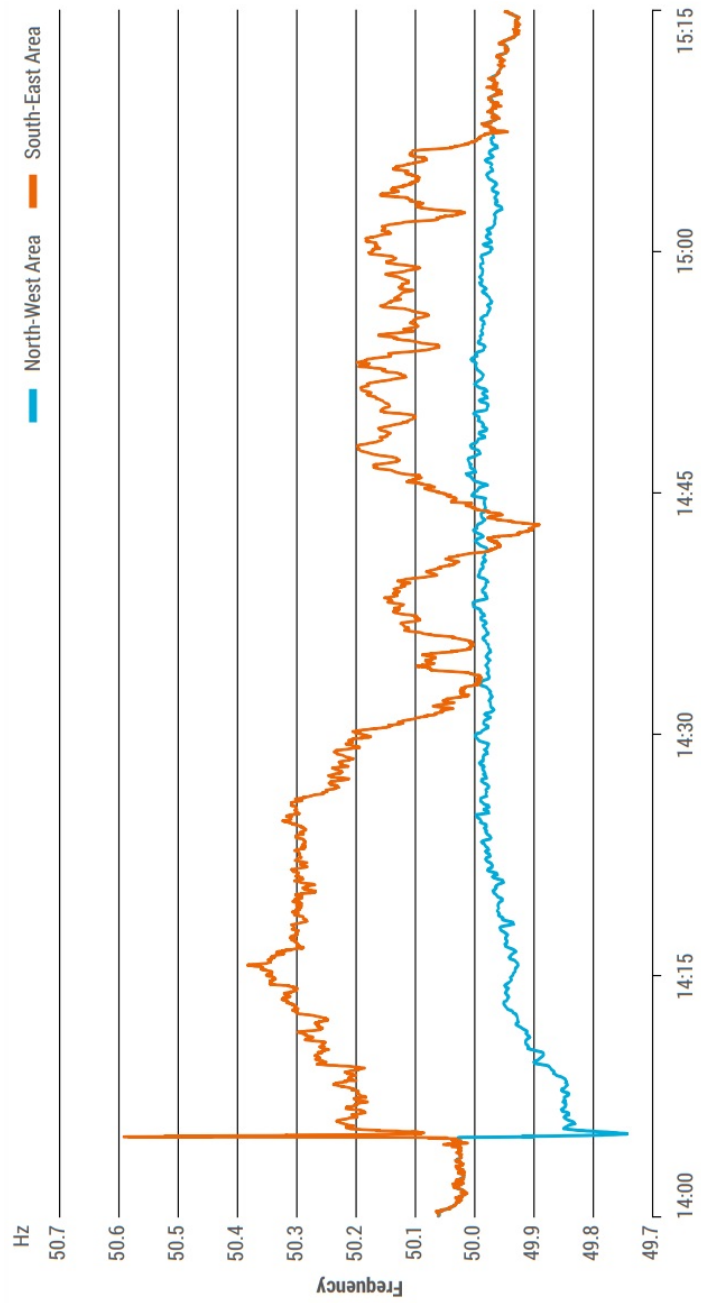

Figure 2.6: Frequency in Continental Europe during the event on 08.01.2021. [21]

rary stop for new companies and institutions that want a connection to the electricity grid. This is because the high-voltage grid in both provinces is almost at maximum capacity due to the rapidly growing demand for electricity, including industrial electrification, large-scale battery systems, mobility charging stations and heat pumps. To solve the issue in the long term, TenneT will invest €2 billion to structurally increase the capacity of the grid [25]. However, the expansion of the networks is taking a lot of time. Hence, TenneT is also focusing on other solutions to make more intensive use of the existing grid and to create additional capacity more quickly.

2.2.4 System restoration

While so far, considerable effort has been put into improving the resilience of power systems against outages, chances for large-scale blackouts still exist. Historically, system restoration has depended on conventional generation. Now, the concern is that increasing the share of renewables and the resulting decommissioning of traditional plants would raise the complexity of the system restoration. Hence, finding novel solutions to restore future power systems quickly and effectively after outages is of high importance.

2.3 Need for flexibility

As mentioned above, increasing share of renewables and power fluctuations affect the optimal operation of power systems [26]. To solve the mentioned challenges and accommodate the net load and generation changes, TSOs take advantage of an ability of the power system called flexibility [27]. Researchers and groups proposed different definitions for flexibility [28, 29]. Ref. [30] has explained the flexibility in power systems as the ability of generators to respond to unanticipated changes in load or the condition of system components. The authors of [31] have defined flexibility as the capability of a power system to use its resources to react to net load changes that are not satisfied by adjustable power production units. Considering the increasing penetration of variable and barely predictable power generation sources, the concept of flexibility in power systems has been redefined. So, next to the demand side uncertainty, the supply side uncertainty should be taken into account. The International Energy Agency (IEA) sees a power system as flexible, if it can, within economic limits, react fast to oscillations in generation and consumption for planned and unexpected events [32, 33].

On a European scale, according to simulated scenarios by Elia for 2050 and before activating the flexibility, the variation of the renewables shows residual oscillations over 600 GW between day and night in summer [34].

In winter, with a lower probable solar infeed, some days with a surplus of solar energy can happen. This might cause a daily spread of up to 400 GW, which highlights the demand for flexibility resources throughout the year. Therefore, without sufficient flexibility, it becomes more challenging to cope with mismatches between electricity consumption and generation arising from their natural deviations in real time. Thus, to deal with both the shortage and the excess of RE generation and to ensure the necessary balance between electrical power production and consumption, flexibility mechanisms in the short, medium and long term are essential. Ref. [35] emphasised the dependency of the functioning of flexibility types on time scale. Flexibility types include very fast and improved frequency response and reserves for seconds to minutes, the capability to ramp up and down for minutes to hours, planning flexibility for hours to a day, and generation and transmission planning for years.

2.4 Potential solutions for flexibility

As previously described, improved flexibility is the most important asset letting the energy systems be dominated by RES. Flexibility must be present in all system elements. Flexibility can be provided through adjustable production units, strong transmission and distribution lines, curtailment, energy storage systems (ESS), and demand-side management [36–38]. Fig. 2.7 gives an overview of several options usually considered for providing flexibility. These flexibility options are already in use today, and some of them will become much more influential in future electrical power systems [39, 40]:

- generation side control,
- curtailment of extra renewable electricity production,
- strong electrical transmission and distribution grids,
- demand-side response,
- energy storage systems,
- sector coupling.

2.4.1 Generation side flexibility

Flexibility in conventional power systems has been ensured by providing reserves and a power generation schedule. Flexibility on the supply side considers load following and partial power production of the power plants connected to the system [35]. For a flexible generation, flexible power plants can be ramped up and down fast and efficiently and operate at low or high output levels as required.

2.4.1.1 Natural gas and nuclear power plants

Natural gas power plants can provide flexibility to the system. Combined cycle gas turbines (CCGT) are the most common as they offer diverse capacities, high efficiencies, and low energy production costs. The new generation of CCGTs is much quicker than traditional ones, with 40-min start-up times [41, 42]. However, the disadvantages of earned flexibility apply to these generation units as the adjustable operation brings wear to mechanical parts, needs more maintenance, and increases running expenses.

Most of the nuclear power plants are developed to be operated at full power and to be stopped only for fuel change or routine maintenance. So,

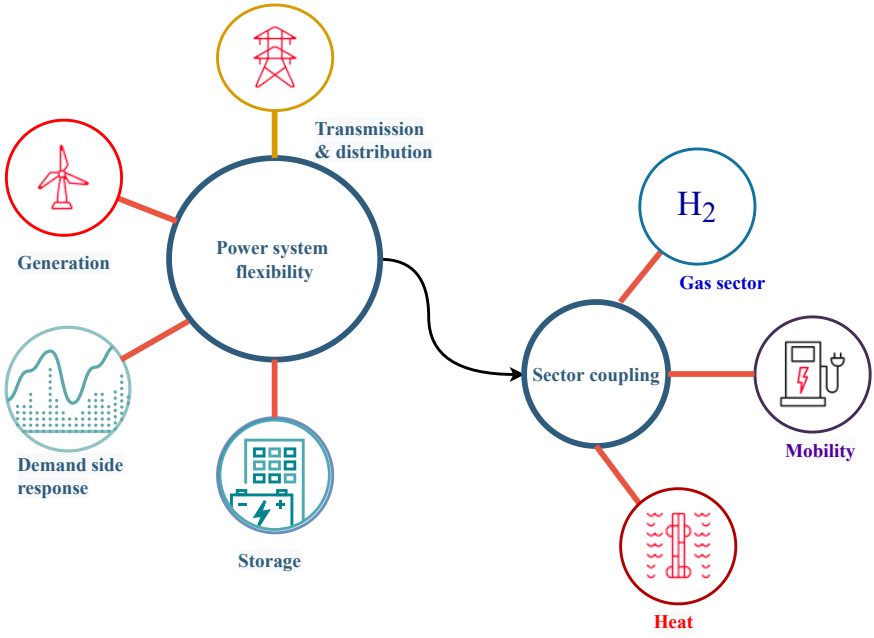

Figure 2.7: Flexibility options

they are viewed as the most inflexible plants. However, flexibility can be provided by these units with the necessary modification in configuration and operation [43]. According to the International Atomic Energy Agency, the majority of the existing nuclear power production plants have an output range between 50% and 100% of the reactor thermal capacity and ramp rates of up to 5%/min. Some countries have the knowledge of operating and developing nuclear power plants with a wide range of flexibility. For example, in France, some nuclear power plants can ramp up their output from 30% to 100% in one hour and from 60% to 100% in 30 min [35].

2.4.1.2 Curtailment of renewables

The curtailment of renewable electricity production can also be introduced under flexibility provision options. When wind and solar farms cause operational constraints, such as grid congestion, the system operator may decide to inject less wind and solar power than what is available to the grid and shave the excess available energy [44]. The renewables integration challenges have increased curtailment levels in recent years. However, curtailment of renewables is not a generally acceptable solution, as it causes a loss of green energy and economic profits. Thus, the operating strategies must be adjusted to guarantee safe and cost-effective integration of the variable RES containing the curtailment at acceptable levels in the future. In recent years, the focus on congestion management has increased, without which further renewable integration seems to be impeded.

2.4.2 Strong transmission and distribution grids

The advantages of strong transmission and distribution grids and cross-border interconnections will be influential. In addition to energy transfer and trading, interconnections can facilitate the exchange of different balancing services and improve the security of supply by sharing generation capacity among regions and countries. In this context, flexibility will be at the core of enabling a resilient and decarbonised pan-European power system while meeting end consumers requirements in a cost-optimal manner.

2.4.3 Energy storage systems

ESS offer flexibility as they can both absorb excess electrical power and supply energy when there is a power deficit. ESS comprise electrical, chemical, electrochemical, and mechanical storage options. Pumped hydroelectric energy storage (PHES) has been used for several decades, covering the

majority of the installed storage capacity [45]. With a high storage capacity, a long discharge time and a fast response time below 1 minute [46], PHES is an option to provide frequency regulation services. However, they are expensive facilities requiring special geographical conditions. Ref. [47] concluded that as short-term and medium-term storage, PHES is the most cost-effective storage technology, while in the long-term, pumped hydro is the costliest means of energy storage compared to hydrogen as a more economic option. Capacitors and batteries, which store energy in an electrochemical form, offer advantages such as rapid response and high levels of efficiency. Home batteries are a great example in this category. They absorb the peaks of solar panels and release the energy at other time slots during the day when sufficient renewable energy is not available. Another storage option is the production of heat and synthetic gases (e.g. hydrogen) with extra available electricity. Once hydrogen is created through electrolysis it can be used in stationary fuel cells, for power generation, to provide fuel for hydrogen-powered vehicles, injected into natural gas grids, or even stored as a compressed gas, cryogenic liquid or wide variety of compounds for later use. The International Energy Agency predicts that hydrogen generated from wind will be cheaper than natural gas by 2030 [48]. More detailed information will be provided in the next sections and chapters about the flexibility potential of hydrogen.

2.4.4 Demand side flexibility

While there are aspects in a power system that will improve flexibility on the supply side, the demand side can also contribute to the smooth operation of electrical girds [49, 50]. Considering the electrification of end-use, consumers such as electric vehicles (EV) and heat pumps do not only offer the carbon reduction in the final energy demand, but they also offer practical flexibility to the system. The flexibility of the demand-side can be achieved through storage and responsive electricity prosumers.

The capability of end-users to manage devices by rescheduling their energy consumption can be split into classes such as consumption increase, decrease, or load shifting [51, 52]. With load shifting, electricity demand does not decrease, but demand is moved to a more suitable time in terms of network operation. Demand response (DR) is already, in many ways, an established concept. Historically, the emphasis of DR has been either on control (e.g. direct control – see Fig. 2.8) or on the value distribution (e.g. day/night tariffs), leading to respectively dispatchable and non-dispatchable DR.

2.4.4.1 Dispatchable (explicit) DR

Dispatchable or explicit DR is dedicated flexibility that concentrates on the control system [53]. The capability of providers to vary the demand profile is contracted to a third party. The contract indicates a responsibility to be ready to respond to signals. This is different from the voluntary characteristic with implicit flexibility. Remuneration can include a part for being ready (expressed in euro/MW/h) and/or a part for activating energy (usually expressed in euro/MWh). Failure to comply to be ready or deliver the flexibility upon demand can lead to penalties.

Direct control of both appliances and industrial processes, like air conditioners and aluminium smelters, has been done for a long time. The provision of ancillary services by loads is one example of dispatchable DR. According to the European association for the cooperation of TSOs for electricity (ENTSO-E), "Ancillary services are measures that TSOs take so that they can ensure system reliability. The most important ones are black start, the provision of reactive power, and frequency services" [54, 55]. Different reserves are triggered sequentially to support the frequency after an imbalance between power generation and demand. The Belgian TSO (Elia) employs the flexibility provided by balancing service providers (BSP) to keep the frequency balanced on the electricity grid. Participants in the flexibility market can provide different FAS, depending on the compatibility of their facilities with the requirements of the respective service. More information about FAS will be presented in Chapter 3.

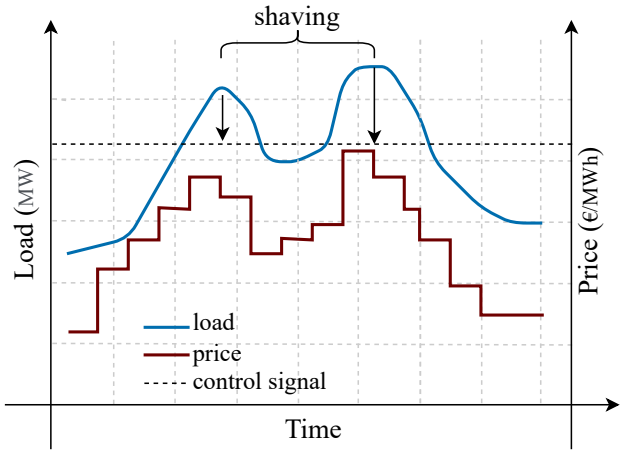

Figure 2.8: Peak shaving

2.4.4.2 Non-dispatchable (implicit) DR

Non-dispatchable or implicit DR focuses on the value distribution system, usually depending on the rationality of customers to modify their consumption in reaction to price changes. This response is a voluntary adjustment of the power consumption, which makes non-dispatchable DR programs not reliable enough to trust for grid stability. Examples are time-of-use and emergency peak pricing. The ability to respond to price signals lets market players reduce costs.

To summarise, Fig. 2.9 illustrates various DR concepts. Each concept communicates on two of three possible axes: power, value and time. One missing axis in each idea is the source of its drawbacks. Dispatchable DR neglects value, while non-dispatchable DR ignores the power and a market approach misses time, resulting in scheduling challenges.

Traditional dispatchable DR directly regulates power consumption. For each time slot, the amount of power is managed by the main control system (as shown in Fig. 2.9-a). In this case, loads (e.g. EVs) are scheduled at the optimal time to help the system operators and balance responsible parties. Technically, it is relatively easy to directly control the loads, but it is not straightforward to evaluate the benefit for the power system and the respective consumer.

Traditional non-dispatchable DR directly sets the value of power (for example, time-of-use prices, shown in Fig. 2.9-b). Time-of-use pricing is somewhat straightforward, and there is a lot of knowledge about day/night tariffs. In this case, consumers are free to respond to prices, but there would not be direct control of loads, which causes uncertainty of the reaction and capability to fine-tune. This could yield probable instability issues if DR automation is used on a large scale.

One solution to reduce the disadvantage of each method is the integration of dispatchable and non-dispatchable DR. Such an integration combines two methods in a mechanism resembling a market, where market-based coordination according to multi-objective optimisation will be conducted (see Fig. 2.9-c). This could bring possible revenues for different stakeholders. The prices charged to customers closely match either the underlying wholesale electricity market or the electricity generation cost. Customers can greatly benefit from variable prices, particularly if they have the ability to modulate their loads in response to market prices.

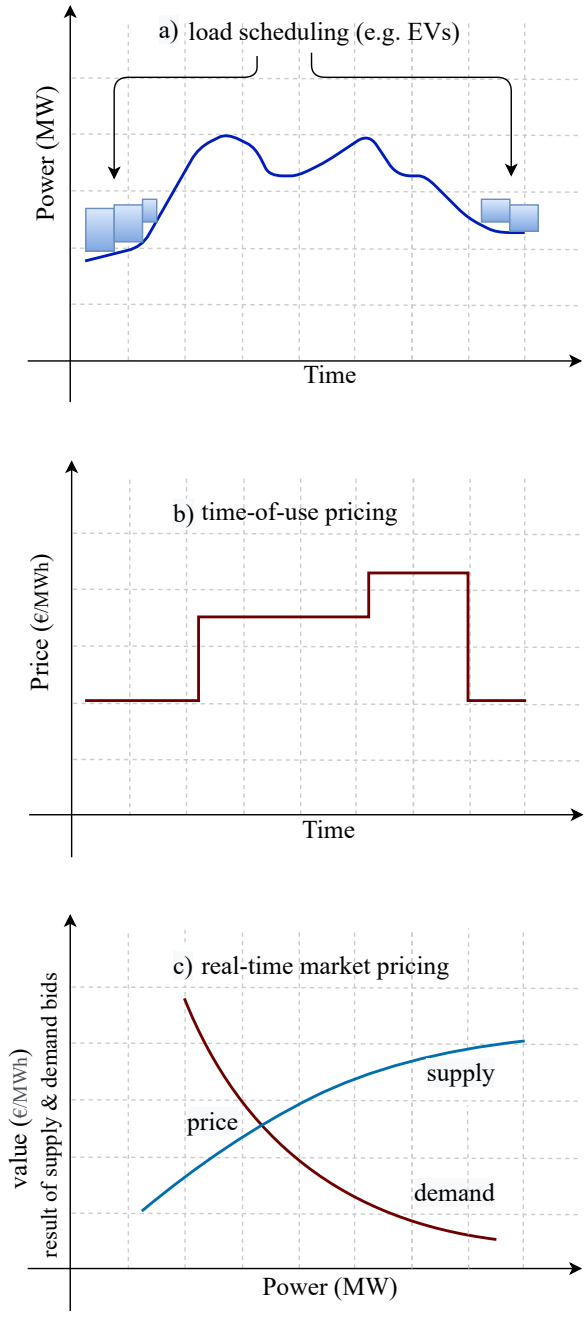

Figure 2.9: Examples of DR concepts

2.5 Summary and conclusions

To achieve the targets for increased penetration of RES into the electricity mix, the modernisation of electricity networks makes testing and implementation of new flexibility options more necessary and viable. On the one hand, voluntary actions and the flexibility of consumers can often be the most affordable and cleanest way to lower energy demand. On the other hand, flexibility is essential for the reliable and stable functioning of the power system. Thus, enhanced flexibility will be key to adapting electricity systems toward the integration of distributed green electricity while avoiding the expensive expansion of electricity networks.

Among various options, demand-side response is a valuable resource to improve the reliability and profitability of the system through enhanced flexibility. Dispatchable and non-dispatchable DR options were introduced in this chapter. Dispatchable DR concentrates on the control system, usually simplifying the value distribution system to payment to the providers. Flexible loads can offer a combination of electrical grid services by load adjustment when asked to do so by grid operators. This not only provides the grid operators more choices, but also brings clear business prospects to the loads. However, it is not easy to modify dispatchable DR plans to the varying desires of consumers without applying an advanced benefit allocation system. A consumer that does not mind the air-conditioning being turned off today, might find it uncomfortable tomorrow. Dispatchable DR thus can feel quite pushy to consumers. That is where non-dispatchable DR programs could kick in. Responsive customers to real-time electricity prices can help the TSO to ensure system reliability while decreasing their electricity procurement costs.

These are exactly the type of solutions given by this thesis focused on developing various optimisation models allowing consumers to increase their profits and help the grid operators by procuring flexibility. Given the efficient regulatory framework and suitable digitalisation of devices and processes on the demand side, consumers can −without any loss of comfort− contribute to the flexibility required in a power system and even benefit from providing FAS and participating in price-based and emergency DR programs.

References

[1] *The Paris Agreement*. [Online, Accessed Nov. 2019]: https://unfccc.int/process-and-meetings/the-parisagreement/the-paris-agreement, 2016.

[2] *European Commission, 2030 climate energy framework.* [Online, Accessed Dec. 2020]: https://ec.europa.eu/clima/eu-action/climate-strategies-targets/2030-climate-energy-framework.

[3] IEA statistics. *Key world energy statistics 2021*. [Online, Accessed May. 2021]: https://iea.blob.core.windows.net/assets/52f66a88-0b63-4ad2-94a5-29d36e864b82/KeyWorldEnergyStatistics2021.pdf, 2021.

[4] International Energy Agency (IEA). *Renewables 2021 - Analysis and forecast to 2026*. [Online, Accessed May. 2020]: https://iea.blob.core.windows.net/assets/5ae32253-7409-4f9a-a91d-1493ffb9777a/Renewables2021-Analysisandforecastto2026.pdf, 2021.

[5] *Share of electricity production from renewables*. [Online, Accessed June 2022]: https://ourworldindata.org/grapher/share-electricity-renewables?tab=chart, 2022.

[6] *Press release: Commission welcomes European Parliament adoption of key files of the Clean Energy for All Europeans package.* [Online, Accessed May. 2021]: europa.eu/rapid/press-release_IP-18-6383_en.htm, 2018.

[7] *REPowerEU: A plan to rapidly reduce dependence on Russian fossil fuels and fast forward the green transition*. [Online, Accessed May. 2022]: https://eur-lex.europa.eu/legal-content/EN/TXT/?uri=COM%3A2022%3A230%3AFIN&qid=1653033742483, 2022.

[8] *Monthly Electricity Statistics, Monthly electricity production and trade data for 47 countries*. [Online, Accessed Jun. 2022]: https://www.iea.org/data-and-statistics/data-product/monthly-electricity-statistics.

[9] K. Poncelet. *Long-term energy-system optimization models-Capturing the challenges of integrating intermittent renewable energy sources and assessing the suitability for descriptive scenario analyses, PhD thesis, KU Leuven, Belgium*. 2018.

[10] IEA. *Belgium 2022 - Energy Policy Review*. [Online, Accessed Jun. 2022]: https://iea.blob.core.windows.net/assets/638cb377-ca57-4c16-847d-ea4d96218d35/Belgium2022_EnergyPolicyReview.pdf, 2022.

[11] *Summary of the Commission assessment of the draft National Energy and Climate Plan 2021-2030*. [Online, Accessed May. 2022]: https://ec.europa.eu/energy/sites/ener/files/documents/necp_factsheet_be_final.pdf.

[12] *Future impact of EVs on the Belgian electricity network*. [Online, Accessed Jun. 2022]: http://www.synergrid.be/download.cfm?fileId=Synergrid_EV_Grid_Impact_ExternalReport_v3_0.pdf&language_code=NED, Nov. 2019.

[13] *Belgium's 2021 electricity mix*. [Online, Accessed Jun 2022]: https://www.elia.be/en/news/press-releases/2022/01/20220107_belgium-2021-electricity-mix, 2022.

[14] International Energy Agency (IEA). *Key energy statistics - Belgium*. [Online, Accessed May. 2022]: https://www.iea.org/countries/belgium, 2022.

[15] *How much renewable electricity can be generated within the Belgian borders?* [Online, Accessed Jun. 2022]: https://bit.ly/3mAMbc7, 2022.

[16] J. Ma, V. Silva, R. Belhomme, D. S. Kirschen, and L. F. Ochoa. *Evaluating and planning flexibility in sustainable power systems*. In 2013 IEEE power & energy society general meeting, pages 1–11. IEEE, 2013.

[17] M. Saffari and M. McPherson. *Assessment of Canada's electricity system potential for variable renewable energy integration*. Energy, 250:123757, 2022.

[18] P. Tielens and D. Van Hertem. *The relevance of inertia in power systems*. Renewable and Sustainable Energy Reviews, 55:999–1009, 2016.

[19] L. Mehigan, D. Al Kez, S. Collins, A. Foley, B. Ó'Gallachóir, and P. Deane. *Renewables in the European power system and the impact on system rotational inertia*. Energy, 203:117776, 2020.

[20] *Final Report on System Disturbance on November 2006*. [Online, Accessed Apr. 2020]: https://eepublicdownloads.entsoe.eu/clean-documents/pre2015/publications/ce/otherreports/Final-Report-20070130.pdf.

[21] ENTSOE. *Continental Europe Synchronous Area Separation on 8 January 2021*. [Online, Accessed March 2022]: https://eepublicdownloads.azureedge.net/clean-documents/Publications/Position%20papers%20and%20reports/entso-e_CESysSep_interim_report_210225.pdf.

[22] B. B. Adetokun, C. M. Muriithi, and J. O. Ojo. *Voltage stability assessment and enhancement of power grid with increasing wind energy penetration*. International Journal of Electrical Power & Energy Systems, 120:105988, 2020.

[23] Y. Kim, G. Lee, J. Yoon, and S. Moon. *Evaluation for Maximum Allowable Capacity of Renewable Energy Source Considering AC System Strength Measures*. IEEE Transactions on Sustainable Energy, 13(2):1123–1134, 2022.

[24] R. Verzijlbergh, L. De Vries, G. Dijkema, and P. Herder. *Institutional challenges caused by the integration of renewable energy sources in the European electricity sector*. Renewable and Sustainable Energy Reviews, 75:660–667, 2017.

[25] *Voorlopige stop voor nieuwe grootverbruikers van elektriciteit in Noord-Brabant en Limburg*. [Online]: https://tinyurl.com/yckkrwx2, Accessed 27 July 2020.

[26] S. Essallah, A. Bouallegue, and A. Khedher. *Integration of automatic voltage regulator and power system stabilizer: small-signal stability in DFIG-based wind farms*. Journal of Modern Power Systems and Clean Energy, 7(5):1115–1128, 2019.

[27] Y. Dvorkin, D. S. Kirschen, and M. A. Ortega-Vazquez. *Assessing flexibility requirements in power systems*. IET Generation, Transmission & Distribution, 8(11):1820–1830, 2014.

[28] H. Nosair and F. Bouffard. *Flexibility envelopes for power system operational planning*. IEEE Transactions on Sustainable Energy, 6(3):800–809, 2015.

[29] J. Villar, R. Bessa, and M. Matos. *Flexibility products and markets: Literature review*. Electric Power Systems Research, 154:329–340, 2018.

[30] M. Z. Degefa, I. B. Sperstad, and H. Sæle. *Comprehensive classifications and characterizations of power system flexibility resources*. Electric Power Systems Research, 194:107022, 2021.

[31] J. Zhang, H. Li, D. Chen, B. Xu, and M. A. Mahmud. *Flexibility assessment of a hybrid power system: Hydroelectric units in balancing the injection of wind power*. Renewable Energy, 171:1313–1326, 2021.

[32] H. Chandler. *Empowering Variable Renewables-Options for Flexible Electricity Systems*. 2008.

[33] International Energy Agency. *Harnessing Variable Renewables: A Guide to the Balancing Challenge*. [Online, Accessed May. 2020]: `https://iea.blob.core.windows.net/assets/2e0cb0c2-d392-4923-b092-ac633531db2b/Harnessing_Variable_Renewables2011.pdf`, 2011.

[34] *Roadmap to Net Zero*. [Online, Accessed Apr 2022]: `https://www.elia.be/-/media/project/elia/shared/documents/elia-group/publications/studies-and-reports/20211203_roadmap-to-net-zero_en.pdf`, 2021.

[35] S. Impram, S. V. Nese, and B. Oral. *Challenges of renewable energy penetration on power system flexibility: A survey*. Energy Strategy Reviews, 31:100539, 2020.

[36] Z. Lu, H. Li, and Y. Qiao. *Probabilistic flexibility evaluation for power system planning considering its association with renewable power curtailment*. IEEE Transactions on Power systems, 33(3):3285–3295, 2018.

[37] B. Mohandes, M. S. El Moursi, N. Hatziargyriou, and S. El Khatib. *A review of power system flexibility with high penetration of renewables*. IEEE Transactions on Power Systems, 34(4):3140–3155, 2019.

[38] P. A. Gunkel, C. Bergaentzlé, I. Jensen, and F. Scheller. *From passive to active: Flexibility from electric vehicles in the context of transmission system development*. Applied Energy, 277:115526, 2020.

[39] K. Hedegaard and P. Meibom. *Wind power impacts and electricity storage–A time scale perspective*. Renewable Energy, 37(1):318–324, 2012.

[40] F. Steinke, Ph. Wolfrum, and C. Hoffmann. *Grid vs. storage in a 100% renewable Europe*. Renewable Energy, 50:826–832, 2013.

[41] S.M. Romero, W. Hughes, et al. *Bringing variable renewable energy up to scale: Options for grid integration using natural gas and energy storage*. Technical report, The World Bank, 2015.

[42] M. Hermans, K. Bruninx, and E. Delarue. *Impact of CCGT start-up flexibility and cycling costs toward renewables integration*. IEEE Transactions on Sustainable Energy, 9(3):1468–1476, 2018.

[43] International Atomic Energy Agency IAEA nuclear energy series. *Non-Baseload Operations in Nuclear Power Plants: Load-Following and Frequency Control Flexible Operations*. [Online, Accessed March 2020]: `https://www-pub.iaea.org/MTCD/Publications/PDF/P1756_web.pdf/`, 2017.

[44] L. Bird, D. Lew, M. Milligan, M. Carlini, A. Estanqueiro, D. Flynn, E. Gomez-Lazaro, H. Holttinen, N. Menemenlis, A. Orths, et al. *Wind and solar energy curtailment: A review of international experience*. Renewable and Sustainable Energy Reviews, 65:577–586, 2016.

[45] B. Dursun and B. Alboyaci. *The contribution of wind-hydro pumped storage systems in meeting Turkey's electric energy demand*. Renewable and Sustainable Energy Reviews, 14(7):1979–1988, 2010.

[46] F. Díaz-González, A. Sumper, O. Gomis-Bellmunt, and R. Villafáfila-Robles. *A review of energy storage technologies for wind power applications*. Renewable and sustainable energy reviews, 16(4):2154–2171, 2012.

[47] F. Klumpp. *Comparison of pumped hydro, hydrogen storage and compressed air energy storage for integrating high shares of renewable*

energies—Potential, cost-comparison and ranking. Journal of Energy storage, 8:119–128, 2016.

[48] *Cost of wind-generated hydrogen to fall below natural gas*. [Online, Accessed Jul. 2022]: https://tinyurl.com/2f2wxber, 24 April 2018.

[49] D. S. Kirschen, J. Rosso, A.and Ma, and L. F. Ochoa. *Flexibility from the demand side*. In 2012 IEEE Power and Energy Society General Meeting, pages 1–6, 2012.

[50] H. W. Anwar, M. B.and Qazi, D. J. Burke, and M. O'Malley. *Harnessing the flexibility of demand-side resources*. IEEE Transactions on Smart Grid, 10(4):4151–4163, 2018.

[51] P. Lund, J. Lindgren, J. Mikkola, and J. Salpakari. *Review of energy system flexibility measures to enable high levels of variable renewable electricity*. Renewable and sustainable energy reviews, 45:785–807, 2015.

[52] A. Pina, C. Silva, and P. Ferrão. *The impact of demand side management strategies in the penetration of renewable electricity*. Energy, 41(1):128–137, 2012.

[53] *European Smart Grids Task Force, Demand Side Flexibility Perceived barriers and proposed recommendations*. [Online, Accessed Aug 2020]: https://ec.europa.eu/energy/sites/ener/files/documents/eg3_final_report_demand_side_flexiblity_2019.04.15.pdf, 2019.

[54] *Operational Reserve Ad Hoc Team Report - Final Version. ENTSO-E,.* [Online, Accessed Aug 2020]: https://eepublicdownloads.entsoe.eu/clean-documents/pre2015/resources/LCFR/2012-06-14_SOC-AhT-OR_Report_final_V9-3.pdf, 2012.

[55] ENTSOE. *Balancing and Ancillary Services Markets*. [Online, Accessed March 2020]: https://docstore.entsoe.eu/about-entso-e/market/balancing-and-ancillary-services-markets/Pages/default.aspx.

3

Grid balancing & role of hydrogen

As stated in Chapter 2, this thesis intends to develop optimisation models allowing consumers to increase their profits and help the grid operators in grid balancing by providing different DRPs and frequency ancillary services (FAS). This chapter gives an overview of grid balancing and the basics of frequency control, together with the potential role of hydrogen systems in the balanced operation of a power system. Section 3.1 presents the principle of grid balancing. In Section 3.2, a summary of the frequency control and services is given. The role of hydrogen and water electrolysers in the provision of FAS will be introduced in Section 3.3. This chapter will be concluded in Section 3.4.

3.1 Principle of balancing in power grids

Each of the ENTSO-E synchronous areas includes several load-frequency control (LFC) blocks in which the assigned TSO is responsible for keeping the power balance. However, as a result of deviations in the production and consumption of electricity, the LFC area can experience a lack or surplus of energy. The area control error (ACE) will show the instantaneous imbalance between actual and scheduled active power flows minus the primary frequency control contribution of the control area [1]. Each control

area will deploy secondary and tertiary FAS to minimise the real-time ACE at each time slot. Additional details on the procured FAS are provided in Section 3.2. The difference between the sum of the volumes of all up- and downward activated services is taken into account by the net regulation volume (NRV). Then, the difference between the ACE and the NRV will define the system imbalance (SI). SI, as an indicator of the quality of the balancing of the LFC area, has to be minimised by the TSO. In order to minimise the SI and decrease the need for activation of reserves, TSOs use the imbalance settlement system as a tool to incentivise balance responsible parties (BRPs) to maintain balance within their portfolio. Then it is up to the BRPs to provide and deploy all available resources to be balanced in real-time on a quarter-hourly basis. To achieve balance at a portfolio level, in addition to internal energy exchanges, a BRP can trade energy with other BRPs for the following day (day-ahead) or the same day (intra-day). Intra-day energy transfer lets the BRP update its position when facing unpredictable events, such as the breakdown of an industrial plant or a generation unit, to avoid imbalances. An intra-day energy transaction is nevertheless intended as a correction on an accurate and complete day-ahead position [2].

3.2 Frequency control and FAS

The frequency in a power system is a measure of the rotation rate of the synchronised generation units and is near but not exactly equal to the nominal value.[1] Power system frequency changes as a consequence of imbalance between power supply and demand. At a constant power generation value, with an increase in the total electricity demand, the frequency will decrease, while with a decrease in the demand, the frequency shows an increase. The frequency change following such an imbalance depends on the system inertia and the size of the power variation as presented in (3.1) [3].

$$\frac{df}{dt} = \frac{\Delta P}{2H} \cdot f_0 + \frac{D}{2H} \cdot \Delta f \tag{3.1}$$

where f_0 is the frequency at the beginning of the imbalance, Δf is the frequency deviation, ΔP is the change between the driving electrical power and the electrical load, H is the system inertia, and D is the load damping factor of the power system.

In classical systems, inertia H is defined as the amount of kinetic energy stored in the rotating masses of electrical machines connected to a

[1] In Europe and most parts of the world, 50 Hz is the nominal frequency, while in some countries (USA, Canada, parts of Japan, etc.), 60 Hz is the norm.

power system. However, in systems with high penetration of technologies, which are connected by converters to the grid, the total system inertia is the sum of the inertia provided by synchronous machines and the synthetic inertia[2] delivered by converter-connected units [4, 5]. Ref. [6] has presented detailed information on how the system inertia and (3.1) will be modified in future grids. Linked to system inertia, the rate of change of frequency (RoCoF) indicates the speed at which the frequency oscillates following a system disturbance or imbalance. With higher inertia values, more stored energy in the rotating machines cause a slower frequency deviation. While the stored energy is injected into the system following any under-frequency event, more energy is absorbed from the system following any over-frequency disturbance.

The load damping factor D models the load response to system frequency variation. This is because the frequency response is not only affected by the change in a generation but also as a result of load variations. By ignoring the damping factor, (3.1) can be expressed as (3.2).

$$\frac{df}{dt} = \frac{\Delta P}{2H} \cdot f_0 \tag{3.2}$$

In order to control the frequency deviations following a disturbance, the inertial response mechanism is the immediate action taken to limit the frequency divergence. However, as mentioned in Section 2.2.1, it is expected that the higher penetration levels of nonsynchronous generation from RES will boost the frequency deviations. Renewable power plants are mostly connected to the power grid by power electronic devices, which makes them isolated from the system. Hence, they do not contribute to the directly-connected inertia except with some extra control loops. With a lower level of inertia, the system is more sensitive to frequency deviations [7]. Thus, the power imbalances caused by the unpredictable production of renewable electricity sources, prediction errors and outage of grid components like generators cause higher levels of frequency divergence. This calls for the activation of FAS, next to the inertial response, to stabilise the operation of the power grid at a frequency of 50 Hz. So, frequency control is designed as a set of services to ensure that the grid frequency stays within a predefined range of the reference frequency at any time.

A general characterisation of frequency control, as outlined by Fig. 3.1[3], is made where different frequency control services are operated

[2]The provision of synthetic inertia is covered in Section 3.2.1.

[3]We note that the pictured frequency incident in Fig. 3.1 is for illustration purposes only. In real-world scenarios with successive frequency deviations, there is a continuous activation of services in both up- down-ward directions.

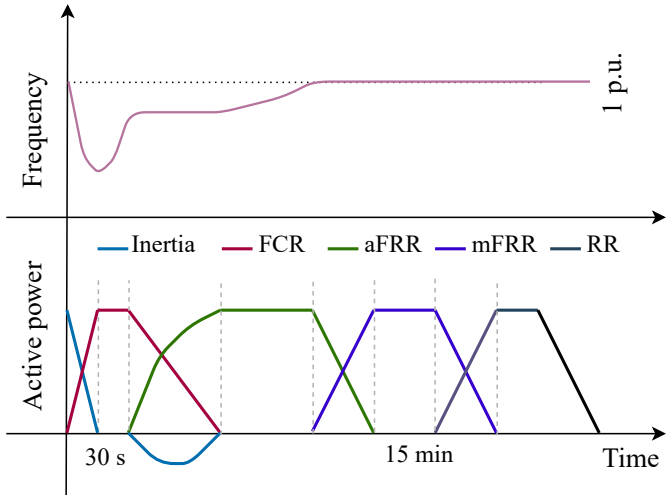

Figure 3.1: General characterisation of frequency control [9]

consecutively at various time scales [8]. After a power imbalance and next to the inertia response, the primary or Frequency Containment Reserve (FCR) is automatically activated and contains the frequency at a stable value. Afterwards, the secondary or automatic Frequency Restoration Reserve (aFRR) will become operational to restore the frequency to its reference value. The following services are the tertiary or manual Frequency Restoration Reserve (mFRR) and Replacement Reserve (RR), which are triggered manually by the TSO. These kick in if there is a frequency deviation even after the aFRR act. RR is available to restore the required level of FRR to be prepared for further system imbalance. In the following sections, the frequency-related ancillary services will be further discussed.

3.2.1 Inertia response

The inertial response in a classical situation with directly-connected synchronous machines was explained in the previous section. However, the increase in non-synchronous production has led to a decrease in rotating inertia in the grid. Assuming that in the future power systems, all units are converter-connected, there should be a mechanism to control the frequency, e.g. in case of power deficit. In such a system, some generation units will function as voltage sources or in a grid-forming way. Then, an inertial response can be implemented by artificially adjusting the velocity of phase angle (i.e. the frequency) of mentioned units based on their active power

output. The possibility of deploying synthetic inertia has already been investigated [10, 11]. The synthetic inertia strategy is able to enhance the inertial response of a variable RES by mimicking the inertial response behaviour of a traditional synchronous generator in case of a disturbance. For example, in the case of a wind turbine, when the grid frequency drops, the reference power of the turbine is increased with an inertial response value, slowing down the turbine and extracting kinetic energy from the rotor. In this way, the output power of the turbine will be temporarily increased and let the wind turbine provide a synthetic inertial response. This response is similar to the behaviour of a synchronous machine where kinetic energy is extracted from the rotor in response to the frequency drop.

While able to be delivered by wind or solar farms, possibilities for the provision of synthetic inertia are also present on the demand side. Technologies like batteries and the combination of electrolysers and fuel cells, with the ability to adjust their working points, can be controlled to mimic the behaviour of synchronous machines and provide synthetic inertia.

While rules regarding the procurement of frequency ancillary services from large RES power parks are already in place in some EU countries, no real market for inertial response is present. However, in Ireland, the synchronous inertial response is contracted with market players [12]. Given a significant share of power generation will be covered by non-synchronous resources in the future, synthetic inertia markets need to be developed in other areas as well.

3.2.2 Frequency Containment Reserve (FCR)

If the frequency deviates from 50 Hz, the primary reserve is activated instantly to avoid a further change in frequency and stabilise the system frequency [13]. Currently, a total FCR capacity of 3000 MW is allocated in the synchronous area of Continental Europe [14, 15]. The FCR market is already partly harmonised, as a capacity of 1400 MW is auctioned jointly in a platform comprised of TSOs from Austria, Belgium, France, Germany, Switzerland, and the Netherlands [16]. In Belgium, until 2020, there were four different products under the FCR scheme (see Fig. 3.2).

- R1 Sym 200 mHz: suppliers must respond proportionally to a deviation within a frequency range of 200 mHz. This product is activated between -200 mHz and + 200 mHz deviation from nominal value.

- R1 Sym 100 mHz: suppliers must respond in proportion to the deviation within a frequency range of 100 mHz. This product is activated between -100 mHz and +100 mHz deviation from nominal value.

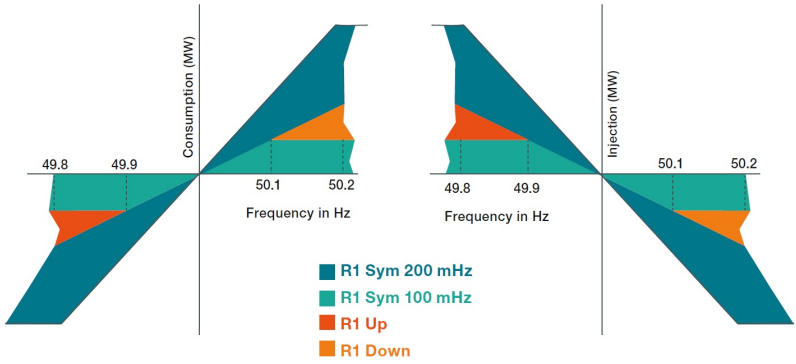

Figure 3.2: FCR products of Elia up until 2020 [13]

- R1 Up: suppliers must reduce their consumption or increase their injection if the frequency drops below 49.9 Hz.

- R1 Down: providers must increase their consumption or reduce their injection if the frequency rise above 50.1 Hz.

Yet, the ancillary services provided by Elia have changed a lot in recent years, to have a better correspondence with the European level. For instance, only one FCR product remains, i.e., the 200 mHz product. A symmetric capacity product is requested (i.e. upward and downward regulation are indivisible), offered in steps of 1 MW and with a minimum bid size of 1 MW. Elia will pay a reservation fee for the service, based on the volume offered [13]. There is no remuneration foreseen for the energy supplied (upward or downward). Moreover, to help integrate RE and decentralised sources, the product procurement of the product has been sped up to 6 hour blocks, so 4 times a day instead of weekly basis (see Fig. 3.3). Belgium's market has a size of 86 MW that must be procured by the Belgian TSO.

In terms of technical requirements, FCR procurement relies on a decentralised linear control able to change the active power output proportionally to the grid frequency deviation (e.g. droop characteristic) [13]. A maximum dead band of 10 mHz around 50 Hz is established in the controller. The full bid has to be activated within 30 seconds for a deviation of 200 mHz or more, and it needs to be online for a short period (up to 15 minutes). Similarly, for a deviation of ±100 mHz, half of the bid must be activated within 15 seconds. The offered service must be 100% accessible during the supply period. This obligation can be illustrated on Fig. 3.4 for equipment contracted for 2 MW FCR-200 mHz.

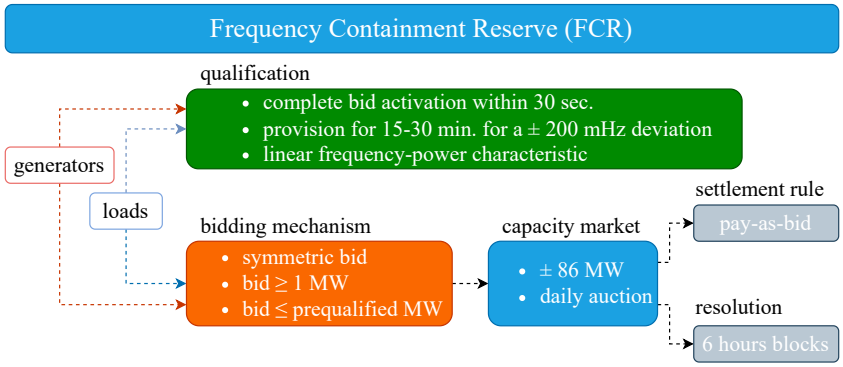

Figure 3.3: FCR general overview

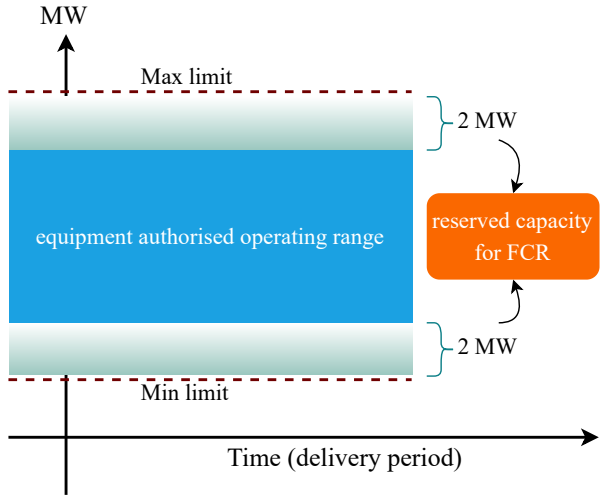

Figure 3.4: Operating range during FCR delivery period

3.2.3 Automatic Frequency Restoration Reserve (aFRR)

After the primary reserve stabilises the frequency, to restore the frequency to 50 Hz, aFRR is employed continuously. In Belgium, the requested energy must be activated within 7.5 minutes and remains active as long as necessary. The aFRR service is divided into upward and downward reserves, often referred to as R2-Up and R2-Down. So, offers can be proposed for each side separately [17]. Some changes in the procurement of aFRR were introduced in September 2020. Since then, the aFRR capacity for the contracting time slots of the day D is procured in two short-term auctions: one arranged on the day $D-2$ and the next on the day $D-1$. These modifications aim to improve the competitiveness of the aFRR market by attracting new sources of flexibility. The aFRR capacity, however, remained fixed at 145 MW in Belgium.

Grid users that provide secondary reserve must have suitable facilities for communicating in real-time with the control centre of Elia over a dedicated SCADA connection, and their units must comply with certain technical requirements. Fig. 3.6 shows how the power generation of a unit participating in the aFRR service should be modified according to the signal sent by the system operator [18]. In case of underproduction, the assets must supply additional power and energy to the system, and we are speaking about aFRR-Up. In case of overproduction, the equipment must absorb power (or reduce the power production) and energy, and we are speaking about aFRR-Down. By delivering both services (down and up), the asset is a symmetric aFRR provider.

Payment for the reserved capacity and also for the activation of the reserve are considered for aFRR providers [18]. The remuneration for the balancing capacity is the product of the unit price [€/MW/h] for the con-

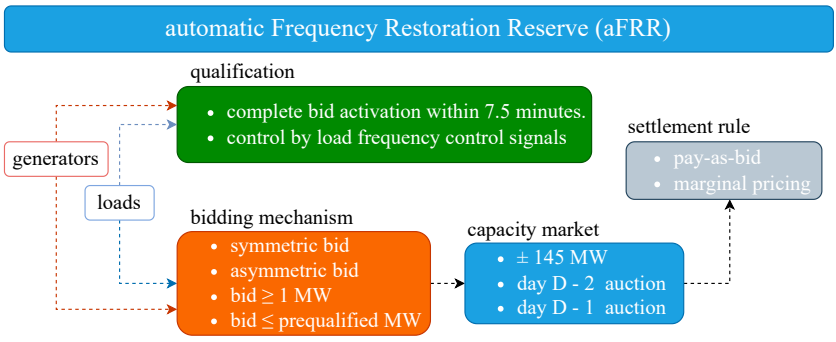

Figure 3.5: aFRR general overview

tracted aFRR capacity, the number of contracted aFRR capacity, and the corresponding hours of the concerned delivery period. The remuneration for the activation is the product of the delivered energy upward (downward) multiplied by the volume-weighted average price of the aFRR offers during the concerned delivery period. The delivered aFRR energy is determined based on the difference between the baseline (reference power) and the measured power, as represented in Fig. 3.7.

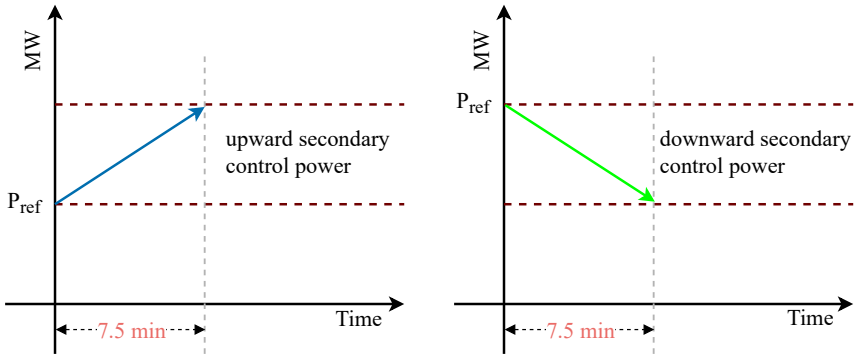

Figure 3.6: Reaction of units providing aFRR

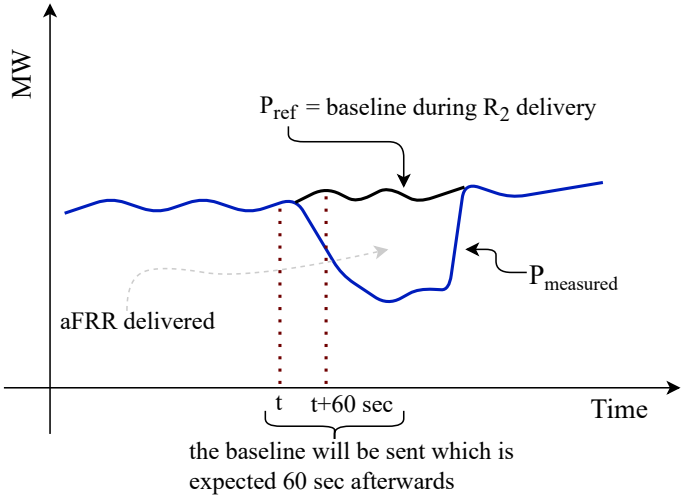

Figure 3.7: Delivered aFRR energy

3.2.4 Manual Frequency Restoration Reserve (mFRR)

After 15 minutes, if necessary, and when aFRR is not enough to alleviate the power imbalance (e.g. a severe outage occurs at a large power plant or long-lasting load changes), aFRR is replaced by the tertiary reserve, activated manually by the TSO. mFRR enables the TSO to cope with a significant or systematic imbalance in the control area and resolve major congestion problems. mFRR could be offered by generation or consumption units. Both generation and production units can provide the mFRR services if they pass the pre-qualification tests. Generation units, which have signed an mFRR contract can inject the extra capacity into the grid, and grid users who have signed an interruptibility contract will reduce the energy offtake.

Several modifications in the opening of the mFRR capacity market appeared with the latest major change in February 2020. Since then, mFRR capacity is no longer procured monthly but daily. The volume to be procured is decided based on daily dimensioning, including limitations on a minimum share of mFRR Standard capacity.

3.2.5 Replacement Reserve (RR)

As mentioned before, RR is the active power capacity available to restore the required levels of other services to be ready for additional system imbalances [19]. Thus, RR will be available to free the formerly activated aFRR and mFRR services so that they are accessible for further activation. The RR generally is a slow service, meaning the full activation time is more than the time to restore the frequency.[4] Generation and consumption units and storage systems can all operate to provide the RR. Trans-European Replacement Reserves Exchange (TERRE) is the European project implemented to exchange the RR in line with the Electricity Balancing guideline [20]. TERRE aims to create the RR Platform and set up the European RR balancing market to offer a harmonised playing field for the market participants. Not all TSOs within the ENTSO-E area activate RR, of which Elia is one.

After all, it is noteworthy that the principle of imbalance netting is implemented to optimise the amount of reserves which need to be activated to counter the ACE. The principal rule is avoiding the activation of FAS (more specifically, the secondary reserve) in opposite directions by enhancing communication between neighbouring LFC areas. As a result, an optimal signal is sent by the International Grid Control Cooperation (IGCC)[5] to the control centre of TSOs, using it to deploy the services in their area.

[4] Time to restore the frequency is 15 minutes in the ENTSO-E area

[5] IGCC is a European platform covering the imbalance netting process since 2016 [21].

3.3 Role of hydrogen in flexibility

Concurrent with the evolution in the energy systems is another movement, i.e. the growing interest in hydrogen as an energy carrier. The role of hydrogen in the energy transition has become more meaningful in recent years due to the trend of coupling different sectors [22]. Hydrogen gained even more interest with the REPowerEU plan. An additional budget of €200 million is granted to accelerate the procedure of turning Europe into a hydrogen economy [23]. According to the plan, Europe must reach a domestic production of 10 million tonnes of renewable and 10 million tonnes of imported hydrogen before 2030. The projected increase in hydrogen production is going to be achieved with several MW of electrolysis capacity.

The EU Hydrogen Strategy aims to reach a European electrolyser capacity of 6 GW and 40 GW in 2024 and 2030, respectively. Such plans for $P2H_2$ conversion have ignited the announcement of a few commercial projects on a large scale, like a 13 MW methanation plant in Austria [24], a 10 MW refinery in Germany [25], the 6 MW P2G plant in Mainz [26] or the 6 MW PEMEL at the steel plant in Linz, Austria [27]. In 2018, the 2.5 MW storage facility near Toronto was the first indoor installation. Afterwards, the next building block of 5 MW has been developed (HyLYZER-1000 product in 2019, see Fig. 3.8). The first commercial project with this product was built for Air Liquide, a 20 MW producing 8,000 kg/day, which was commissioned end of 2020 [28]. At the country level, the National Recovery and Resilience Plan of Belgium has granted funding to support the installation of at least 150 MW of electrolysis capacity by 2026 [29].

3.3.1 Technical aspects of grid balancing by hydrogen

As a sustainable solution, hydrogen systems have also been integrated with RES to reduce the stability problems and provide grid balancing [31, 32]. For instance, fleets of electrolysers have been coordinated with large RES to help mitigate the fluctuations of generated power [33, 34]. Moreover, in congestion management, large scale electrolysers are able to decrease the aggregated load in peak hours by reducing their electricity consumption or even by stopping the operation. In situations that network operator needs to quickly relieve the congestion, the fast dynamical reaction of electrolysers is an advantage over other large loads with slower responses. An external signal is sent by the TSO to the electrolyser operator to modify the setpoint of the active power. However, location dependency of this service implies that only a few large-capacity electrolysers located in specific locations can provide this service.

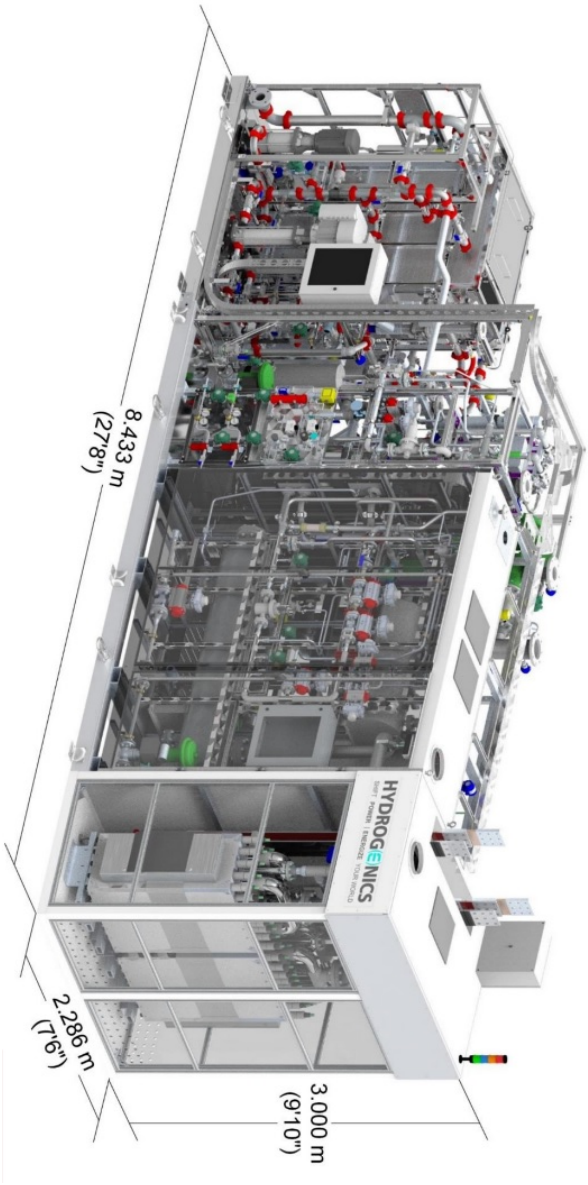

Figure 3.8: 5 MW PEMEL, product Hylyzer 1000 [30]

Electrolysers should support the reactive power when running at a partial or nominal load to provide voltage control services. By working at partial load, the remaining capacity of the converter can be utilised to inject or consume reactive power to or from the grid. However, one should note that the power factor must not be lower than 0.9, regardless of the active power consumption [35]. This follows the requirements for the provision of MVAR ancillary service by transmission-connected demand facilities. In this regard, the range for importing and exporting reactive power shall not be wider than 48% of the maximum import or export capacity of active power. The provision of voltage control, when the electrolyser operates at nominal power, requires extra controllers. Thus, the ability of electrical converters and grid codes impact the potential of electrolysers for offering voltage control. It should be mentioned that, like congestion management, voltage control is a very location-dependent service. Given the above-mentioned points, the techno-economic feasibility of water electrolysers to provide this service is not clear yet.

Coming to FAS, any technology is able to participate given that it passes the qualification tests. However, each technology has some advantages and drawbacks to provide FAS. Traditionally, synchronous generators were the main source of FCR provision. For example, in Belgium, the FCR was provided by thermal power plants working with a derating (at a power lower than the base load) to be able to increase their production to stabilise the network. This situation is rapidly changing due to the increasing penetration of distributed, nonsynchronous converter-interfaced generation and ESS causing reduction of the total system inertia. Thus, TSOs are looking for new technologies to counter the challenges of these modifications in the system fuel mix [36, 37]. Since 2017, most of the Belgian FCR capacity has been provided by battery energy storage (18 MW owned by Centrica). Large responsive loads like electrolysers are also able to provide new and flexible balancing services to the grid. Grid operators could ask large electrolysers to quickly ramp-up their consumption when there is an excess of renewable energy production. They also can command the electrolysers to reduce their consumption when the power generation is less than the electricity consumption of aggregated loads. Previous studies have pointed out that the use of fast DR with large-scale electrolysers offers a positive effect on power system frequency balance [38].

Looking at different electrolysis technologies, polymer electrolyte membrane electrolysers (PEMELs) show more flexibility than the others. Particularly their cold start-up and shut-down times range from 1 second to 5 minutes compared to 1–10 minutes for Alkaline (AEL) and less than 60 minutes for solid oxide electrolyser cell (SOEC) [39]. As an example

and according to the data provided by Cummins, the HYLYZER®-4000-30 PEMEL with the nominal power of 20 MW is able to ramp up from the minimum to the nominal power in less than 10 seconds [40]. PEMELs are also able to adjust their electricity consumption (100 %) from standby mode to nominal capacity in one second compared to 0.2 – 20 % per second for AEL. A broad operating range (0 –160 % of the nominal capacity) is another advantage of PEMEL over AEL (10 –110 %) and SOEC (20 –125 %). It should be mentioned that there is limited information on the flexibility potential of SOEC electrolysers as they are still in development, with recent demonstration projects reaching 1 MW [39]. So, among diverse electrolysis technologies, PEMELs offer better start-up and dynamic operation, as well as a compact system design with high power densities [41]. Thus, the PEMELs have a great potential to contribute to the inertial response and for the procurement of FAS, and that is why the PEM technology has been chosen for this study.

Several studies have tested the viability of using PEMELs for providing different frequency balancing services. The ITM 300 kW PEM plant was tested for providing FCR and aFRR services [42]. In the H2Future project, researchers, with the help of the Austrian transmission operator, worked on the pre-qualification tests of a SIEMENS PEM electrolyser with 6 MW power to provide grid services [43]. In [44], the ability of a 2 MW PEMEL to provide frequency regulation services has been examined. Outcomes of [45, 46] show that electrolysers respond to frequency deviations much faster than the required activation times for primary and secondary frequency control.

As mentioned above, electrolysers can flexibly produce hydrogen according to the availability of RE and grid conditions. However, the flexibility not only from the electricity grid point of view but also the use of hydrogen as feedstock in industry should be considered [47]. Access to secure sources of electricity and hydrogen, as an energy carrier or feedstock, is crucial for sectors with low flexibility and in activities that need a baseload of hydrogen to support profitable production. Thus, the optimal operation of hydrogen systems integrated with renewable sources and hydrogen storage, is required. Considering hydrogen as a fuel in gas turbines (GT) at various blending rates is an innovative flexibility-related research domain as well. One promising option to supply the electricity demand at the times of low energy production from renewables, is to replace the whole or some of the natural gas used at the plant with green hydrogen. In recent years, development of hydrogen-fuelled GTs has gained attention and companies have started working on commercialisation as it would reduce CO_2 from the cycle of industrial processes.

3.3.2 Economic aspects of grid balancing by hydrogen

While various hydrogen projects have been materialised already around the world, participation of such systems in the FAS markets comes with some challenges. For example, after a steep increase in aFRR and mFRR procurement costs seen in 2018, costs have declined in the following years. Moreover, as a result of expensive materials and the much smaller-scale production volume of PEMELs, existing investment costs are higher compared to other technologies [48, 49]. So, one might say that considering the high investment cost of PEMELs and the downtrend of FAS remuneration prices, there will be no business opportunity for a this technology in balancing markets.

However, it is noteworthy that the availability prices for FCR, aFRR and mFRR have grown dramatically since the fourth quarter of 2020 (see Fig. 3.9). The natural gas and carbon prices have had the main influence on these prices. Next to that, the total procurement cost of balancing capacity increased in 2021 to 182.4 M€. A 147% increase of the total cost compared to 2018 and a 234% increase compared to 2020 (see Table. 3.1) [51]. The steep boost is attributed to the even more increase in the gas price, especially since the outbreak of the war in Ukraine. As this drives up the generation cost of thermal power plants, they need to compensate for the difference between marginal generation cost and day-ahead price by increasing their bids for availability on the capacity markets. Also, the settlement rules for FCR, for example, will possibly be adjusted to marginal pricing, leading to slightly higher prices. In line with the planned market modifications, the technical conditions will likely become more strict at some point, either by shortening the full activation time or by supporting the participation of quicker technologies, such as PEMELs. Thus, as flexibility will continue to become more imminent, insights into availability and activation prices are essential for anyone having flexible equipment or processes.

3.4 Summary and conclusions

This chapter mainly focused on different flexibility options that could support the reliable operation of electrical grids. The potential of demand-side response, especially $P2H_2$ systems by using electrolysers to provide ancillary services was introduced. According to literature, MW class PEM electrolysers (PEMELs) are in principle capable of meeting the technical prerequisites of most existing TSO grid services, particularly for ones requiring merely active power control. Literature and demonstration projects have shown that the technical characteristics of PEMEL widely fulfil the

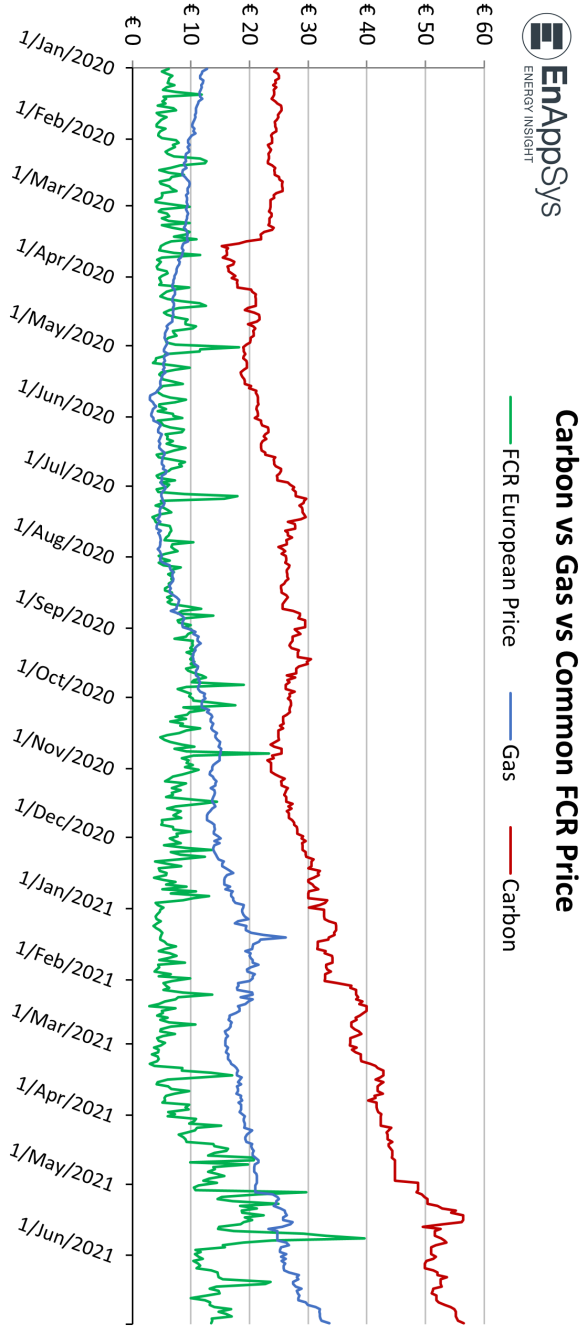

Figure 3.9: Carbon, natural gas and FCR prices [50]

Table 3.1: Procurement costs for each of the balancing reserve types procured in the LFC Area of Elia (M€)

	FCR	aFRR	mFRR	Total
2015	22.1	28.8	18.9	69.8
2016	11.7	33.5	21.5	66.7
2017	10.3	34.7	23.9	69.1
2018	9.6	43.3	71.1	124.0
2019	6.7	25.7	48.5	80.8
2020	7.1	27.1	43.7	78.0
2021	24.2	121.0	37.2	182.4

minimum prequalification requirements of ancillary services for frequency balancing. Especially, their capability to quickly ramp up or ramp down to change the consumption set point is remarkably valuable for frequency support. In this context, $P2H_2$ systems equipped with PEMELs as a type of adjustable load along with storage facilities, are able to offset the volatile renewable power generation and offer FAS to the grid operators. Whereas the operation of a PEMELs to provide FAS may be viable from a technical point of view, it may be economically unfeasible. Since PEMELs will compete with other technologies, optimisation of hydrogen production costs and ancillary service provision has become more critical. Thus, the next two chapters will investigate the techno-economic aspects of providing FAS by $P2H_2$ systems.

References

[1] *ENTSO-E Operation Handbook Glossary v2.2.* : https://eepublicdownloads.entsoe.eu/clean-documents/pre2015/publications/entsoe/Operation_Handbook/glossary_v22.pdf.

[2] Elia. *The role of the BRP*. [accessed Aug. 2022]: https://www.elia.be/en/electricity-market-and-system/role-of-brp.

[3] L. Wu. *Power System Frequency Measurement Based Data Analytics and Situational Awareness, PhD thesis, University of Tennessee*. 2018.

[4] P. Makolo, R. Zamora, and T. Lie. *The role of inertia for grid flexibility under high penetration of variable renewables-A review of challenges and solutions*. Renewable and Sustainable Energy Reviews, 147:111223, 2021.

[5] G. Magdy, H. Ali, and D. Xu. *A new synthetic inertia system based on electric vehicles to support the frequency stability of low-inertia modern power grids*. Journal of Cleaner Production, 297:126595, 2021.

[6] Y. Qi, H. Deng, X. Liu, and Y. Tang. *Synthetic inertia control of grid-connected inverter considering the synchronization dynamics*. IEEE Transactions on Power Electronics, 37(2):1411–1421, 2021.

[7] P. Tielens and D. Van Hertem. *The relevance of inertia in power systems*. Renewable and Sustainable Energy Reviews, 55:999–1009, 2016.

[8] A. Kaushal and D. Van Hertem. *An overview of ancillary services and HVDC systems in European context*. Energies, 12(18):3481, 2019.

[9] J. Baetens. *Electrical flexibility in the chemical process industry*. PhD thesis, Ghent University, 2021.

[10] ENTSO-E. *Need for synthetic inertia for frequency regulation*. 2017.

[11] J. Van de Vyver, J. D. M. De Kooning, B. Meersman, L. Vandevelde, and T. L. Vandoorn. *Droop Control as an Alternative Inertial Response Strategy for the Synthetic Inertia on Wind Turbines*. IEEE Transactions on Power Systems, 31(2):1129–1138, 2016.

[12] Eirgrid. *Consultation on DS3 System Services Volume Capped Fixed Contracts, DS3 System Services Implementation Project*, 25 October 2018.

[13] *FCR design note*. [Online, Accessed Jun. 2021]: https://tinyurl.com/yx3vu5z7, Apr. 2019.

[14] L. Meeus. *The evolution of electricity markets in Europe*. Edward Elgar Publishing, 2020.

[15] Tennet. *Dutch Ancillary Services*. [Online, Accessed Jun 2021]: https://www.tennet.eu/electricity-market/dutch-ancillary-services/.

[16] *Internetplattform zur Vergabe von Regelleistung*. [Online, Accessed Jun. 2020]: https://www.regelleistung.net.

[17] *Separated procurement of FCR and aFRR products*. [Online, Accessed Apr. 2021]: https://www.elia.be/-/media/project/elia/elia-site/public-consultations/20181009_consultation_document_2_separated_procurement_of_fcr_and_afrr_products_en.pdf?la=en, Dec. 2019.

[18] *General Framework for Secondary Control Service by CIPU Technical Units*. [Online, Accessed Feb. 2021]: https://www.elia.be/-/media/project/elia/elia-site/electricity-market/system-services/system-services-pdf-document-library/03-balancing-services-bsp/04-afrr/01-contract-templates/2019-contract-afrr-cipu.pdf, 2019.

[19] European Union Emissions Trading Scheme. *Replacement Reserve*. [Online, Accessed Jun. 2022]: https://tinyurl.com/wwkf73hk, Nov. 2021.

[20] ENTSO-E. *TERRE*. [accessed Jul. 2022]: https://www.entsoe.eu/network_codes/eb/terre/.

[21] *Commission Regulation (EU) 2017/2195 of 23 November 2017 establishing a guideline on electricity balancing.* [accessed Jul. 2022]: https://eur-lex.europa.eu/legal-content/EN/TXT/?uri=uriserv:OJ.L_.2017.312.01.0006.01.ENG&toc=OJ:L:2017:312:TOC.

[22] I. Petkov and P. Gabrielli. *Power-to-hydrogen as seasonal energy storage: an uncertainty analysis for optimal design of low-carbon multi-energy systems*. Applied Energy, 274:115197, 2020.

[23] *REPowerEU: A plan to rapidly reduce dependence on Russian fossil fuels and fast forward the green transition*. [Online, Accessed May. 2022]: https://eur-lex.europa.eu/legal-content/EN/TXT/?uri=COM%3A2022%3A230%3AFIN&qid=1653033742483, 2022.

[24] *McPhy wins a €1.3M equipment contract in Austria for an innovative methanation plant operated by RAG*. [Online, Accessed Feb 2020]: https://mcphy.com/en/press-releases/power-to-gas-in-austria/.

[25] *Shell, ITM Power to install 10 MW electrolyzer for refinery hydrogen*. [Online, Accessed Jan 2020]: https://www.greencarcongress.com/2017/09/20170901-shell.html, 2017.

[26] *Technical data about the Energiepark Mainz*. [Online, Accessed Dec. 2019]: https://www.energiepark-mainz.de/en/technology/technical-data.

[27] *H2FUTURE project - Technology*. [Online, Accessed Nov. 2019]: https://h2future-project.eu/technology.

[28] *Air Liquide a commencé la production industrielle d'hydrogène vert à Bécancour*. [Online, Accessed Jan. 2020]: https://bit.ly/3Nox7Jq.

[29] IEA. *Belgium 2022 - Energy Policy Review*. [Online, Accessed Jun. 2022]: https://iea.blob.core.windows.net/assets/638cb377-ca57-4c16-847d-ea4d96218d35/Belgium2022_EnergyPolicyReview.pdf, 2022.

[30] *Hylyzer®, water electrolysers*. [Online, Accessed Jan. 2022]: https://www.cummins.com/sites/default/files/2021-08/cummins-hylyzer-1000-specsheet.pdf, 2020.

[31] G. Maggio, A. Nicita, and G. Squadrito. *How the hydrogen production from RES could change energy and fuel markets: A review of recent literature*. International Journal of Hydrogen Energy, 44(23):11371–11384, 2019.

[32] V. Oldenbroek, S. Wijtzes, K. Blok, and A. van Wijk. *Fuel cell electric vehicles and hydrogen balancing 100 percent renewable and integrated national transportation and energy systems*. Energy Conversion and Management, 9:100077, 2021.

[33] J. Eichman, K. Harrison, and M. Peters. *Novel electrolyzer applications: providing more than just hydrogen*. Technical report, National Renewable Energy Lab.(NREL), Golden, CO (United States), 2014.

[34] Y. Zhang, L. Wang, N. Wang, L. Duan, Y. Zong, S. You, F. Maréchal, Y. Yang, et al. *Balancing wind-power fluctuation via onsite storage under uncertainty: Power-to-hydrogen-to-power versus lithium battery*. Renewable and Sustainable Energy Reviews, 116:109465, 2019.

[35] *Study on the future design of the ancillary service of voltage and reactive power control*. [Online, Accessed May 2020]: `https://tinyurl.com/4buvx8cd`, Oct. 2019.

[36] P. Moutis, A. Vassilakis, A. Sampani, and N. D. Hatziargyriou. *DC switch driven active power output control of photovoltaic inverters for the provision of frequency regulation*. IEEE Transactions on Sustainable Energy, 6(4):1485–1493, 2015.

[37] Á. Ortega and F. Milano. *Modeling, Simulation, and Comparison of Control Techniques for Energy Storage Systems*. IEEE Transactions on Power Systems, 32(3):2445–2454, 2017.

[38] B. W. Tuinema, E. Adabi, P. KS Ayivor, V. G. Suárez, L. Liu, A. Perilla, Z. Ahmad, J. L. R. Torres, M. van der Meijden, and P. Palensky. *Modelling of large-sized electrolysers for real-time simulation and study of the possibility of frequency support by electrolysers*. IET Generation, Transmission & Distribution, 14(10):1985–1992, 2020.

[39] *Potential of P2H technologies to provide system services*. [Online]: `https://eepublicdownloads.blob.core.windows.net/public-cdn-container/clean-documents/Publications/Position%20papers%20and%20reports/ENTSO-E_Study_on_Flexibility_from_Power-to-Hydrogen__P2H2_.pdf`, Accessed 27 Jun 2022.

[40] Hydrogenics. [Online, Accessed Sep. 2019]: `https://www.hydrogenics.com/hydrogen-products-solutions/energy-storage-fueling-solutions/power-to-gas/`.

[41] K. A. Lewinski, D. van der Vliet, and S. M. Luopa. *NSTF advances for PEM electrolysis-the effect of alloying on activity of NSTF electrolyzer catalysts and performance of NSTF based PEM electrolyzers*. ECS Transactions, 69(17):893, 2015.

[42] *Thüga Aktiengesellschaft. Project webpage Strom zu Gas Demonstrationsanlage.* [Online, Accessed Jul. 2021]: `http://www.szg-energiespeicher.de/`, 2017.

[43] Eva Maria Plunger. *H2FUTURE Hydrogen meeting future needs of low carbon manufacturing value chains*. [Online, Accessed Dec. 2021]: `https://www.fch.europa.eu/sites/default/files/documents/ga2011/6_Session%206_H2FUTURE%20%28ID%204811834%29.pdf`, 2018.

[44] U. Mukherjee, S. Walker, A. Maroufmashat, M. Fowler, and A. Elkamel. *Power-to-gas to meet transportation demand while providing ancillary services to the electrical grid.* In 2016 IEEE Smart Energy Grid Engineering (SEGE), pages 221–225, 2016.

[45] L. Allidières, A. Brisse, P. Millet, S. Valentin, and M. Zeller. *On the ability of PEM water electrolysers to provide power grid services*. International Journal of Hydrogen Energy, 44(20):9690–9700, 2019.

[46] M. Kopp, D. Coleman, Ch. Stiller, K. Scheffer, J. Aichinger, and B. Scheppat. *Energiepark Mainz: Technical and economic analysis of the worldwide largest Power-to-Gas plant with PEM electrolysis*. International Journal of Hydrogen Energy, 42(19):13311–13320, 2017.

[47] A. Valera-Medina, H. Xiao, M. Owen-Jones, W. I. David, and P.J. Bowen. *Ammonia for power*. Progress in Energy and Combustion Science, 69:63–102, 2018.

[48] O. Schmidt, A. Gambhir, I. Staffell, A. Hawkes, J. Nelson, and Sh. Few. *Future cost and performance of water electrolysis: An expert elicitation study*. International Journal of Hydrogen Energy, 42(52):30470–30492, 2017.

[49] *ITM Power, Scaling PEM Electrolysis to 100 MW, Hannover Messe, Germany*. [Online, Accessed Dec. 2020]: `https://www.h2fc-fair.com/hm17/images/forum/tf/2017-04-25-1100.pdf`, Apr. 2017.

[50] *Carbon and gas prices drive ancillary services up in the Netherlands*. [Online, Accessed Jun. 2022]: https://bit.ly/3xX6GVB, 2021.

[51] *Study on the functioning and price evolution of the Belgian wholesale electricity market – Monitoring Report 2021*. [Online, Accessed Jun. 2022]: https://www.creg.be/sites/default/files/assets/Publications/Studies/F2355EN.pdf, May 2022.

4

Operation & investment plans of $P2H_2$ systems providing FCR

As mentioned in previous chapters, hydrogen plays a major role in mitigating GHG emissions and supporting the security and flexibility of future European energy systems. In this context, $P2H_2$ plants equipped with PEMELs can provide flexibility to the grid by adjusting their electricity consumption and compensating for supply and demand mismatches. This chapter investigates the implications of providing primary frequency reserve on the design and operation of $P2H_2$ systems, specifically for a hydrogen refuelling station. A techno-economic model is introduced to analyse the total annual profits (TAP) of the plant, considering investment and operational costs and different revenue streams coming from the mobility, natural gas and ancillary service markets. The prices on electricity and ancillary service markets, characteristics of sub-components in the $P2H_2$ plant, and other technical constraints are used based on real data of the Belgian energy system.

The rest of this chapter is structured as follows: Section 4.1 reviews the literature and presents the novelty of this chapter to cover the research gap. Section 4.2 defines the test system and the proposed method based on the specifications of the

HRS. Section 4.3 describes the input data and the frameworks in Belgium that are applied to the model. Then, the results of the sizing and scheduling method for different scenarios are presented in Section 4.4. Finally, Section 4.5 draws the conclusions. The content of this chapter has been published in [1].

On the optimal planning of a hydrogen refuelling station participating in the electricity and balancing markets

Akbar Dadkhah, Dimitar Bozalakov, Jeroen D.M. De Kooning and Lieven Vandevelde

Published in International Journal of Hydrogen Energy, 2021
DOI: 10.1016/j.ijhydene.2020.10.130

Abstract: *This work presents an optimisation model to assess the techno-economic feasibility of a hydrogen refuelling station, which purchases power from the electricity market, supplies the mobility sector with hydrogen, and participates in the ancillary service market. The problem is formed as a mixed-integer nonlinear programming model to investigate the optimal operational plans considering the nonlinear behaviour of an electrolyser. Obtained results from various scenarios in 2020 and 2030 show that participation in the reserve market considering optimal sizing and dispatch of components increase revenues up to 16%, and as a result, decrease the hydrogen break-even price by up to 4.7% and 6.4% in 2020 and 2030, respectively. Exemption from tax and levies for connection to the grid reduces the hydrogen break-even price by up to 13%. Plant operators could benefit from the proposed approach to schedule components reliably while meeting the hydrogen demand and maximising the annual profits.*

4.1 Introduction

Road transportation was responsible for nearly 21% of total CO_2 emissions of the European Union (EU) in 2016. In 2019, the EU set out a new target of 23% emissions reduction from road transport by 2030 compared to 2005 [2]. To reach this target, the growing use of alternative fuels is indispensable, and hydrogen as one of these alternatives has begun to take its place in the transportation sector. In recent years, hydrogen-powered vehicles and HRSs have become more available to the public. The major factors to be considered for the implementation of an HRS are financial issues and technical operation of the system, which make the techno-economic analysis of an HRS crucial for investors and decision makers.

Many studies have analysed the techno-economic feasibility of hydrogen systems and HRSs around the world. The technical potential of hydrogen production by placing wind turbines next to the existing fuelling stations has been studied in [3]. Ref. [4] has examined the techno-economic viability of small-scale HRSs, which produce hydrogen via alkaline electrolysers. In [5], a strategy has been proposed for the operation of an electrolyser, which consumes energy at times of low electricity prices in the

spot market. The proposed method has considered the predictions of electricity prices and wind energy production. However, optimal sizing has not been included, and electricity grid costs and taxes were assumed as constant per unit values. Ref. [6] has used an optimisation strategy to minimise the operation costs of an HRS considering electrolysis process and wind energy production. However, investment costs were not included in the analysis. With a focus on reducing design costs, a Simulink model consisted of an electrolyser, a compressor, storages, and a hydrogen consumer block has been developed in [7]. While some detailed aspects of an HRS were described in this reference, its simulations lack elaborate operational details such as optimal planning of the electrolyser electricity consumption. Moreover, the authors have not considered sizing of subcomponents, and other sources of revenue, such as participation in the ancillary service markets.

The reasonable sizing and siting of HRSs both improve the hydrogen infrastructure and reduce the production cost of hydrogen. In [8], a deployment plan has been developed to find the optimal location and the required number of refuelling stations in the Republic of Korea. Ref. [9] has considered the growing hydrogen demand and offered an optimised design for an HRS network. The economic feasibility of an HRS network in Romania considering the annual hydrogen consumption, investments, and net present value at the end of the period has been studied in [10]. The results showed that the primary barrier for the expansion of hydrogen infrastructures is the unfavourable economic issues rather than technical requirements. While Refs. [9, 10] have done thorough analyses, they made assumptions about the capacity of the stations, mainly focused on economic evaluation of HRS rollout plans, and technical aspects and hourly operation of stations were not taken into account. In [11], an HRS siting optimisation model has been proposed, highlighting that attention should be paid to all aspects of hydrogen cost including the cost of production, transport, storage, and the annual investment and operational costs.

In addition to siting, the HRS subcomponents should be sized correctly to meet the hydrogen demand at any given time. If the size of the subcomponents is not optimised, not all produced hydrogen will be used for the mobility sector and the excess amount will be supplied to the gas grid or will be vented to atmosphere. Besides, capacity optimisation of each unit at the planning stage is of vital importance to decrease substantial investment expenses. Recently, some articles have focused on the techno-economic analysis of hydrogen systems together with size optimisation. Ref. [12] has designed a photovoltaic-powered HRS to supply a taxi fleet in a Brazilian city. Results pointed out that the levelised cost of hydrogen is inversely proportional to the hydrogen production volume. However, the authors have

only considered a topology for supplying cars, but not heavy-duty vehicles. Besides, a constant value for the efficiency of the electrolyser was assumed, and injection to the gas grid and grid costs were not included in the analysis. In [13], a method has been proposed to find the optimal size of the electrolysers in a system consisting of wind turbines, electrolysers, and hydrogen fuel cells. The authors studied the trade-offs between selling the hydrogen to consumers or store it at times when the electricity price is high. In [14], the authors have determined the optimal location, size, and the number of wind turbines, electrolysers, compressors, storages, and fuel cells in a test system. This source has mainly dealt with the excess wind power through the electrolysis process, while the interaction between the power grid and hydrogen production and consumption has not been taken into account. Moreover, hydrogen demand has not been considered for the mobility sector, or authors assumed a constant value for the daily demand based on the nominal capacity of the electrolyser in [13, 14].

The authors have analysed different HRS architectures from the economic point of view for 2015 and 2050 in [15]. They have dimensioned compressor and high-pressure hydrogen storage to minimise capital and electricity costs. However, costs and energy consumption scheduling associated with the electrolyser were not considered, and therefore, grid connection costs excluded the electrolyser. Ref. [16] has introduced a siting and sizing method to achieve the optimal cost for hydrogen consumers. While the proposed model covers various techniques of hydrogen production, transportation, and storage, the authors have mainly focused on the economic features of a group of stations, and the technical aspects and operational scheduling of electrolysers, storages and compressors in an HRS were not taken into account. Ref. [17] has presented a model to evaluate the HRS profitability and to find the optimal size of the electrolyser and storage for different car-sharing fleets. However, operational aspects, such as electrolyser scheduling and the model of grid costs have not been included.

In addition to sizing, it is also important to explore possible markets that are properly suited for HRS. The first clear business model relies on trading between the markets for selling hydrogen and the electricity market during times of low electricity price. For example, [18] has designed an HRS in which hydrogen is produced by a proton exchange membrane electrolyser (PEMEL) using electricity from a photovoltaic plant and the power grid. The authors have evaluated the feasibility of case studies with several objective functions. However, they have studied a topology for supplying cars, but not heavy-duty vehicles, and assumed an amount for the capacity of subcomponents such as hydrogen storage.

Other business models that provide added incomes aim at the provision of ancillary services to guarantee the reliable performance of power systems [19, 20]. Contribution of water electrolysers in providing ancillary services has already been investigated in some papers. Ref. [21] has studied the economic profitability of an electrolyser participating in the French primary reserve market. The authors concluded that the provision of the primary reserve with the current requirements is an unattractive option as it increases hydrogen production cost. A model was developed in [22] to study the performance of an HRS. While the authors have considered participation in the reserve market, their research lacks the optimal sizing of the primary reserve capacities, the nonlinear model of the electrolyser, and simulation of electricity grid costs. Participation in the secondary reserve market has also been taken into account in detail in [23, 24]. An overview of a 6 MW power to gas plant in which a part of the produced hydrogen is delivered to an HRS has been given in [23]. Providing secondary reserve was among the different operating modes. They found 1 €/kg as the production costs because they did not include either taxes and grid costs on purchased electricity or investment costs of compressors and storages. Furthermore, hydrogen demand has not been included as a limitation in the study. Ref. [24] has proposed a model to evaluate the economic feasibility of hydrogen plants that provide secondary frequency service in addition to supplying hydrogen for different markets. Instead of sizing HRS components, the authors have determined the minimum demand expected from the hydrogen-powered vehicles so that an electrolysis facility with 5 MW size and the assumed hydrogen selling price returns enough profits. They have considered a constant efficiency for the electrolyser, and hourly operation of the electrolyser and other subcomponents has not been presented.

4.1.1 Gap and contribution

Various parameters such as refuelling pressure make the design of an HRS complex. Heavy- and light-duty vehicles refuel at 350 bar and cars at 700 bar, respectively. The estimated daily and hourly refuelling demand should be considered in the HRS design as well. Considering the above-mentioned factors and the notable impact of investment and operation costs of equipment on the hydrogen production costs, the authors were inspired to develop a model to identify the optimum size and hourly working points of subcomponents. The introduced method optimises the operation of an HRS to be compatible with the power and balancing markets and provides the lowest hydrogen break-even price while meeting the hydrogen demand for the mobility sector.

While the aforementioned research set a precious foundation for this study, they have not analysed the size optimisation of an HRS together with optimal hourly provision of FCR to get the minimum hydrogen break-even price. They also have not employed a detailed model for calculating grid costs; instead, they have assumed a constant price for each MWh energy consumption. This work considers a more detailed model of an HRS that supplies hydrogen vehicles at both 350 and 700 bar combined with the possibility of injection into the gas grid. The proposed approach considers FCR provision, and employs exact models of the electrolyser and grid costs components including taxes, levies, public service obligations, etc.

4.2 Test system and methodology

In this chapter, an onsite grid-connected HRS, which buys electricity on the electricity market was analysed. Fig. 4.1 shows the HRS system configuration, which serves both light and heavy-duty vehicles with tanks at 350 bar and cars with tanks at 700 bar. The HRS design considers a refuelling plan in which two compressors feed the medium and high-pressure storages. The first compressor supplies the medium pressure (450 bar) storage with hydrogen coming from the electrolyser and the second compressor supplies the high-pressure (900 bar) storage with hydrogen coming from the medium-pressure storage. Both 350 and 700 bar types of dispensers as an interface with the customers are considered [25]. It is assumed that the produced hydrogen with an output pressure of 30 bar could also be injected to the natural gas network using the third compressor with a pressure up to 70 bar [26].

The proposed method finds the optimal size of components and FCR capacities, and accordingly, the resulting optimal electrolyser electricity demand, the amount of produced and stored hydrogen, and the injected hydrogen to the gas grid are determined at every hour over one year. A mixed-integer nonlinear programming (MINLP) model was employed as the given strategy uses nonlinear models of the electrolyser. To consider uncertainties in future electricity and reserve markets and investment costs [27], the impact of change in energy and FCR prices and the efficiency improvement and potential cost reduction of subcomponents on the economic feasibility of the HRS design in different scenarios for 2020 and 2030 were analysed. Moreover, the hydrogen break-even price ρ_{ab}^{be} (€/kg), which is the hydrogen selling price required to match revenues and costs where the benefits become zero was also introduced as an indicator.

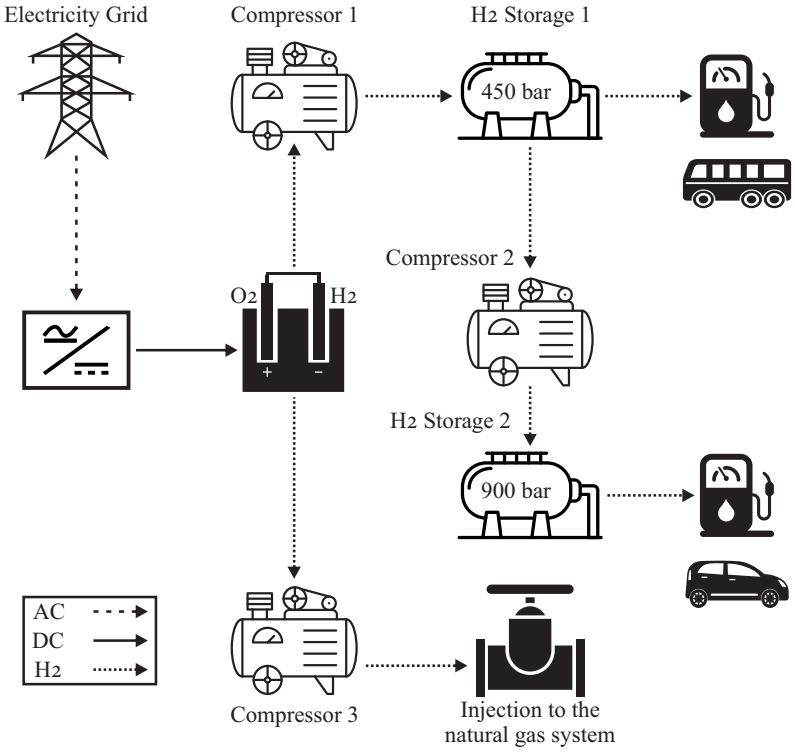

Figure 4.1: The HRS system evaluated in the scenarios

Fig. 4.2 gives a summary of the simulation method. Although the problem consists of sizing and scheduling, the proposed method solves both in one run. The optimisation problem was solved for all hours over a year.

The model attempts to maximise TAP by optimal sizing of subcomponents and flexible electrolyser operation. The annual profit TAP is represented as the difference between annual revenues TAR and annual costs TAC. TAR includes the revenues from selling hydrogen to the mobility sector and the natural gas system, selling O_2 as a by-product, and the revenue obtained from the provision of frequency containment reserve (FCR). The following equation defines the TAR:

$$\begin{aligned} \text{TAR} = \sum_{h=1}^{8760} \Big\{ & (H_h^b + H_h^a) \cdot \rho_{ab} + H_h^g \cdot \rho_g \\ & + C_h^{\text{FCR}} \cdot \rho_h^{\text{FCR}} + H_h^p \cdot K_{O_2} \Big\} \end{aligned} \tag{4.1}$$

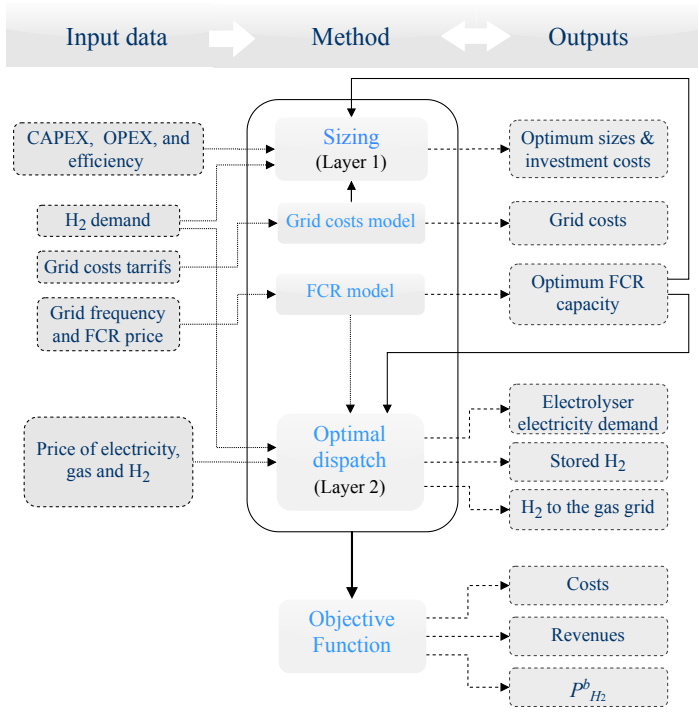

Figure 4.2: Schematic diagram of the proposed approach

Revenue from the mobility sector depends on the hydrogen price ρ_{ab} and demand. H_h^b and H_h^a are the hourly hydrogen demand for light and heavy-duty vehicles and cars, respectively. FCR revenue depends on hourly FCR capacity C_h^{FCR} and hourly availability payments ρ_h^{FCR}, in € per MW per hour allocated each hour for providing the FCR service. Revenue from selling hydrogen to the gas grid is related to the hydrogen price in the gas sector ρ_g and the amount of hydrogen injected to the gas grid H_h^g. Revenue from selling oxygen was calculated by multiplying the produced hydrogen and $K_{O_2} = 0.0123$ €/kg as the O_2 revenue factor. The O_2 revenue factor was obtained according to the O_2 selling price and the information provided by Cummins related to the amount of produced O_2 per kg produced H_2.

The total annual cost TAC is represented as the sum of the equipment costs, bought electricity expenses, water costs WC, electricity grid costs GC, and the cost for connection to the gas grid IC^g. Equipment costs covers the annual investment IC$_{\mathrm{pu}}^u$ and operation costs OC$_{\mathrm{pu}}^u$ of subcomponent u and annual stack replacement costs ARC. The model also considers other expenses, such as construction costs and costs of control and energy man-

agement systems, which are estimated based on a fixed percentage (10%) of total annual investment costs of the HRS system (see (4.2)). The installation costs are reported in the order of 5-15% of the capital costs [28, 29].

$$\begin{aligned} \text{TAC} = \sum_{h=1}^{8760} P_h \cdot \rho_h^e + \text{WC} + \text{GC} + \\ 1.1 \cdot \left[\text{IC}^g + C^E \cdot \text{RC}_{pu} + \sum_{s=1}^{8} C^u \cdot \text{IC}_{\text{pu}}^u\right] \\ + \sum_{u=1}^{8} C^u \cdot \text{OC}_{\text{pu}}^u \end{aligned} \tag{4.2}$$

P_h is the electrolyser hourly electricity demand, ρ_h^e is the electricity price, C^E is the electrolyser capacity, and C^u is the capacity of subcomponent u.

The simulation of grid costs (GC) shows how the costs related to the access to the grid are computed. The region in which the access point is located and the infrastructure level were also taken into account. Grid costs were calculated according to the tariffs applicable for the given access point linked to the terms for access to the grid, public service obligations and taxes and levies. Eq. (4.3) shows the breakdown of the GC:

$$\text{GC} = \text{MDC} + \text{MEC} + \text{PRC} + \text{MIC} + \text{PSC} + \text{TLC} \tag{4.3}$$

where MDC represents the costs of the management and the development of the grid infrastructure, MEC defines the costs of the management of the electric system, PRC represents the costs of power reserves and black-start, MIC defines the market integration costs, PSC considers public service obligations costs, and TLC represents tax and levies. The abovementioned parts depend on the monthly and yearly energy consumption, monthly and yearly power peaks, and the power put at disposal. So, the size of the electrolyser, its hourly working points, and FCR hourly capacities affect the grid costs.

The net present cost (NPC) method was used to perform the investment cost-related calculations:

$$\text{NPC}_{\text{pu}}^u = \frac{\text{IC}_{\text{pu}}^u}{\text{CRF}} \tag{4.4}$$

$$\text{CRF} = \frac{d \cdot (1+d)^y}{(1+d)^y - 1} \tag{4.5}$$

where $\mathrm{IC}_{\mathrm{pu}}^{u}$ is the annualised cost per unit capacity, CRF is the capital recovery factor, y is the number of years, and d is the real discount rate. The annual real discount rate is calculated as given in (4.6):

$$d = \frac{d' - i}{1 + i} \tag{4.6}$$

d' is the nominal discount rate (assumed 5%) and i is the expected inflation rate (assumed 2%). Here, the economic analysis of the considered system was performed assuming 20 years as the lifetime of the project.

The model employed in this work considers some constraints shown in (4.7)-(4.26) to ensure the desired operation of the HRS system. Eq. (4.7) and (4.8) ensure that the power consumption of the electrolyser remains in its operating range. The electrolyser is capable of operating between 5 and 100% of its nominal power (see (4.7)). Eq. (4.8) shows that the electricity load of the electrolyser is limited by C_{EG}, the capacity of the feeder that electrolyser is connected to via the AC/DC converter.

$$0.05 \cdot C^{E} \leq P_h \leq C^{E} \tag{4.7}$$

$$P_h \leq C_{EG} \tag{4.8}$$

4.2.1 Power specifications for FCR

As stated before, the Belgian TSO (Elia) has balance responsible parties (BRP) in order to keep the balance between generation and consumption. If BRPs are incapable to balance their customer portfolio, Elia itself takes the essential steps and asks power system players to provide FAS [30]. FAS in Belgium has changed recently, to have a better correspondence with the European level. For instance, for providing primary reserve, only the 200 mHz FCR product has remained. The loads intending to participate in the FCR market with a power amount of C^{FCR} MW (in 1 MW integer steps), should prove that they can adjust their baseline power P^0 over the $(P^0 - C^{\mathrm{FCR}})$ to $(P^0 + C^{\mathrm{FCR}})$ power range in maximum 30 s [31]. The C^{FCR} is delivered proportionally to the grid frequency variation, and the total C^{FCR} amount is delivered for a frequency change of 200 mHz. Eq. (4.9) and Fig. 4.3 illustrate the amount of power to be delivered according to the grid frequency.

The dead band, which is specified as the minimum magnitude of change in the frequency that causes a change in power consumption is 10 mHz. FCR regulation is a dynamic process in which the instant setpoints are provided by the grid operator. Let ΔP_h be the power difference between the setpoint power P_h, and the baseline power of the equipment P_h^0. ΔP_h is a function of C_h^{FCR} and of the grid frequency f_h.

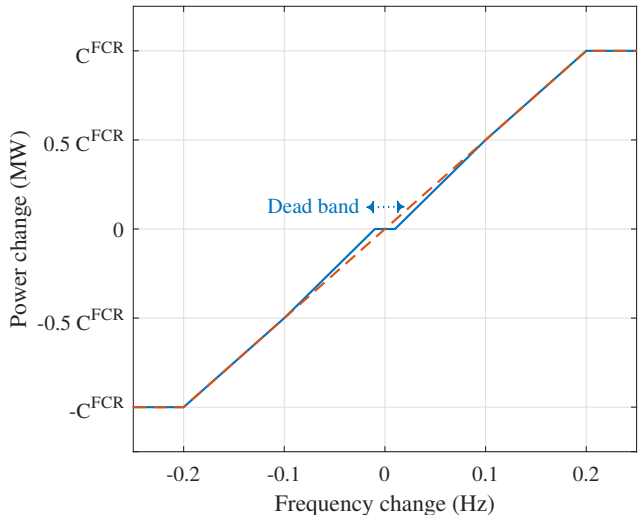

Figure 4.3: The description of FCR product.

$$\Delta P_h = \begin{cases} 0, & |\Delta f_h| \leq 0.01\text{Hz} \\ (\Delta f_h - 0.01) \cdot \frac{C_h^{\text{FCR}}}{0.2}, & 0.01\text{Hz} < |\Delta \text{f}_\text{h}| \leq 0.2\text{Hz} \\ C_h^{\text{FCR}}, & |\Delta f_h| > 0.2\text{Hz} \end{cases} \tag{4.9}$$

$$P_h = P_h^0 + \Delta P_h \tag{4.10}$$

$$\Delta f_h = f_h - 50 \tag{4.11}$$

Participation in FCR would require operation at an optimal baseline load P_h^0, which enables the load to increase or decrease the consumption (see (4.12)). Transient states of load operation can be neglected in this thesis due to their low duration in the order of seconds.

$$0.05 \cdot C^E + C_h^{\text{FCR}} \leq P_h^0 \leq C^E - C_h^{\text{FCR}} \tag{4.12}$$

The hydrogen produced in a particular hour h was calculated by (4.13) as a function of the electrolyser consumption and the relative power $P_{n,h}$. Eq. (4.13) was obtained from a calculation to estimate the amount of hydrogen production based on the efficiency of the electrolyser and the higher heating values. The efficiency of the electrolyser is modelled as a second order polynomial curve in the function of the relative power on experimental data for a PEMEL provided by Cummins.

$$H_h^p = [-5.9 \cdot P_{n,h}^2 + 5.07 \cdot P_{n,h} + 20.17] \cdot P_h \tag{4.13}$$

$$P_{n,h} = \frac{P_h}{C^E} \tag{4.14}$$

The following equations consider the balance of hydrogen flows in the HRS. Eq. (4.15) divides the hydrogen coming from the electrolyser into $H_h^{C_3}$ and $H_h^{C_1}$. The $H_h^{C_1}$ is the share of produced hydrogen that goes to the medium-pressure compressor, while the $H_h^{C_3}$ represents the amount of hydrogen that goes to the third compressor for injection to the gas pipeline.

$$H_h^p = H_h^{C_3} + H_h^{C_1} \tag{4.15}$$

Eq. (4.16) defines the amount of injected hydrogen into the gas grid, while (4.17) works as a constraint that limits the amount of hydrogen injection into the gas system in a way that hydrogen concentration does not surpass the gas grid limits. η_{C_3} is the efficiency of the third compressor.

$$H_h^g = H_h^{C_3} \cdot \eta_{C_3} \tag{4.16}$$

$$H_h^g \leq C_G \tag{4.17}$$

Eq. (4.18) calculates the amount of compressed hydrogen by the first compressor $C_{1,h}$, where η_{C_1} is the efficiency of the first compressor.

$$C_{1,h} = H_h^{C_1} \cdot \eta_{C_1} \tag{4.18}$$

The amount of hydrogen within the first storage at a particular hour h is obtained by (4.19). Assuming 5% leakage for the hydrogen storages according to the results of [32, 33], the term $0.95 \cdot S_{1,h-1}$ expresses the amount of hydrogen present in the storage at the beginning of each hour. The stream $-H_h^b/\eta_{D_1} - H_h^{C_2}$, divides the hydrogen coming from the first storage into H_h^b/η_{D_1} and $H_h^{C_2}$. The $H_h^{C_2}$ is the share of hydrogen that goes to the high-pressure compressor, while the H_h^b/η_{D_1} represents the amount of hydrogen that goes to the dispenser for light and heavy-duty vehicles.

$$S_{1,h} = 0.95 \cdot S_{1,h-1} + C_{1,h} \cdot \eta_{S_1} - H_h^b/\eta_{D_1} - H_h^{C_2} \tag{4.19}$$

Eq. (4.20) calculates the amount of compressed hydrogen by the second compressor $C_{2,h}$, where η_{C_2} is the efficiency of the compressor.

$$C_{2,h} = H_h^{C_2} \cdot \eta_{C_2} \tag{4.20}$$

The amount of hydrogen within the second storage at a particular hour h is obtained by (4.21). The term $0.95 \cdot S_{2,h-1}$ represents the amount of existing hydrogen in the storage at the beginning of each hour. The stream H_h^a/η_{D_2} gets the hydrogen coming from the second storage to the second dispenser for cars.

$$S_{2,h} = 0.95 \cdot S_{2,h-1} + C_{2,h} \cdot \eta_{S_2} - H_h^a/\eta_{D_2} \tag{4.21}$$

The model finds the optimal volume of hydrogen that needs to be produced and then stored such that the hydrogen demand of vehicles is satisfied (see (4.22)-(4.24)).

$$\sum_{h=1}^{8760} \frac{\frac{H_h^a}{\eta_{C_2} \cdot \eta_{S_2} \cdot \eta_{D_2}} + \frac{H_h^b}{\eta_{D_1}}}{\eta_{C_1} \cdot \eta_{S_1}} + \frac{H_h^g}{\eta_{C_3}} \leq \sum_{h=1}^{8760} H_h^p \tag{4.22}$$

$$\sum_{h=1}^{8760} S_{1,h} \geq \sum_{h=1}^{8760} \frac{H_h^b}{\eta_{D_1}} + \frac{H_h^a}{\eta_{C_2} \cdot \eta_{S_2} \cdot \eta_{D_2}} \tag{4.23}$$

$$\sum_{h=1}^{8760} S_{1,h} \geq \sum_{h=1}^{8760} \frac{H_h^a}{\eta_{D_2}} \tag{4.24}$$

The maximum amount of compressed and stored hydrogen by compressors and in storages depend on the decision variables C_{C_1}, C_{C_2}, C_{C_3}, C_{S_1}, and C_{S_2}. Eq. (4.25) and (4.26) were considered as constraints in the model, as the state of compressors and storages at each hour should be less than the size of the respective component.

$$C_{1,h} \leq C_{C_1}, \qquad C_{2,h} \leq C_{C_2}, \qquad C_{3,h} \leq C_{C_3} \tag{4.25}$$

$$S_{1,h} \leq C_{S_1}, \qquad S_{2,h} \leq C_{S_2} \tag{4.26}$$

4.3 Simulation inputs

The current investigation was conducted based on the regulatory situation in Belgium, and therefore all electricity-related input data, including energy prices, grid tariffs and taxes, and FCR remuneration scheme were chosen for Belgium. Table 4.1 provides up-to-date techno-economic data gathered in projects from suppliers or obtained from companies around Europe. Specifically, given data for the electrolyser, cell stacks, and power electronic equipment, which are provided by Cummins, are close to the information in the references mentioned in Table 4.1. CAPEX and OPEX introduce capital and operational expenditure, respectively.

Table 4.1: Components parameters and characteristics of a PEMEL

Subcomponents	CAPEX		OPEX/year	Lifetime	Sources
	2020	2030	% of CAPEX		
Cell stack	0.39 M€/MW	0.27 M€/MW	5%	56,000 hours	[24, 26, 28, 34]
Electrolyser	0.77 M€/MW	0.54 M€/MW		20 years	[24, 26, 28, 34]
Compressor 1	1,525 [€/Nm3/h]	1,322 [€/Nm3/h]			[26, 35]
Compressor 2	538 [€/Nm3/h]	496 [€/Nm3/h]			[26, 35]
Compressor 3	333 [€/Nm3/h]	266 [€/Nm3/h]			[17, 26]
Dispenser & precooling 1	€116,689	€116,689			[35]
Dispenser & precooling 2	€162,570	€162,570			[35]
Storage 1	1,400€/kg	960€/kg	1%		[17, 26]
Storage 2	1,900€/kg	1,320€/kg	1%		[17, 26]
Gas grid connection	1.5M€	1.27M€	8%	35 years	[26, 36]

4.3.1 Electricity market data

The costs related to the electricity consumption were integrated into the model based on electricity price and the grid costs simulator provided by Elia (TSO in Belgium and Germany) for 2019, since those were the most up-to-date data of a whole year accessible to the author [37]. The potential revenue of FCR was also evaluated based on the capacity payments for all weeks of 2019. Frequency values are extracted from Elia platform [38].

4.3.2 Hydrogen demand data

Including the hydrogen demand in the objective function lets the impact of increasing hydrogen demand to be considered. The normalised time series of the hydrogen demand for vehicles were obtained from a fuel station profile and adjusted according to the hydrogen demand for mobility in Belgium [39]. The demand varies within hours and weekdays, which forms recurrent arrays of one week for the hydrogen consumption over one year. Hourly demand in 2020 amounts to 75 kg on average, a maximum of 273 kg, and for the year 2030, was modified and scaled up based on plans for HRSs in Belgium. The distribution of hydrogen demand will be given in Section 4.4 to be compared with produced and stored hydrogen. It is noteworthy that different assumptions for hydrogen demand lead to different results, and they all need to be compared to produce useful outputs for decision makers. Considering that Belgium is still lagging the national plans in terms of hydrogen refuelling infrastructure, the author compared the obtained results using the data presented in [40] as the current situation in Belgium in 2020 with the results considering the hydrogen targets. For hydrogen injection into the natural gas system, it was assumed that the hydrogen injection tariff and natural gas price are the same (based on the caloric value) for the corresponding scenario, i.e. hydrogen price of 1.5 €/kg in 2020 and 1.7 €/kg in 2030, which is not competitive with price in the mobility market.

4.4 Results

Simulations are run for two situations according to the hydrogen targets [39] and according to the current conditions in Belgium [40]. Sections 4.4.1 and 4.4.2 discuss the simulation outputs in more detail.

4.4.1 Results considering the hydrogen targets

For this situation, the introduced method is implemented in two cases, including eight scenarios in total. The first case consists of three scenarios and evaluates the techno-economic feasibility of an HRS considering techno-economic conditions and an FCR compensation scheme. Since investment in an HRS can last for years, the growth of energy prices during the HRS lifetime should be covered in the feasibility studies [41]. Besides, in the coming years, the capital and operation costs of components are expected to decrease because of technological improvements [28]. So, the second case consists of five scenarios, which consider the operation of the HRS in 2030 and evaluate the results following the change in some techno-economic data displayed in Table 4.1. Changes in input parameters include reduction of investment and operation costs of subcomponents and increase in cell stack lifetime and efficiency of the electrolyser and compressors. Moreover, the effect of change in energy prices and FCR remuneration were examined. After performing the first round of simulations, the maximum amount of optimised hourly FCR capacities were calculated 3 MW and 8 MW for 2020 and 2030, respectively. With increased FCR prices, this reached 10 MW. So, the following scenarios are presented:

(1) Case 1: 2020

- Scenario 1: Operation without FCR provision
- Scenario 2: Operation with optimal hourly FCR
- Scenario 3: Operation with constant FCR reserve, C^{FCR} = 3 MW

(2) Case 2: 2030

- Scenario 4: Operation without FCR provision
- Scenario 5: Optimal FCR reserves, 10% reduced FCR prices
- Scenario 6: Operation with optimal hourly FCR
- Scenario 7: Optimal FCR reserves, 10% increased FCR prices
- Scenario 8: Operation with constant FCR reserve, C^{FCR} = 8 MW

Considering the abovementioned scenarios, the electrolyser and other components were dimensioned, and HRS hourly operation was optimised to maximise the benefit by providing the hydrogen for the mobility sector, injecting the extra produced hydrogen into the natural gas system, and participating in the FCR market. The first part of the results focuses on the operational aspects of the HRS in various scenarios. The outputs of the

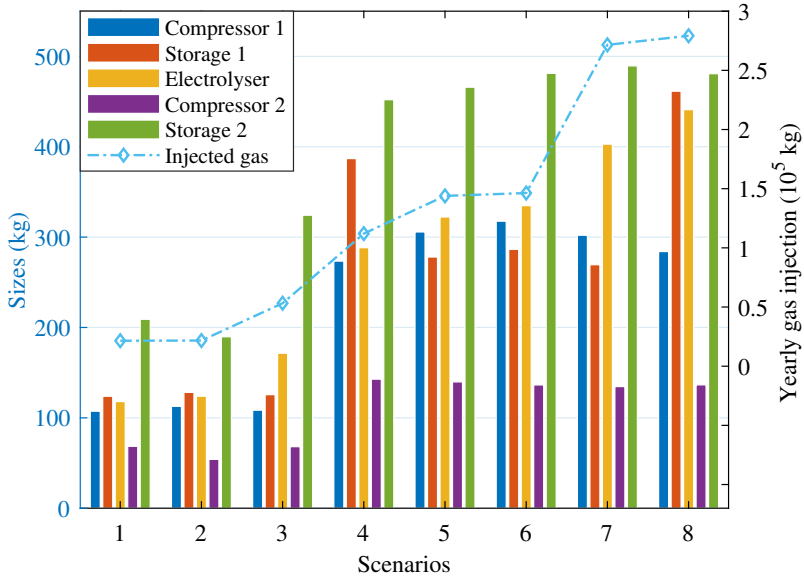

Figure 4.4: Optimised capacity of components and annual injected hydrogen to the gas grid.

simulation are the size of subcomponents, hourly FCR capacities, electrolyser dispatch, and hydrogen injection into the gas grid.

Fig. 4.4 shows the optimal sizes of the electrolyser, medium and high-pressure compressors, and storages for eight scenarios. All of the capacities were scaled to kg to be comparable with each other. Results prove that participation in the FCR market with higher reserve needs the higher size of the electrolyser, and as a result, more hydrogen will be injected into the gas grid compared to the scenarios with smaller capacities of the electrolyser. In the first and fourth scenarios, where the system does not participate in the FCR market, the lowest sizes of electrolyser 6.2 MW and 15.1 MW were obtained for 2020 and 2030, respectively. This increase in size (243%) reflects the increase in the amount of hydrogen demand. The maximum capacity of the electrolyser was obtained for scenario 8 (23.1 MW). The sizing of the hydrogen storages enables the possibility of storing excess produced hydrogen when electricity prices and/or hydrogen demand are low and using some amount of stored hydrogen when electricity prices or/and hydrogen demand are high so that the electrolyser operates at a lower electricity demand. Employing hydrogen storage enables the electrolyser to participate in the FCR provision with high availability as well. However, it should be

noted that there is a trade-off between the availability for the provision of grid services and storage capacity: an increase in the sizes of the storage and the electrolyser will improve availability but also increase HRS costs. Hence, the optimal size of components does not follow the same trend, as the model tries to minimise the investment costs, which increase for larger subcomponents. Hence, whereas from scenario 4 to scenarios 5 and 7, a larger electrolyser is required to deliver higher FCR capacities, a smaller storage ensures the minimum investment costs.

The excess hydrogen that was not used for the mobility sector, and could not be stored, was injected into the gas grid by the third compressor. The size of the third compressor follows the same trend as the electrolyser and hydrogen injection to the gas grid: from 119 kg capacity for scenario 1 to 415 kg for scenario 8. Comparing scenario 7 to scenarios 5 and 6 shows a strong difference for the injected hydrogen to the natural gas grid. That sharp rise after a +10% FCR price change could be explained by the fact that the optimum FCR capacity increases from 8 MW to 10 MW and also the number of hours that the electrolyser works at the maximum FCR capacity increases as a result of the FCR price increase, whereas with a -10% change in FCR price, the number of hours working at the maximum of 8 MW FCR capacity is decreased. Hence, following the larger FCR capacity and working more hours to provide the maximum FCR capacity, the size of the electrolyser and consequently the hydrogen production will increase. This will cause more hydrogen injection to the natural gas grid while the hydrogen demand from the mobility is not changed.

In a situation where there is no strict hydrogen demand, the electrolyser runs at nominal power as long as the difference between the price of electricity and equivalent price of selling hydrogen is high enough to cover equipment losses and investment costs. But for the proposed system in this study that should meet hourly hydrogen demand, the situation is different. In addition to the price of electricity and hydrogen, hourly hydrogen demand, the size of storages, FCR prices, and hourly FCR capacities affect the optimal dispatch of the electrolyser and hydrogen production. All these parameters form a multi-dimensional optimisation problem, in which even at some hours with low electricity price the electrolyser works at low power levels because the hydrogen demand is low or the storages are full, or the electricity price is lower at next hours and the operator prefers to fill the storages at lower electricity prices. It should also be considered that at some hours, the revenue from consumption adjustment for FCR provisions exceeds the benefit of arbitrage trading.

Based on the electricity price time series, grid frequency, and hydrogen demand and its price, the optimal electrolyser dispatch considering cross-

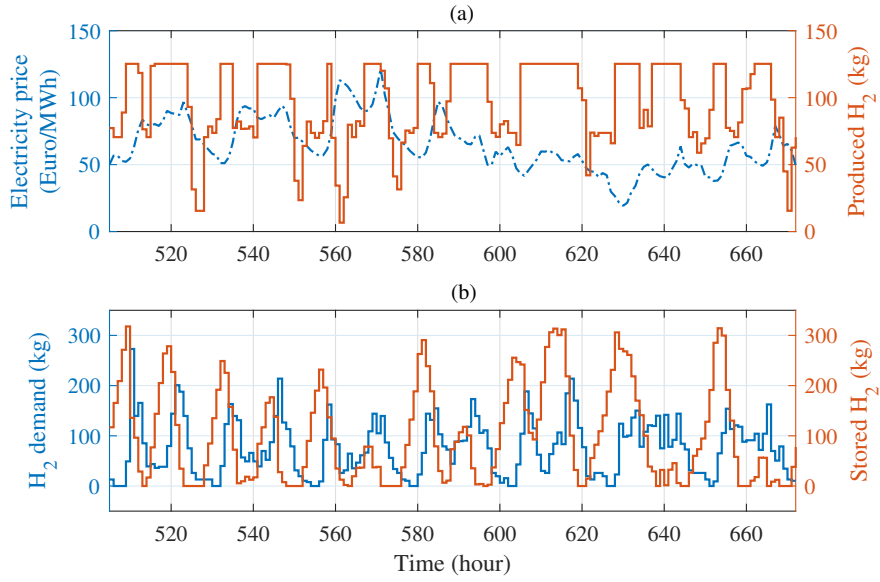

Figure 4.5: Scenario 2- Electrolyser dispatch, hydrogen demand and storage state

commodity arbitrage trading and FCR provision were obtained. The hydrogen production curves are revealed as the orange line in Fig. 4.5 (a) and Fig. 4.6 (a), while the electricity price data can be found as the blue line. The stored hydrogen is shown by the orange line in Fig. 4.5 (b) and Fig. 4.6 (b), while the hydrogen demand (demand from mobility sector plus injection to the gas grid) can be found as the blue line. Figures are given for the fourth week of 2020 and 2030.

The optimal sizing of the hydrogen storages and compressors alongside the electrolyser forms a multi-period MINLP problem and allows the electrolyser to participate in the FCR market with high availability. The HRS operator uses the spare capacity for FCR provision in hours that are not profitable for cross-commodity arbitrage trading. As stated before, the electrolyser produces a higher volume of hydrogen and part of the extra amount is stored in the storages when the electricity tariff is low, or benefit of up-FCR is higher than the costs of electricity purchase. This, in turn, allows the electrolyser to operate at lower power when the electricity tariff increases or the benefit of down-FCR is high enough to cover the revenue of cross-commodity arbitrage trading. At these hours, dispensers withdraw part of the hydrogen that was previously stored in the storages. Comparing subfigures (a) and (b) in Fig. 4.5 and 4.6 clearly shows that when the hydrogen demand is lower than hydrogen production, the system fills the

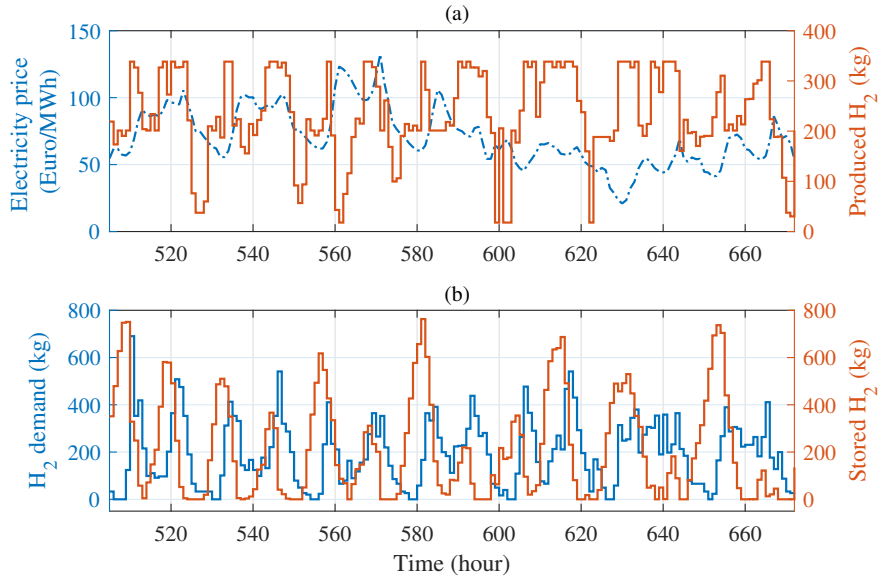

Figure 4.6: Scenario 6- Electrolyser dispatch, hydrogen demand and storage state

storages to withdraw hydrogen at hours with lower hydrogen production than hydrogen consumption.

For scenarios with constant FCR size in the whole year, the method focuses on an electrolyser employing cross-commodity arbitrage trading strategy while offering 3 MW and 8 MW reserve, either upward or downward. But, for scenarios considering FCR capacity optimisation, the FCR reserve is optimised on an hourly basis during the year. The optimal FCR hourly capacities are revealed as the orange line in Fig. 4.7 (a) and Fig. 4.8 (a) while the grid frequency can be found as the dashed blue line. For the sake of transparency, only the first two days of the fourth week of the year are plotted. To show how the HRS operator manages the electrolyser consumption to provide FCR service, the optimal electrolyser hourly electricity demand after responding to the frequency signals are revealed as the dashed orange line in Fig. 4.7 (b) and Fig. 4.8 (b) while the electrolyser baseline power before activating FCR service can be found as the blue line.

Fig. 4.9 shows the optimised FCR capacities and allotted number of hours to each of them in a year for the scenarios with optimal hourly FCR capacity calculation. Comparing scenario 2 with the other three shows that increase in hydrogen demand, which is reflected in the electrolyser size, as previously shown in Fig. 4.4, increases the maximum FCR capacity. The results of scenario 7 show that 10% increase in FCR revenue payment can

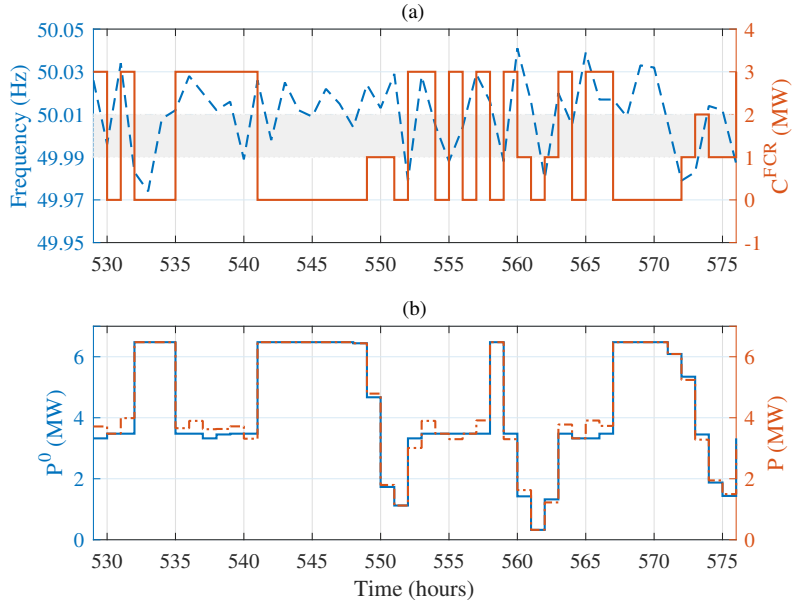

Figure 4.7: Scenario 2- Frequency, FCR capacity, optimal electrolyser demand

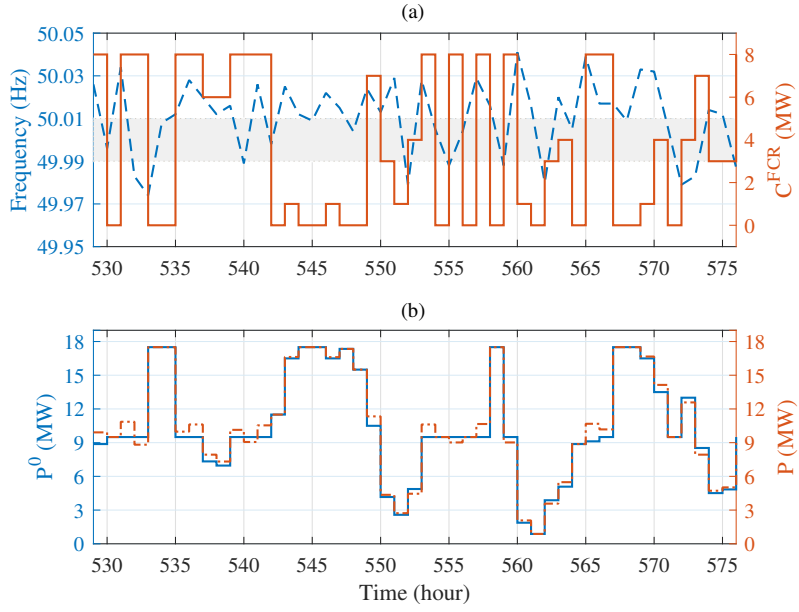

Figure 4.8: Scenario 6- Frequency, FCR capacity, optimal electrolyser demand

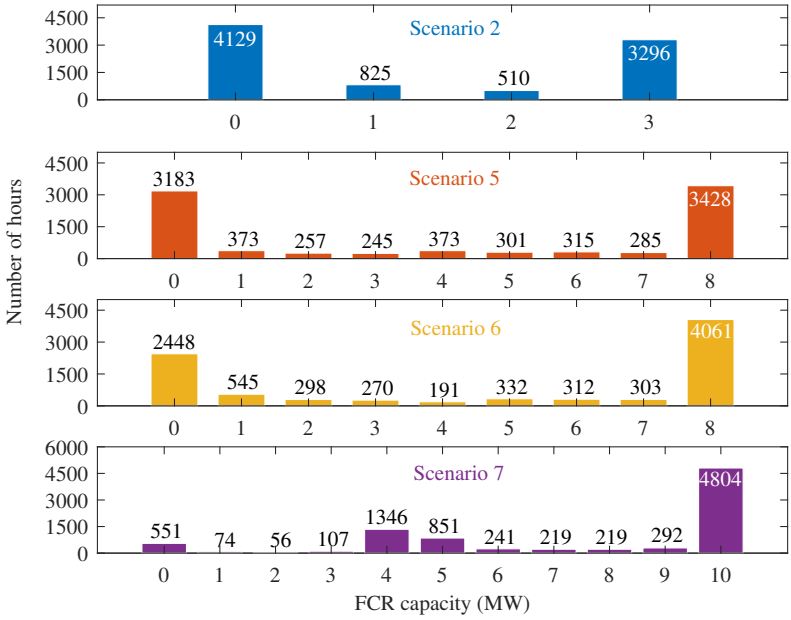

Figure 4.9: Distribution of optimal hourly FCR capacities

compensate for the higher investment costs as a result of the larger size of components. This increase in FCR remuneration price raises the number of hours allotted to maximum FCR capacity and lowers the number of hours allotted to zero FCR capacity.

It is notable that while the maximum size of the FCR capacity in scenario 7 goes up to 10 MW, the size of the electrolyser for this scenario is lower than the one for scenario 8 where an FCR capacity of 8 MW is considered. It is because in scenario 7, the electrolyser participates optimally with high capacities when the base line load is low or when the system should activate down-FCR and, as a result, the size of the electrolyser does not increase too much. This scenario proves the necessity of optimal FCR reserve calculation.

The second part of the results focuses on the economic aspects of the HRS in various scenarios. Tables 4.2 and 4.3 summarise the obtained costs and revenues in various scenarios. Costs related to the HRS system (investment, operation and replacement costs) and grid costs (GC) account for 23-27% and 18-24% of the total annual costs, respectively. Costs linked to electricity costs (EC) despite grid costs are considerably high, varying from

48% of total annualised costs in scenario 3 to 58% in scenario 4. While the size of equipment increases in 2030, the share of costs related to the HRS system remains constant or decreases, because of the lower per-unit investment costs and higher efficiency. Higher efficiency causes lower relative energy consumption per kilogram of the produced hydrogen.

Table 4.2 shows that the impact of participating in the FCR market on the annual costs is directly linked to the size of power reserved for this service. In 2020, a 2% increase in the total cost is observed when assigning optimal hourly capacities, while the total costs increase by 15% when the electrolyser reserves a constant capacity of 3 MW for frequency regulation. In 2030, this increase reaches around 5% for assigning optimal hourly capacities and 17% considering a constant capacity of 8 MW for the FCR service. This difference can be explained by the increase of grid costs, electricity costs, and investment costs because of the higher size of the electrolyser and other subcomponents. It is also noteworthy that compared to 2020, in 2030, the share of grid costs decreased while the share of electricity costs increased. The nonlinear behaviour of the grid cost simulator is then one of the reasons for the reduction in the share of grid costs.

The last row in Table 4.2 shows that the exemption from charges related to tax and public service obligation is vital for economic efficiency of the HRS as the share of tax and public service obligation costs is between 7% to 15% for different scenarios. Besides, significant reductions in power prices are necessary because of their undeniable influence on the economic feasibility of the system.

Table 4.3 shows the total revenues and the share of different sources of revenues, assuming the hydrogen price of 5 €/kg. While the contribution of selling hydrogen to the gas grid (GR) is not very promising, the share from participation in FCR (FASR) is notable, varying from 6.3% in scenario 5 to 10.7% in scenario 7. It is also noteworthy that in the case of ancillary service provision, the total annual revenue can be increased by 12% in 2020 and by 16% in 2030 compared to the scenarios that do not consider FCR provision. However, the crucial factor is to receive sufficient compensation from selling hydrogen, which depends on the hydrogen demand and its selling price.

As stated before, optimisations have been performed to maximise the annual benefits, and consequently, minimise the hydrogen break-even price. Fig. 4.10 illustrates the hydrogen break-even price, costs, and revenues for different scenarios. Comparison of the results of 2020 and 2030 shows that in 2030, the total annual costs and revenues increase notably with the growing demand of hydrogen, while the break-even price of hydrogen decreases due to the increasing gap between revenues and costs. In 2030,

Table 4.2: Components of annual costs (€)

Scenario	**1**	**2**	**3**	**4**	**5**	**6**	**7**	**8**
TAC	3,151,034	3,207,488	3,614,342	6,828,946	7,072,804	7,152,739	7,716,413	8,019,127
GC	718,766	736,176	875,679	1,218,383	1,318,131	1,355,030	1,554,543	1,666,635
	23%	23%	24%	18%	19%	19%	20%	21%
EC	1,631,840	1,648,558	1,737,113	3,994,487	4,030,872	4,032,344	4,241,397	4,366,329
	52%	51%	48%	58%	57%	56%	55%	54%
IC	783,110	805,457	983,320	1,573,411	1,680,936	1,722,383	1,874,865	1,940,095
	25%	25%	27%	23%	24%	24%	24%	24%
TAC w/o tax	2,729,721	2,783,720	3,068,287	6,337,189	6,566,977	6,641,707	7,109,294	7,195,518

Table 4.3: Components of annual revenues (€)

Scenario	**1**	**2**	**3**	**4**	**5**	**6**	**7**	**8**
TAR	3,327,539	3,553,739	3,710,708	8,535,145	9,167,271	9,274,541	9,870,388	9,726,653
GR	32,281	32,521	79,830	198,316	254,702	258,993	480,652	494,230
	1%	0.9%	2.2%	2.3%	2.8%	2.8%	4.8%	5.1%
MR	3,285,065	3,285,065	3,285,065	8,311,215	8,311,215	8,311,215	8,311,215	8,311,215
	99%	92.4%	88.5%	97.4%	90.7%	89.6%	84.2%	85.5%
FASR	0	225,972	335,081	0	575,619	678,528	1,051,132	893,549
	-	6.4%	9.0%	-	6.3%	7.3%	10.7%	9.2%

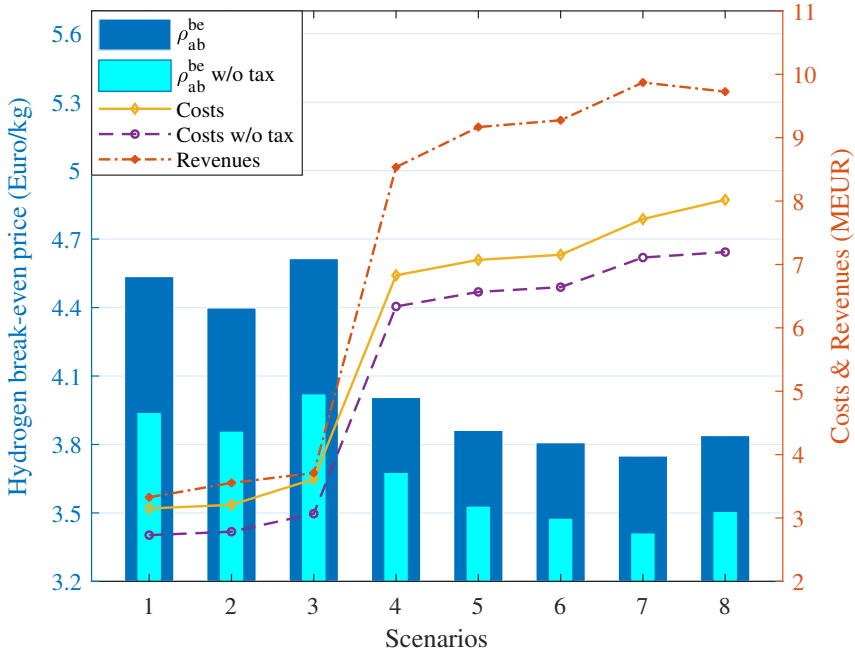

Figure 4.10: Costs, revenues, and hydrogen break-even prices

the combined effect of lower investments per unit capacity, more space for participation in FCR market, and selling hydrogen in a broader scale will make the operation of an HRS more economically effective with a lower hydrogen break-even price. Scenarios 5 and 7 considered the modification of the FCR price in 2030, where it was set to 90% and 110% of the price in 2020, respectively. As illustrated in Fig. 4.10, the effect is pretty significant compared to scenario 6 with an FCR price equal to the one in 2020, where the hydrogen break-even price was 3.74 €/kg. The price increases to 3.80 €/kg in scenario 5 and reduces to 3.68 €/kg in scenario 7. A comparison was also made between the hydrogen break-even price with and without considering tax and levies in the grid costs calculation. Exemption from tax and public service obligations amounts to an 8 to 17% reduction in hydrogen price compared to the situation where tax is included.

4.4.2 Comparing the current situation with targets

This section explains and compares the simulation results considering the current situation with the outcomes of simulations assuming the hydrogen targets for Belgium in 2020. Although it was planned to have 1000 fuel cell electric vehicles (FCEV) and 50 hydrogen-powered buses on the road by the end of 2020, the number of active FCEVs and hydrogen buses by September 2020 have been 48 and 5, respectively. Thus, in this section, the hydrogen demand is modified accordingly. For this situation, the introduced method is implemented in three scenarios and evaluates the techno-economic feasibility of the HRS. After performing the first round of simulations, the maximum amount of optimised hourly FCR capacity was calculated to be 1 MW. So, the following scenarios are presented:

- Scenario R1: Operation without FCR provision
- Scenario R2: Operation with optimal hourly FCR
- Scenario R3: Operation with maximum constant FCR reserve at all hours, C_{FCR} = 1 MW

Fig. 4.11 shows the optimal sizes of the components (C1-C2: Compressors, S1-S2: Storages, E: Electrolyser) for the three mentioned scenarios. Similar to Section 4.4.1, results illustrate that participation in the FCR market needs a larger electrolyser, and as a result, more hydrogen will be

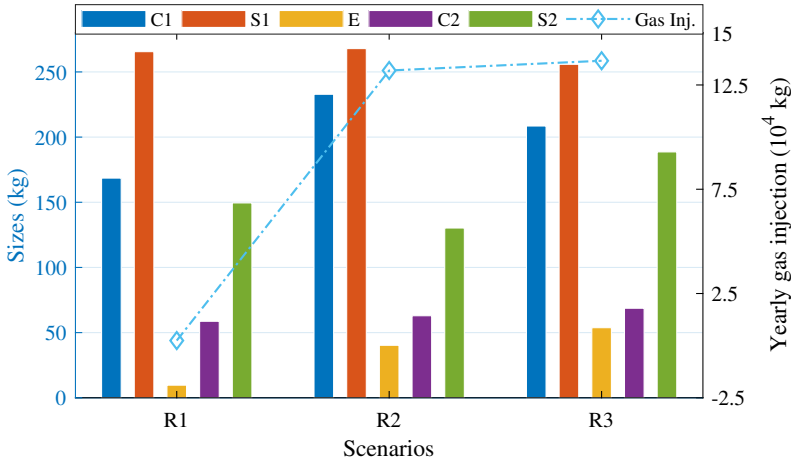

Figure 4.11: Optimised capacity of components and annual injected hydrogen to the gas grid for current situation in 2020

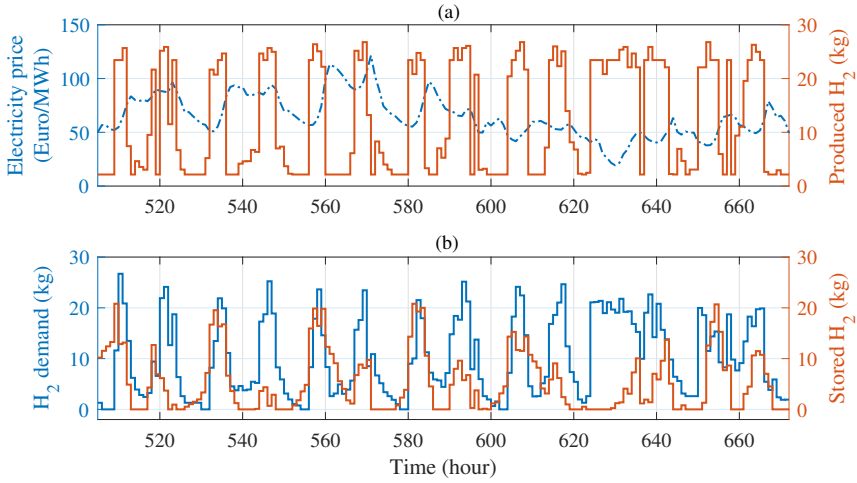

Figure 4.12: Electrolyser dispatch, hydrogen demand and storage state for situation in 2020

injected into the gas grid. In scenario R1, where the system does not participate in the FCR market, the smallest size of the electrolyser, 506 KW, was obtained. The optimal capacity of the electrolyser for scenarios R2 and R3 is 2.1 MW and 2.8 MW, respectively. The sizing results clarify the significant effect of lower demand from the mobility sector on the sizing of the components.

The optimal electrolyser dispatch considering the electricity price time series, grid frequency for FCR provision, and hydrogen demand were obtained. The hydrogen production curves are depicted by an orange line in Fig. 4.12 (a), while the electricity price data can be found as the blue line. The stored hydrogen is shown by the orange line in Fig. 4.12 (b), while the hydrogen demand (demand from mobility sector plus injection to the gas grid) can be found as the blue line.

For scenario R2 considering the FCR capacity optimisation, the FCR reserve is calculated on an hourly basis during the year. In this scenario, the electrolyser is scheduled to participate in the reserve market with 1 MW capacity for 6728 hours while in the remaining 2032 hours it works with an FCR capacity of zero. Compared to the results from Section 4.4.1, it is clear that hydrogen demand reduction has decreased the maximum capacity of the reserve to participate in the FCR market.

To focus on the economic aspects, Table 4.4 summarises the obtained costs and revenues in scenarios R1-R3. Investment and grid costs account for 29-32% and 19-28% of the total annual costs, respectively. Electricity

Table 4.4: Costs and revenues for current conditions (€)

Scenario	R1	R2	R3
GC	62,459	172,436	224,188
EC	159,190	255,899	389,963
IC	103,262	182,976	249,508
TAC w/o tax	288,236	513,329	729,947
GR	3,657	197,895	204,904
MR	265,300	265,300	265,300
FASR	0	99,110	111,694
ρ_{ab}^{be} (€/kg)	6.1	5.9	8.3
ρ_{ab}^{be} w/o tax (€/kg)	5.3	4.0	6.2

costs despite grid costs varying from 42% of total annualised costs in scenario 2 to 49% in scenario 1. These results show a small increase in the share of investment and grid costs and a decrease in the share of electricity costs compared to the results in Section 4.4.1. From the revenue point of view, in scenarios R2 and R3, the contribution of selling hydrogen to the gas grid and participation in FCR is notable, 35% and 19%, respectively. This increase compared to Section 4.4.1 shows how the electrolyser operator could use the proposed algorithm to increase the share of revenues from the gas grid and FCR market when the hydrogen demand from the mobility sector is low.

The last two rows in Table 4.4 illustrate the hydrogen break-even price for different scenarios. The lowest prices were obtained for scenario R2, where the electrolyser participate optimally in the reserve market. Increase in these prices illustrates how important the amount of hydrogen demand is for HRS owners. While the obtained prices have increased compared to prices in Section 4.4.1, HRS operators could still benefit from selling hydrogen as long as the margin with the selling price of hydrogen is enough.

4.5 Summary and conclusions

Considering the role of hydrogen in mitigating GHG emissions and supporting the security of future power systems mentioned in Chapter 3, this chapter studied the operation of a $P2H_2$ plant equipped with a PEMEL that provides flexibility to the grid by adjusting its electricity consumption. This study investigated the implications of providing primary frequency reserve on the design and operation of $P2H_2$ systems, specifically for an HRS. An

optimisation method was presented to evaluate the techno-economic feasibility of the HRS. The model optimised both the size and hourly operation of the subcomponents to perform an energy arbitrage in electricity, natural gas, hydrogen, and FCR markets.

The results revealed that the operational costs depend extremely on electricity price and grid costs, which are directly associated with the size of the electrolyser. Hence optimal sizing of components and exemptions from tax and levies or other components of grid costs are essential to reach economic viability.

Up to 19% contribution in revenues from FCR provision proved the possibility of participation in regulation markets as a promising opportunity to minimise hydrogen price for the mobility sector.

In addition to FCR revenues, higher hydrogen demand, higher efficiency of components, and lower capital and operation costs can reduce the break-even price of hydrogen. The calculations in different scenarios show that the minimum hydrogen break-even price in 2020 will be 4.40 €/kg, while mobility users will be able to refuel their vehicles for 3.75 €/kg at the station in 2030. Comparing the break-even price for current conditions with the value obtained according to the Belgium hydrogen targets proved the significant effect of hydrogen demand from the mobility sector on the profitability of an HRS.

The explained method could be used to determine optimal investment plans, and HRS operators together with grid operators could benefit from the offered method to schedule the electrolyser in a way that meets the hydrogen demand, and provide FCR simultaneously. The obtained results demonstrated that the proposed methodology is generic and scalable enough to deal with various amounts of hydrogen demand. The optimisation algorithm is able to optimise any cases with different hydrogen demand for the real or forecasted situation.

While this chapter examined the impact of FCR provision on the investment and operation strategies in an HRS, the implications of providing other FASs, including aFRR and mFRR, need to be studied. The uncertain behaviour of hydrogen demand and capacity market prices should be considered in the modelling as well. Thus, Chapter 5 will propose a probabilistic optimisation method for optimal sizing and the flexible operation of a $P2H_2$ plant, considering different scheduling strategies for various FASs, i.e., the FCR, aFRR, and mFRR.

References

[1] A. Dadkhah, D. Bozalakov, J. D. M. De Kooning, and L. Vandevelde. *On the optimal planning of a hydrogen refuelling station participating in the electricity and balancing markets*. International Journal of Hydrogen Energy, 46(2):1488–1500, 2021.

[2] *CO_2 emission performance standards (2020 onwards)*. [Online, accessed 13 March 2020]: `https://ec.europa.eu/clima/policies/transport/vehicles/regulation_en`.

[3] N. Chrysochoidis-Antsos, M. R. Escudé, and A. J. M. van Wijk. *Technical potential of on-site wind powered hydrogen producing refuelling stations in the Netherlands*. International Journal of Hydrogen Energy, 45(46):25096–25108, 2020.

[4] D. Apostolou, P. Enevoldsen, and G. Xydis. *Supporting green Urban mobility–The case of a small-scale autonomous hydrogen refuelling station*. International Journal of Hydrogen Energy, 44(20):9675–9689, 2019.

[5] F. Grüger, O. Hoch, J. Hartmann, M. Robinius, and D. Stolten. *Optimized electrolyzer operation: Employing forecasts of wind energy availability, hydrogen demand, and electricity prices*. International Journal of Hydrogen Energy, 44(9):4387–4397, 2019.

[6] F. Carr, S.and Zhang, F. Liu, Z. Du, and J. Maddy. *Optimal operation of a hydrogen refuelling station combined with wind power in the electricity market*. International Journal of Hydrogen Energy, 41(46):21057–21066, 2016.

[7] S. Riedl. *Development of a hydrogen refueling station design tool*. International Journal of Hydrogen Energy, 45(1):1–9, 2020.

[8] H. Kim, M. Eom, and B. Kim. *Development of strategic hydrogen refueling station deployment plan for Korea*. International Journal of Hydrogen Energy, 45(38):19900–19911, 2020.

[9] Y. Li, F. Cui, and L. Li. *An integrated optimization model for the location of hydrogen refueling stations*. International Journal of Hydrogen Energy, 43(42):19636–19649, 2018.

[10] I. Iordache, D. Schitea, and M. Iordache. *Hydrogen refueling station infrastructure roll-up, an indicative assessment of the commercial vi-*

ability and profitability. International Journal of Hydrogen Energy, 42(8):4721–4732, 2017.

[11] Ch. He, H. Sun, Y. Xu, and S. Lv. *Hydrogen refueling station siting of expressway based on the optimization of hydrogen life cycle cost*. International Journal of Hydrogen Energy, 42(26):16313–16324, 2017.

[12] R. P. Micena, O. R. Llerena-Pizarro, T. M. de Souza, and J. L. Silveira. *Solar-powered Hydrogen Refueling Stations: A techno-economic analysis*. International Journal of Hydrogen Energy, 45(3):2308–2318, 2020.

[13] P. Hou, P. Enevoldsen, J. Eichman, W. Hu, M. Z. Jacobson, and Z. Chen. *Optimizing investments in coupled offshore wind-electrolytic hydrogen storage systems in Denmark*. Journal of Power Sources, 359:186–197, 2017.

[14] M. Kim and J. Kim. *An integrated decision support model for design and operation of a wind-based hydrogen supply system*. International Journal of Hydrogen Energy, 42(7):3899–3915, 2017.

[15] T. Mayer, M. Semmel, M. A. Morales, K. M. Schmidt, and J. Bauer, A.and Wind. *Techno-economic evaluation of hydrogen refueling stations with liquid or gaseous stored hydrogen*. International Journal of Hydrogen Energy, 44(47):25809–25833, 2019.

[16] H. Sun, C. He, X. Yu, M. Wu, and Y. Ling. *Optimal siting and sizing of hydrogen refueling stations considering distributed hydrogen production and cost reduction for regional consumers*. International Journal of Energy Research, 43(9):4184–4200, 2019.

[17] F. Grüger, L. Dylewski, M. Robinius, and D. Stolten. *Carsharing with fuel cell vehicles: Sizing hydrogen refueling stations based on refueling behavior*. Applied Energy, 228:1540–1549, 2018.

[18] H. Aki, I. Sugimoto, T. Sugai, M. Toda, M. Kobayashi, and M. Ishida. *Optimal operation of a photovoltaic generation-powered hydrogen production system at a hydrogen refueling station*. International Journal of Hydrogen Energy, 43(32):14892–14904, 2018.

[19] P. Larscheid, L. Lück, and A. Moser. *Potential of new business models for grid integrated water electrolysis*. Renewable Energy, 125:599–608, 2018.

[20] L. Allidières, A. Brisse, P. Millet, S. Valentin, and M. Zeller. *On the ability of PEM water electrolysers to provide power grid services*. International Journal of Hydrogen Energy, 44(20):9690–9700, 2019.

[21] B. Guinot, F. Montignac, B. Champel, and D. Vannucci. *Profitability of an electrolysis based hydrogen production plant providing grid balancing services*. International Journal of Hydrogen Energy, 40(29):8778–8787, 2015.

[22] A. Dadkhah, D. Bozalakov, J. D. M. De Kooning, and L. Vandevelde. *Optimal Sizing and Economic Analysis of a Hydrogen Refuelling Station Providing Frequency Containment Reserve*. In 2020 IEEE International Conference on Environment and Electrical Engineering and 2020 IEEE Industrial and Commercial Power Systems Europe (EEEIC/I&CPS Europe), 2020.

[23] M. Kopp, D. Coleman, Ch. Stiller, K. Scheffer, J. Aichinger, and B. Scheppat. *Energiepark Mainz: Technical and economic analysis of the worldwide largest Power-to-Gas plant with PEM electrolysis*. International Journal of Hydrogen Energy, 42(19):13311–13320, 2017.

[24] G. Matute, J. M. Yusta, and L. C. Correas. *Techno-economic modelling of water electrolysers in the range of several MW to provide grid services while generating hydrogen for different applications: A case study in Spain applied to mobility with FCEVs*. International Journal of Hydrogen Energy, 44(33):17431–17442, 2019.

[25] M. Honselaar, G. Pasaoglu, and A. Martens. *Hydrogen refuelling stations in the Netherlands: An intercomparison of quantitative risk assessments used for permitting*. International Journal of Hydrogen Energy, 43(27):12278–12294, 2018.

[26] D. Thomas, D. Mertens, M. Meeus, W. van der Laak, and I. Francois. *Power-to-Gas Roadmap for Flanders*. [Online, Accessed Dec. 2019]: `https://www.waterstofnet.eu/_asset/_public/powertogas/P2G-Roadmap-for-Flanders.pdf`, 2016.

[27] A. Mayyas and M. Mann. *Manufacturing competitiveness analysis for hydrogen refueling stations*. International Journal of Hydrogen Energy, 44(18):9121–9142, 2019.

[28] A. Buttler and H. Spliethoff. *Current status of water electrolysis for energy storage, grid balancing and sector coupling via power-to-gas and power-to-liquids: A review*. Renewable and Sustainable Energy Reviews, 82:2440–2454, 2018.

[29] K. Poncelet. *Long-term energy-system optimization models-Capturing the challenges of integrating intermittent renewable energy sources and assessing the suitability for descriptive scenario analyses, PhD thesis, KU Leuven, Belgium*. 2018.

[30] Elia. *Keeping the Balance*. [Online, Accessed Jun 2020]: https://www.elia.be/en/electricity-market-and-system/system-services/keeping-the-balance.

[31] *FCR design note*. [Online, Accessed Jun. 2021]: https://tinyurl.com/yx3vu5z7, Apr. 2019.

[32] *Hydrogen Leakage: A Potential Risk for the Hydrogen Economy*. [Online]: https://tinyurl.com/3kb4ntr2.

[33] *Scientists warn against global warming effect of hydrogen leaks*. [Online]: https://tinyurl.com/4ca9cp3m.

[34] O. Schmidt, A. Gambhir, I. Staffell, A. Hawkes, J. Nelson, and Sh. Few. *Future cost and performance of water electrolysis: An expert elicitation study*. International Journal of Hydrogen Energy, 42(52):30470–30492, 2017.

[35] Ø. Ulleberg and R. Hancke. *Techno-economic calculations of small-scale hydrogen supply systems for zero emission transport in Norway*. International Journal of Hydrogen Energy, 45(2):1201–1211, 2020.

[36] *Development of Business Cases for Fuel Cells and Hydrogen Applications for Regions and Cities*. [Online, accessed 7 September 2019]: https://www.fch.europa.eu/sites/default/files/FCH%20Docs/171121_FCH2JU_Application-Package_WG5_P2H_Hydrogen%20into%20gas%20grid%20%28ID%202910558%29%20%28ID%202911642%29.pdf.

[37] *EPEX spot market*. [Online, accessed 17 December 2019]: https://www.epexspot.com/en.

[38] Elia. *Data download*. [Online]: https://www.elia.be/en/grid-data/data-download-page?csrt=14870108954399801490.

[39] W. van der Laak, A. Mertens, S. Neis, and J. Proost. *National Implementation Plan, Hydrogen Refuelling Infrastructure Belgium*. Technical Report, WaterstofNet, (2015).

[40] *European alternative fuels observatory*. [Online]: `https://www.eafo.eu/`, Accessed 26 September 2020.

[41] D. Parra and M. K. Patel. *Techno-economic implications of the electrolyser technology and size for power-to-gas systems*. International Journal of Hydrogen Energy, 41(6):3748–3761, 2016.

5

Opportunities for $P2H_2$ systems to provide FCR, aFRR & mFRR

Given the technical characteristic of PEMELs, the $P2H_2$ systems can play a key role in accelerating the transition toward a low-carbon economy. They can offer new forms of flexibility using their storage and fast adjustable consumption capabilities. Thus, the design of novel optimisation algorithms will become necessary to facilitate the flexible operation of hydrogen plants while assuring secure investment in such facilities. Chapter 4 investigated the effects of providing FCR by electrolysers on the investment and operational strategies in an HRS. Still, the implications of providing other frequency ancillary services (FAS), including aFRR and mFRR need to be studied. The uncertain behaviour of hydrogen demand and capacity market prices should be considered in the modelling as well. Thus, this chapter proposes a probabilistic optimisation method for optimal sizing and the flexible operation of a $P2H_2$ plant. The test system is coupled with electricity, natural gas, and industrial hydrogen networks while supplying the mobility sector with hydrogen. Different scheduling strategies for various FAS, i.e., the FCR, aFRR, and mFRR, are compared in terms of power adjustment, the influence on costs and revenues and the final hydrogen break-even price. The rest of this

chapter is structured as follows: Section 5.1 reviews the literature and presents the novelty of this chapter to cover the research gap. The test system and the proposed model are introduced in Section 5.2. Numerical studies are represented in Section 5.3. Finally, Section 5.4 summarises the main conclusions. The content of this chapter has been published in [1, 2].

Techno-Economic Analysis and Optimal Operation of a Hydrogen Refueling Station Providing Frequency Ancillary Services

Akbar Dadkhah, Dimitar Bozalakov, Jeroen D.M. De Kooning and Lieven Vandevelde

Published in IEEE Transactions on Industry Applications, 2022
DOI: 10.1109/TIA.2022.3167377

Abstract: *Following the urgency of climate change issues, investments in renewable energy sources and electrification of the transportation sector have increased to facilitate the transition to a more sustainable future. However, as renewable resources like wind parks are replacing conventional power plants, new balancing solutions are required to strengthen grid stability. As responsive loads with quick dynamics, electrolysers operating in HRSs can present flexible balancing services to the power grid. To exploit this benefit, this work examines the techno-economic features of providing different frequency grid services by an HRS, considering the possibility of hydrogen injection into the industrial and natural gas pipelines. The ratings of the subcomponents and dispatch plans are optimised to enhance the performance of the plant. A probabilistic mixed-integer linear programming problem is solved over one year with a time resolution of one hour and using real-world historical data based on the European electricity market. Simulation results indicate that economic profits can be increased significantly as a result of participating in the ancillary service markets and meeting the HRS specifications while stable performance is guaranteed.*

5.1 Introduction

As a connection between electricity and commodity markets, the Power-to-Hydrogen ($P2H_2$) concept has a great potential to convert sustainable electricity into sustainable hydrogen for different applications such as mobility and industry. In such a concept, electrolysis is the most well-known method for hydrogen production, where electricity is used to split water into hydrogen and oxygen [1]. The produced hydrogen can be deposited in tanks for later use and facilitates the flexible operation of different sectors [3]. Plenty of publications have already reviewed $P2H_2$ projects and their techno-economic performance [4, 5]. Some lately announced projects suggest hydrogen injection into the natural gas grid or the use of green hydrogen in industries [6]. Hydrogen usage in transportation is also growing, yet HRSs account for a low percentage of filling stations, as their economic profitability is still not sufficiently clear. The present selling cost of hydrogen has been reported around €7-10 [7, 8]. To make fuel cells com-

petitive with batteries as a power source for electric vehicles by 2030, the selling cost of hydrogen should go below €4-5. Hence, different feasible routes should be investigated to reduce the present high selling prices. Refs. [9–11] have investigated scheduling models to decrease hydrogen generation costs in HRSs connected to wind parks and small wind turbines.

Apart from selling hydrogen to vehicles, HRS operators could look for a promising source of extra revenue by providing flexibility to the power system, where growing penetration of intermittent renewable sources has raised the challenge of frequency deviations [12]. In response, grid operators have to let new frequency service providers support the grid stability [13]. A great deal of research has been performed on the provision of frequency grid services by various technologies. Ref. [14] has introduced a control design for the provision of FASs, where the ramping capacity of photovoltaic systems has been employed to enhance system security. In [15], a secondary frequency reserve provision method was offered for a system comprising of a wind turbine and a photovoltaic array. The authors have reviewed the strategies for the charging of electric vehicles participating in FAS markets [16, 17]. Ref. [18] has analysed the possibility of improving frequency stability by a supercapacitor in an energy system with a high share of renewables. An economic model has been presented in [19] to study the profitability of the provision of frequency services by batteries.

P2G and HRSs have also been considered as a source of flexibility in some papers. A control system has been realised in [20, 21] to optimise hydrogen production and ensure the stable operation of the electricity grid using electrolysers. An optimisation technique has been presented in [22] to design the integration patterns of Hydrogen-Power systems and to guide the planning of HRSs. A scheduling scheme has been introduced in [23] to increase the flexibility of energy systems, where the excess wind power is converted into natural gas, i.e. P2G. Ref. [24] has investigated the operation of a chlor-alkali process considering a short-term price forecast for the delivery of FCR. The economic viability of the FCR provision using a 25 MW electrolyser has been studied in [25]. Ref. [26] has looked at the technical ability of electrolysers in providing grid services. Yet, the economic aspects have not been elaborated. The operation of HRSs has been examined in [1] and [27], considering the FCR provision. However, the provision of aFRR and mFRR has not been studied.

Refs. [28, 29] have introduced scheduling models for the operation of hydrogen storages and fuel cells with predefined sizes to serve both the transport sector and the regulation market. It should be pointed out that hydrogen production by electrolysis and using a fuel cell to reconvert the stored hydrogen into electricity might not be economically feasible for grid-

connected systems. This is due to the relatively low-efficient process (30-50%) of double energy conversion [30]. Provision of secondary reserve with regulation steps of 1 MW has been analysed for a 5 MW electrolyser in [31]. However, it was assumed that the electrolyser was not used for other goals and remained shut off when no service signals were issued.

While electrolysers have a great potential in providing regulation services owing to their quick load flexibility in the order of a few seconds [32], providing FAS with electrolysers might face financial risks due to the high investment that might be needed. Hence, new approaches should consider sizing aspects of the HRSs to reduce the investment costs. The optimal ratings of the hydrogen production and storage units in HRSs for different fleet sizes of vehicles have been determined in [33]. Ref. [34] has introduced a sizing method for various components to maximise the net profit of hydrogen fueling stations.

5.1.1 Gap and contribution

While the operation of HRSs has been examined in literature, an applicable approach for the optimal planning and scheduling of multiple subcomponents considering the provision of FCR, aFRR, and mFRR services has not been adequately examined. Most recent studies have used predefined sizes for subcomponents or estimated the sizes according to the hydrogen demand. Then they looked at additional revenue stemming from the provision of grid services considering an average price for the service throughout the year. However, the average values do not reflect the weekly, daily, nor hourly variation of remuneration prices of FAS. As a result, the hourly scheduling of the electrolyser and other subcomponents and, consequently, total costs and revenues would be calculated based on an unrealistic average price. To employ and compare the potential of the plant in providing different FAS, their impact on both the operation and design of the HRS has to be included in the optimisation model. In particular and without loss of generality, this chapter presents the following contributions:

- A new optimisation model for the performance of an HRS considering the energy supply to hydrogen-powered vehicles, providing hydrogen as a feedstock for industry and hydrogen injection into the natural gas grid.
- Detailed operation mechanisms and optimisation constraints of FCR, aFRR, and mFRR are presented to compare all FAS from the techno-economic viewpoint. The model exploits the electrolyser potential to serve the grid considering real signals issued by the grid operator.

- Further, the offered model evaluates revenues versus investments and running expenses using real-world data. The economic feasibility of the investment in such a plant is further improved via optimal sizing of subcomponents acknowledging the effect of providing various grid services on the system rating.

- The uncertainty of the hydrogen demand and the price of grid services are embedded into the optimisation model to reflect the effect of uncertain parameters on the system operation. Based on this concept, the HRS might have different response behaviour according to the regulation signals, the price of grid services, the electricity price and the hydrogen demand.

5.2 Test system and model

The test system, illustrated in Fig. 5.1, is assumed to be located in the port of Zeebrugge in Flanders, Belgium. This area was picked because of the increasing wind capacity in the North Sea and the high number of industrial sites currently running in the region. An AC–DC converter, connected to the power grid, provides the electrolyser with electricity required for hydrogen production. The generated hydrogen, after the compression stages, is stored in medium pressure (450 bar) and high pressure (900 bar) storage tanks to satisfy the hydrogen demand from the mobility sector. Heavy-duty vehicles like buses refuel at 350 bar, while passenger cars are filled at 700 bar. An industrial pipeline network, which connects Zeebrugge with the port of Antwerp, facilitates hydrogen transport across industrial clusters [35]. Hence, the extra produced hydrogen could be injected into this industry or the natural gas network via separate pipelines. The test system is a hybrid energy hotspot in which all the above-mentioned subcomponents are in close proximity.

While employing the entire potential of the plant for multiple applications can improve economic efficiency by accumulating revenue from various sources, new models have to be developed to optimise the planning and scheduling of the plant. However, this is a challenging task because of different factors: (i) While asymmetric frequency regulation is possible for aFRR and mFRR, the transmission system operator (TSO) expects symmetric FCR capacities. The electrolyser flexibility is also restricted by its technical capabilities and the hydrogen demand. Hence, coordination between the terms of providing grid services and meeting the hydrogen demand is a vital factor. (ii) As the HRS will receive remuneration to follow the TSO signals, a trade-off should be made between the regulation per-

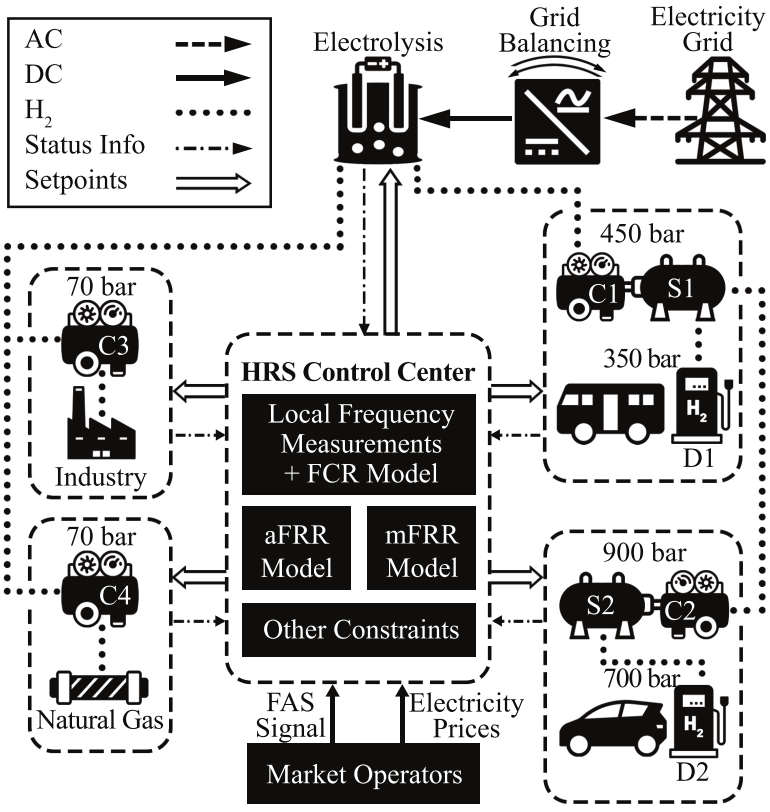

Figure 5.1: The studied HRS test system.

formance and the obtained revenues. (iii) The remuneration price of FAS and hydrogen demand from the mobility sector are among the uncertain parameters, which raise the complexity of the optimal scheduling. (iv) The model should define to which extent the HRS has to be redesigned to make the plant available for grid services while at the same time satisfying the hydrogen demand. So, how to size different subcomponents in the HRS remains to be answered. The model should also give a clear response on what the consequences of the possible redesign for the investment and operation costs of the plant are and to which extent the revenues from grid services will compensate these extra costs.

An optimisation model is developed to tackle the above-mentioned challenges and determine the optimal operation of the electrolyser. Considering detailed models of FCR, aFRR, and mFRR services, the electrolyser operator follows TSO signals while maximizing the economic opera-

tion of the plant to deal with challenges (i) and (ii). To take into account the stochastic behaviour of the considered uncertain parameters and solve challenge (iii), a normal distribution was used to generate 10 scenarios for each source of uncertainty. Then, 100 scenarios are produced by scenario combination. The optimal sizing of the plant solves challenge (iv) to find a balance between the availability of the system for grid balancing and the required size of subcomponents for a continued supply of the consumers.

5.2.1 Objective function

The proposed method in this work is meant to determine the maximum economic potential when optimally operating the system. Thus, the model attempts to maximise TAP by optimal sizing of subcomponents and flexible electrolyser operation considering the frequency regulation signals. The annual profits are measured as the difference between annual revenues and costs in (5.1), where s is the index for scenarios, h is the index for time steps and u is the index for different subcomponents. Based on the hydrogen sales to multiple sectors and revenues from the provision of grid services, annual revenues are calculated in the first line. Revenues from the mobility sector (terms 1 and 2) depend on the hydrogen prices (ρ_b and ρ_a) and hydrogen demands ($H^b_{h,s}$ and $H^a_{h,s}$) for buses and passenger cars, respectively. Additional possible revenues come from injecting hydrogen ($H^g_{h,s}$ and $H^i_{h,s}$) at the prices ρ_g and ρ_i into the natural gas network and industry (terms 3 and 4). While the remuneration of FCR covers only the remuneration for the reserved capacity, the compensations of aFRR and mFRR include the reservation payments, complemented with a payment for the activated energy (terms 5 and 6). The payment for the balancing capacity is the product of the remuneration price $\alpha_{h,s}$ times the contracted capacity $R_{h,s}$. The remuneration for the activated energy is the product of the absolute value of the activated energy $|\Delta P_{h,s}|$ multiplied by the service activation price $\beta_{h,s}$.

The cost of electricity bought from the grid is obtained in the second line as the product of the electricity price ρ^e_h times hourly electricity consumption of the electrolyser $P_{h,s}$, compressors and dispensers. The electricity consumption of compressor c is calculated by multiplying the compressed hydrogen in the compressor $C_{c,h,s}$ and the energy consumption per kg compressed hydrogen κ_{C_c}. The electricity consumption of dispensers is determined in the same way, where κ_{D_1} and κ_{D_2} are the energy efficiency of the dispensers. Annual costs for investment, replacement and operational expenditures of subcomponents are added to the function (third line), where C^u_s is the size of the subcomponent u, while $\mathrm{IC}^u_{\mathrm{pu}}$, $\mathrm{RC}^u_{\mathrm{pu}}$, and $\mathrm{OC}^u_{\mathrm{pu}}$

$$\begin{aligned}
\mathrm{TAP} = \sum_{s=1}^{100} \gamma_s \cdot \sum_{h=1}^{8784} \Big[& H^b_{h,s} \cdot \rho_b + H^a_{h,s} \cdot \rho_a + H^i_{h,s} \cdot \rho_i + H^g_{h,s} \cdot \rho_g + R_s \cdot \alpha_{h,s} + |\Delta P_{h,s}| \cdot \beta_{h,s} \Big] \\
& - \sum_{s=1}^{100} \gamma_s \cdot \sum_{h=1}^{8784} \left[P_{h,s} + H^b_{h,s} \cdot \kappa_{D_1} + H^a_{h,s} \cdot \kappa_{D_2} + \sum_{c=1}^{4} C_{c,h,s} \cdot \kappa_{C_c} \right] \cdot \rho^e_h \\
& - \sum_{u=1}^{9} \left[1.1 \cdot C^u_s \cdot (\mathrm{IC}^u_{\mathrm{pu}} + \mathrm{RC}^u_{\mathrm{pu}}) + C^u_s \cdot \mathrm{OC}^u_{\mathrm{pu}} \right]
\end{aligned} \tag{5.1}$$

are the per-unit investment, replacement and operation costs of subcomponent u, respectively. An extra 10% of the investment and replacement costs of subcomponents are assumed as the additional costs of installation, planning and preparation. The annual investment and operation costs for each subcomponent are calculated using the capital recovery factor [36].

While providing FAS needs short-term consideration, hydrogen production and storage can be optimised over a longer period. Thus, the management of these requirements is important in the optimisation model. On the one hand, the electrolyser responds to the issued FAS signals on an hourly basis considering constraints linked to the ancillary services. On the other hand, the produced hydrogen will be stored in hydrogen tanks for use in longer time frames considering hydrogen flow constraints.

5.2.2 Constraints linked to the ancillary services

The technical aspects of FAS have to be considered in the model in addition to the economic parts, which have been taken into account in (5.1). Considering the requirement that units with the ability to provide a minimum capacity of 1 MW are allowed to participate in the capacity market, (5.2a)-(5.5b) cover the specifications of FAS, including FCR, aFRR and mFRR.

FCR is implemented symmetrically according to the measured frequency signals. To allow the symmetric support, the power bounds must guarantee that the full contracted capacity can be activated in both directions (see (5.2a)). In other words, the loads participating in the FCR market with a contracted capacity of R_s have to be flexible to modify their baseline power $P^0_{h,s}$ over the $(P^0_{h,s} - R_s)$ to $(P^0_{h,s} + R_s)$ range [37]. An FCR provider has to activate the reserved capacity in less than 30 seconds. Thus, to meet the fast dynamics requirement of FCR, the electrolyser should not be turned off: (5.2a) implies that the electrolyser is always running between 5 and 100% of its nominal power. The power to be delivered according to the changes in grid frequency is shown in (5.2b) [37]. The electrolyser delivers the reserved capacity R_s proportionally to the change in frequency, where at a deviation of 200 mHz, the total reserved capacity is released.

$$0.05 \cdot C^E_s + R_s \leq P^0_{h,s} \leq C^E_s - R_s \tag{5.2a}$$

$$\Delta P_{h,s} = \begin{cases} 0, & |\Delta f_h| \leq 0.01 \text{ Hz} \\ (\Delta f_h - 0.01) \cdot \frac{R_s}{0.2}, & 0.01 \text{ Hz} < |\Delta f_h| \leq 0.2 \text{ Hz} \\ R_s, & |\Delta f_h| > 0.2 \text{ Hz} \end{cases} \tag{5.2b}$$

In (5.2a), C_s^E is the electrolyser optimal capacity, and Δf_h is the difference between the frequency signal and the optimal target of 50 Hz in scenario s. $\Delta P_{h,s}$ is the power difference between the modified electrolyser consumption $P_{h,s}$, and the baseline electricity demand $P_{h,s}^0$ before the TSO signals are issued in different frequency ancillary services.

$$\Delta P_{h,s} = P_{h,s} - P_{h,s}^0 \tag{5.3}$$

After FCR, the TSO asks providers to activate aFRR in less than 7.5 minutes by communicating control signals, separated into downward (aFRR-Down) and upward (aFRR-Up) values [38]. For aFRR-Up, the TSO asks the load to decrease the net off-take, while for aFRR-Down the service provider manages the consumption by increasing the net off-take (see (5.4b)). The instant values of the control signals communicated by the TSO for aFRR-Down I_h^D and aFRR-Up I_h^U are values between 0 to +1 and -1 to 0, respectively.

$$P_{h,s}^0 : \begin{cases} 0 \leq P_{h,s}^0 \leq C_s^E - R_s, & \text{aFRR} - \text{Down} \\ R_s \leq P_{h,s}^0 \leq C_s^E, & \text{aFRR} - \text{Up} \end{cases} \tag{5.4a}$$

$$\Delta P_{h,s} = \begin{cases} R_s \cdot I_h^D, & \text{aFRR} - \text{Down} \\ R_s \cdot I_h^U, & \text{aFRR} - \text{Up} \end{cases} \tag{5.4b}$$

In case of a large imbalance between generation and consumption that cannot be recovered by activating the FCR and aFRR products, the TSO initiates the mFRR service, which should be activated in less than 15 minutes. For loads like electrolysers, mFRR is only allowed as an upward service, which means the TSO signals J_h^U are amounts between -1 to 0. The constraint in (5.5b) assures that the system can act as per the TSO signal.

$$R_s \leq P_{h,s}^0 \leq C_s^E \tag{5.5a}$$

$$\Delta P_{h,s} = R_s \cdot J_h^U \tag{5.5b}$$

The baseline power $P_{h,s}^0$ is a vital aspect for delivering aFRR and mFRR services. The baseline constraints (see (5.4a) and (5.5a)) guarantee that if the electrolyser works at peak loads (e.g., because electricity prices are low) and it is requested to increase the power consumption (down services), enough capacity has been reserved beforehand. The same would happen if the TSO asks the service provider to decrease its power consumption (up services) and the unit is in low-load conditions. Once the signal is issued by the market operator, the electrolyser is scheduled accordingly to

modify the intake power compared to the baseline consumption. Moreover, based on the baseline, the delivered aFRR and mFRR energy $\Delta P_{h,s}$ are calculated [39].

The TSO signal delay might impact the technical aspects of the provision of ancillary services in an optimisation problem with a short time frame. However, instead of the transient state of electrolyser response and delay in TSO signals, this study looks at a larger time frame for the hourly operation of the system with an annual optimisation horizon. Thus, it is assumed that delay associated with the TSO signal does not impact the outcome of this study.

5.2.3 Hydrogen flow constraints

The objective function is subject to the balance of hydrogen flow in the HRS. Eq. (5.6) distributes the hydrogen produced by the electrolyser between compressors. The produced hydrogen $H^{p}_{h,s}$ is computed as the product of the electrolyser energy efficiency κ_E times the electrolyser power consumption. $H^{C_c}_{h,s}$ is the share of hydrogen that goes to the c^{th} compressor.

$$H^{p}_{h,s} = \kappa_E \cdot P_{h,s} = \sum_{\substack{c=1 \\ c\neq 2}}^{4} H^{C_c}_{h,s} \tag{5.6}$$

Eq. (5.7) determines the volume of compressed hydrogen by compressor c, where η_{C_c} is its efficiency.

$$C_{c,h,s} = H^{C_c}_{h,s} \cdot \eta_{C_c}, \quad \forall c \in \{1,2,3,4\} \tag{5.7}$$

The amount of injected hydrogen into the industrial pipeline $H^{i}_{h,s}$ is given by (5.8), while (5.9) calculates the amount of hydrogen injected into the natural gas grid, $H^{g}_{h,s}$.

$$H^{i}_{h,s} = H^{C_3}_{h,s} \cdot \eta_{C_3} \tag{5.8}$$

$$H^{g}_{h,s} = H^{C_4}_{h,s} \cdot \eta_{C_4} \tag{5.9}$$

Eq. (5.10) limits the amount of injected hydrogen into the industry and natural gas grid to make sure that pipeline constraints are not surpassed. C_I and C_G are equal to 500 and 1,000 kg, respectively. There is no demand constraint here, and hydrogen will be injected into the natural gas grid and into the industrial hydrogen pipeline whenever it is profitable.

$$H^i_{h,s} \leq C_I \quad , \quad H^g_{h,s} \leq C_G \tag{5.10}$$

The objective function is also subjected to the balance of hydrogen in the storage tanks. Supposing a leakage of 5% for the storage units and having η_{S_1} as the storage efficiency, (5.11) implies that the available hydrogen in the first storage at any given hour is equal to the remaining hydrogen from the previous timeslot $0.95 \cdot S_{1,h-1,s}$ plus the inflow of the compressed hydrogen by the first compressor $C_{1,h,s}$. The hydrogen that goes to the first dispenser $H^b_{h,s}$ and the share of hydrogen that goes to the high-pressure compressor $H^{C_2}_{h,s}$ are subtracted.

$$S_{1,h,s} = 0.95 \cdot S_{1,h-1,s} + C_{1,h,s} \cdot \eta_{S_1} - H^b_{h,s} - H^{C_2}_{h,s} \tag{5.11}$$

As for the first storage, (5.12) implies that the available hydrogen in the second tank at any given time is equal to the remaining hydrogen from the previous hour $0.95 \cdot S_{2,h-1,s}$ plus the inflow of the compressed hydrogen by the second compressor $C_{2,h,s}$, while the hydrogen that goes to the second dispenser $H^a_{h,s}$ is subtracted.

$$S_{2,h,s} = 0.95 \cdot S_{2,h-1,s} + C_{2,h,s} \cdot \eta_{S_2} - H^a_{h,s} \tag{5.12}$$

Eqs. (5.13)-(5.15) ensure that the optimal volume of hydrogen is produced and then stored such that the hydrogen demand of vehicles is satisfied in each scenario and in the whole optimisation period.

$$\sum_{h=1}^{8784} \left(H^p_{h,s} - \left(\frac{H^i_{h,s}}{\eta_{C_3}} + \frac{H^g_{h,s}}{\eta_{C_4}} + \frac{\frac{H^a_{h,s}}{\eta_{C_2} \cdot \eta_{S_2}} + H^b_{h,s}}{\eta_{C_1} \cdot \eta_{S_1}} \right) \right) \geq 0 \tag{5.13}$$

$$\sum_{h=1}^{8784} \left(S_{1,h,s} - H^b_{h,s} - \frac{H^a_{h,s}}{\eta_{C_2} \cdot \eta_{S_2}} \right) \geq 0 \tag{5.14}$$

$$\sum_{h=1}^{8784} S_{2,h,s} - H^a_{h,s} \geq 0 \tag{5.15}$$

Eq. (5.16) is proposed to limit the amount of compressed and stored hydrogen at each hour and scenario considering the decision variables C_{C_c} as the optimal capacity of compressor c and C_{S_t} as the optimal capacity of the storage t.

$$\begin{cases} C_{c,h,s} \leq C_{C_c}, & \forall c \in \{1,2,3,4\} \\ S_{t,h,s} \leq C_{S_t}, & \forall t \in \{1,2\} \end{cases} \tag{5.16}$$

A balance between the full availability of the system for grid balancing, the size of the hydrogen tanks and the amount of reserved hydrogen has to be found to enable the continued supply of consumers. Thus, to guarantee that the demand is always met if the maximum consumption happens at any time or an unplanned outage occurs, (5.17) ensures that there is always a reserved amount of hydrogen equal to the maximum hourly consumption.

$$\begin{cases} \max H^b_{h,s} \leq S_{1,h,s} \\ \max H^a_{h,s} \leq S_{2,h,s} \end{cases} \tag{5.17}$$

5.3 Numerical assessment

The efficiency of the introduced model is examined by using the real energy market data [40]. The potential of providing FAS is assessed based on the given capacity and energy payments during the year 2020 [41]. The most important modelling parameters are listed in Table 5.1. Two types of efficiency parameters have been used for compressors: energy efficiency κ_C and hydrogen flow efficiency η_C. The specific energy consumption of the system (including utilities and rectification) is given by Cummins, a developer and manufacturer of hydrogen generation and fuel cell products. The annual investment costs are computed assuming a project lifetime of 20 years, a discount rate of 5%, an expected inflation rate of 2%, and the operation and maintenance costs of 1% for storage tanks and 5% for other subcomponents relative to the initial investment.

Knowledge of hydrogen demand is also essential to support the development and performance of a hydrogen station. This chapter assumes that existing data from gasoline fills can be adopted to build a hydrogen demand profile for mobility. The normalised time series of the demand was obtained from a fuel station and modified according to the patterns given in [42, 43] considering the supply capacity of an HRS in Belgium. The consumption changes within hours and days create repetitive patterns of one week (see Fig. 5.2) for hydrogen demand over one year. Hydrogen selling prices of

Table 5.1: Test system modelling parameters

	CAPEX	Energy efficiency [kWh/kg]	H_2 flow efficiency
E	0.77 M€/MW	$\kappa_E = 54.4$	-
C_1	1525 [€/Nm3/h]	$\kappa_{C_1} = 2.0$	$\eta_{C_1} = 0.90$
C_2	538 [€/Nm3/h]	$\kappa_{C_2} = 2.7$	$\eta_{C_2} = 0.90$
$C_{3,4}$	333 [€/Nm3/h]	$\kappa_{C_{3,4}} = 2.0$	$\eta_{C_{3,4}} = 0.90$
S_1	1400 €/kg	-	$\eta_{S_1} = 0.99$
S_2	1900 €/kg	-	$\eta_{S_2} = 0.99$
D_1	116,689 €	$\kappa_{D_1} = 6.0$	-
D_2	162,570 €	$\kappa_{D_2} = 6.0$	-

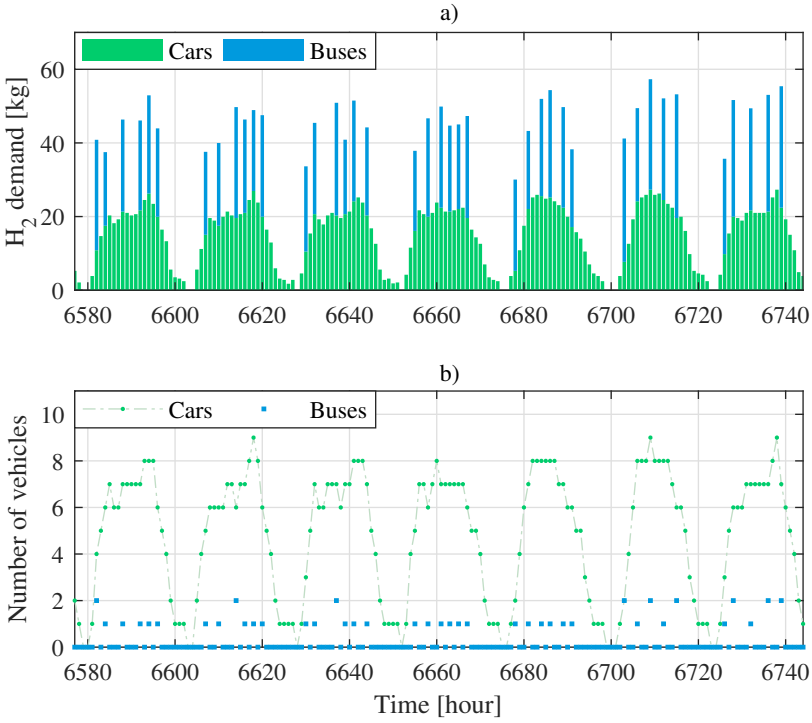

Figure 5.2: a) Hourly H_2 demand, b) Number of refilled vehicles.

7.6 €/kg for cars and 7.2 €/kg for buses are used for the numerical investigations [44]. According to [44], an average hydrogen selling price of 2 €/kg could be assumed for the industry, while the prices for injection into the gas grid are calculated based on the hydrogen caloric value and data provided in [45].

Proper sizing and operation schedules of an HRS are expected to be considerably influenced by the grid services constrained by (5.2a)-(5.5b). Hence, the operation of the introduced system is optimised based on a probabilistic mixed integer linear programming (PMILP) model for different cases as follows: Case 1 examines the operation without the provision of frequency grid services, while Cases 2-5 study the system performance under the provision of respectively FCR, aFRR-Down, aFRR-Up and mFRR-Up. CPLEX, a high-performance solver is used to solve the proposed model. Conducting each simulation took around 8 minutes on a 2.11 GHz Windows-based system with 16 GB of RAM. From some initial simulations, it was seen that the optimal capacity for FCR, aFRR, and mFRR contracts, at maximum, are 2, 50, and 50 MW, respectively. However, because of the limited space for electrolysers to participate in FAS markets and to compare the effect of different services on the system operation, the capacity of 2 MW is considered as the maximum limit for reserved capacity in all grid services.

5.3.1 Sizing

The ratings of the electrolyser, compressors and storage tanks are optimised according to filling demands, the FAS market condition and considering the possible injection of the extra produced hydrogen into the industry and the natural gas system. The obtained ratings for subcomponents in five cases are shown in Table 5.2. Ratings are scaled to kg to be analogous to each other. The size of the electrolyser can increase with fixed steps of 0.5 MW, while 5 kg increment steps are assumed for other subcomponents. The lowest size of electrolyser, 4.5 MW, is obtained for the situation without the provision of grid services, where the system only has to meet the hydrogen demand from the vehicles. However, providing grid services will add other constraints to the operation of the plant. As shown in (5.2a), before receiving any FCR signals, and considering the maximum reserve of 2 MW, the electrolyser must work at a baseline power between $(2+0.05\cdot C^E)$ MW and $(C^E - 2)$ MW. At the same time, it must have enough production around 4.5 MW obtained in the first case to supply the mobility. As a result, the model finds the size of 6.5 MW for the electrolyser in Case 2. aFRR-Down is provided asymmetrically where the system should have a 2 MW reserve

Table 5.2: Subcomponents sizes in different cases

	No FAS	FCR	$aFRR_{Down}$	$aFRR_{Up}$	$mFRR_{Up}$
E (MW)	4.5	6.5	6.5	5.0	4.5
C_1 (kg)	70	65	65	70	65
S_1 (kg)	75	75	75	80	75
C_2 (kg)	35	30	30	35	30
S_2 (kg)	175	175	175	175	175
C_3 (kg)	65	65	75	65	65
C_4 (kg)	0	25	0	15	10

to provide the service by increasing the electricity consumption. Same as the case of FCR, the electrolyser works at a maximum of 4.5 MW as the baseline power to provide enough hydrogen for mobility, and considering 2 MW as the maximum reserved capacity results in 6.5 MW electrolyser capacity in Case 3.

aFRR-Up and mFRR-Up are also provided asymmetrically, but the electrolyser must work at a minimum of 2 MW baseline power to have enough reserve to serve the FAS market, and then can decrease its power demand according to the grid signals or increase it according to the hydrogen demand. Considering a large number of activation and high amount of activated energy volumes, the electrolyser operator decreases consumption for a large number of hours. Hence, the electrolyser should work at higher capacities at some hours to provide enough hydrogen for the vehicles. Thus, the size of 5 MW for the electrolyser is obtained in Case 4.

It is even possible to provide aFRR-Up without changing the size of the electrolyser obtained in Case 1. However, the requirements of modifying electricity consumption for providing aFRR-Up and meeting hydrogen demand simultaneously do not ensure optimum profits. This is because in Case 4, the high number and volumes of aFRR-Up activation will reduce the electrolyser electricity consumption and hydrogen production at some hours, even with cheap electricity. In return, the production of more hydrogen at hours with expensive electricity would reduce the total profits. By having a 5 MW electrolyser, the reduction in electrolyser electricity consumption will be the same, but the level of hydrogen production at hours with low electricity prices can increase due to the higher size of the electrolyser. This facilitates cost minimisation by producing less hydrogen at hours with expensive electricity. Thus, a slight increase in the size of the electrolyser would improve the total profits in Case 4.

However, in case of mFRR, the lower number of activations and the smaller amount of activated energy volumes let the electrolyser decrease consumption for a limited number of hours. This, in turn, makes working at lower power values compared to aFRR-Up suitable to provide enough hydrogen for mobility. As a result, the size of the electrolyser amounts to 4.5 MW in Case 5. The results prove that participation in the FAS markets, especially those with downside activation, requires a larger electrolyser.

The ratings for compressor 1 are more or less the same in all cases as it works as the first compression stage to supply heavy-duty vehicles. However, in Cases 2, 3 and 5, the size of compressor 1 is decreased to reduce the costs. The same occurs for compressor 2, which supplies the second storage for passenger cars. The sizing of compressors 3 and 4 implies another story, though. The excess hydrogen that is not used for the mobility sector, and is not profitable to be stored, will be injected into the industry or natural gas pipelines. Larger sizes for compressor 3 imply a higher revenue potential from selling hydrogen to the industry.

The sizing of the storage tanks allows the HRS operator to store excess produced hydrogen when electricity prices and/or hydrogen demand are low. In turn, amounts of stored hydrogen can be extracted when electricity prices and/or hydrogen demand are high, so that the electrolyser operates at a lower electricity demand. It should be noted that there is a trade-off between the optimal arbitrage trading, participation in grid services and storage capacity: larger storage tanks and electrolyser will increase optimal arbitrage plans but also HRS costs. Minimum storage capacity limits of 175 and 75 kg are assumed for supplying cars and buses, respectively. This assures the continued supply of hydrogen to the customers in case of an emergency where the electrolyser cannot produce hydrogen for half a day and, thus, may need to be changed for other HRSs. The largest size for the first storage is obtained in Case 4, where, as mentioned before, the electrolyser should work at higher capacities at some hours to store hydrogen. The stored amount will be extracted by the dispensers in later time-steps when hydrogen production will be reduced due to service provision. However, the size of the second storage is equal to the minimum limit in all cases. This is because the model tries to reduce the investment costs, and a size of 75 kg for the first storage and 175 kg for the second one are enough to meet the hydrogen flow requirement in most cases.

5.3.2 Scheduling

While simulation studies are performed for a year and the financial parameters are computed on an annual basis, scheduling curves are depicted for the first two days of the week, starting from 1 October 2020 in all cases for detailed studies when looking at the grid services.

When there is no specified hydrogen demand, the electrolyser runs at maximum power as long as the equivalent price of hydrogen is high enough to cover the electricity costs, equipment losses and investment costs. However, for the suggested model of this study, in which the hourly hydrogen demand should be met, the situation is different. Hence, in addition to electricity costs, hydrogen demand and the ratings of storage tanks influence the optimal dispatch of the electrolyser. In the case of grid services, the remuneration price and activation signals add to the complexity of the system performance. All these parameters shape a multi-dimensional optimisation problem in which, even at some hours with low electricity prices, the electrolyser works at low power levels. This is due to the low hydrogen demand, the fully-filled storage tanks, or lower values for the electricity price in the next hours where the operator prefers to fill the storage units.

Considering all these points, the electrolyser under different working conditions is scheduled to maximise the profits while meeting the requirement of grid services. The produced hydrogen, electricity price ρ^e, demand from vehicles, injected hydrogen to the industry and stored hydrogen in Case 1 are represented in Fig. 5.3(a)-(c). The model schedules the electrolyser to operate and produce at lower electricity prices, when possible, to minimise the power purchase cost. The operational setpoints are also impacted by the hydrogen demand at different hours. The storages state of charge (SOC) is represented in Fig. 5.3(c). Storage tanks are mainly filled at hours with low electricity prices or low hydrogen demand. Later, the storage units supply a part of the hydrogen load when demand surpasses the production. After the storage tanks, industrial pipeline and the natural gas grid are prioritised to be supplied with the surplus hydrogen production.

For Cases 2-5, the electrolyser is programmed under different FAS schemes to absorb the excess power from the grid or/and consume less when such an activity is requested. The optimal electrolyser operation considering cross-commodity arbitrage trading and FCR provision is investigated in Case 2. The grid frequency deviation signals, electricity price values, electrolyser scheduling and hydrogen flow are represented in Fig. 5.4(a)-(d). The electrolyser electricity consumption after reacting to the frequency deviation signals are shown as the black line in Fig. 5.4(b), while the electrolyser consumption before FCR activation can be found as

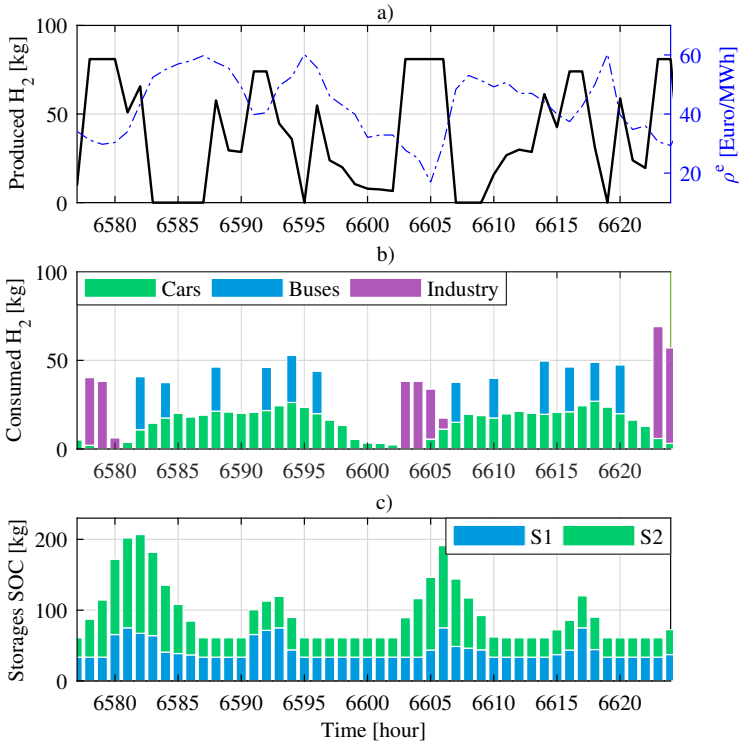

Figure 5.3: Case 1- a) H_2 production vs. electricity prices, b) Consumed H_2 in various sectors, c) SOC of storage units.

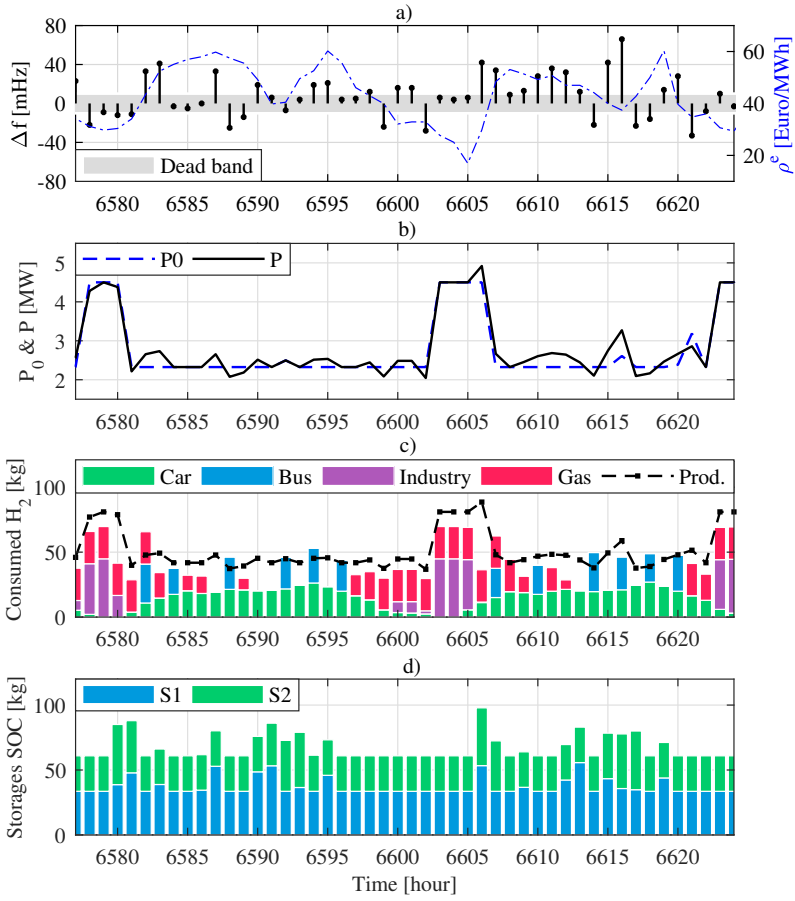

Figure 5.4: Case 2- a) Frequency variation, b) Electrolyser power, c) Produced H_2 vs. consumed H_2 in various sectors, d) State of charge of storage units.

the dashed blue line. The hydrogen production and consumption (demand from cars and buses and injection to the industry and natural gas network) curves are depicted in Fig. 5.4(c), while the SOC of storage tanks can be found in Fig. 5.4(d).

The electrolyser produces higher volumes of hydrogen, and part of the extra amount is stored in the tanks when the electricity tariff is low, or the benefit of FCR to increase the consumption is higher than the costs of electricity. This, in turn, allows the electrolyser to consume less when the electricity tariff increases or the benefit of FCR to decrease the power demand is higher than the revenue of selling hydrogen to different sectors. In these instances, the mobility sector is partly supplied by the stored hydrogen in the tanks. As illustrated in (5.2a), baseline electricity demand is limited at both ends while providing FCR. It would require purchasing non-zero electrical energy, which increases the costs that exceed the possible remuneration of FCR. Hence, the operator cannot use the best strategy.

The optimal electrolyser operation considering cross-commodity arbitrage trading and providing aFRR-Down, aFRR-Up, and mFRR-Up are investigated in Cases 3-5. The TSO signals, electricity price values, electrolyser scheduling, and hydrogen flow are represented in Figs. 5.5(a)- 5.7(d). The electrolyser electricity consumption after reacting to the TSO signals are shown as the black line in subfigures (b) of Figs. 5.5- 5.7, while the electrolyser consumption before activating grid services can be found as the dashed blue line. The hydrogen production and consumption curves are depicted in subfigures (c) of Fig. 5.5 to Fig. 5.7, while the SOC of storage tanks can be found in subfigures (d) of Fig. 5.5 to Fig. 5.7.

In Case 3, the electrolyser produces higher volumes of hydrogen and part of the extra amount is stored in the storage tanks when the electricity tariff is low, and/or the aFRR-Down signal is issued, and the electrolyser has to increase its consumption. This, in turn, allows the electrolyser to consume less when the electricity tariff increases. However, it is noteworthy that the benefit of aFRR-Down might not be high enough to cover the costs when the electricity prices are high. This indicates that due to the flexibility provision, arbitrage trading is not optimally possible in some instances.

In Case 4, on the other hand, when the aFRR-Up signal is issued, the electrolyser operator has to decrease its consumption. When the TSO signal is not issued or has a small value, the electrolyser works at a base load of around 2 MW because of the capacity reserve requirement of the service. In that case, the benefit of aFRR-Up might not be high enough to cover the costs when the electricity prices are high. This means, similar to the aFRR-Down, flexibility provision might decrease the optimal arbitrage trading benefits at some timeslots.

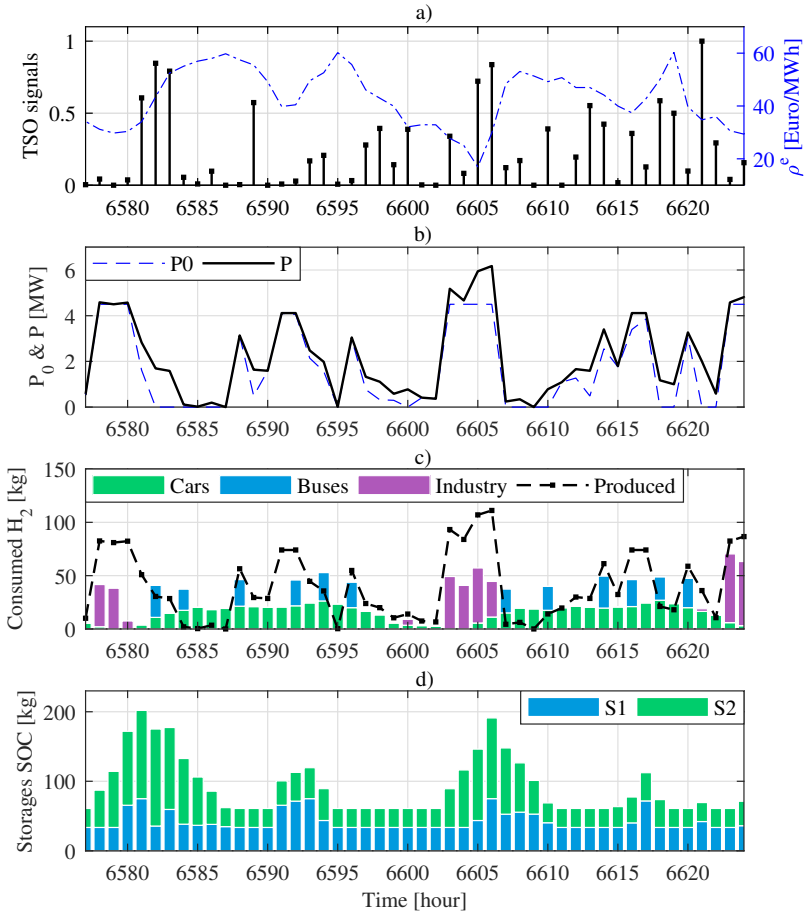

Figure 5.5: Case 3- a) aFRR-D TSO signals, b) Electrolyser power, c) Produced H_2 vs. consumed H_2 in various sectors, d) State of charge of storage units.

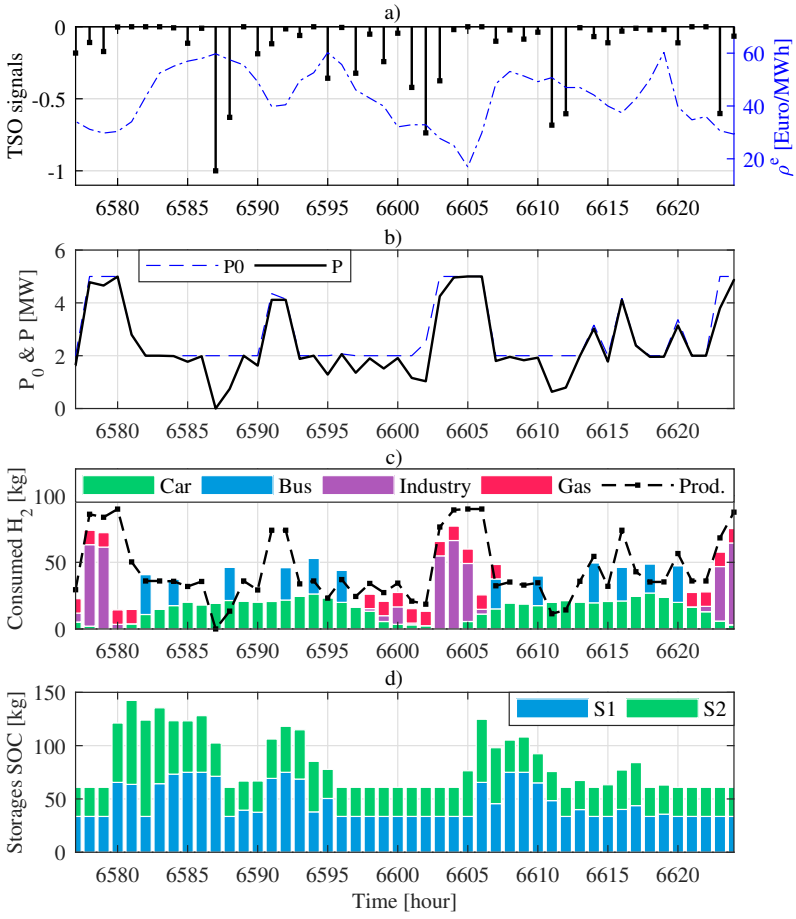

Figure 5.6: Case 4- a) aFRR-U TSO signals, b) Electrolyser power, c) Produced H_2 vs. consumed H_2 in various sectors, d) State of charge of storage units.

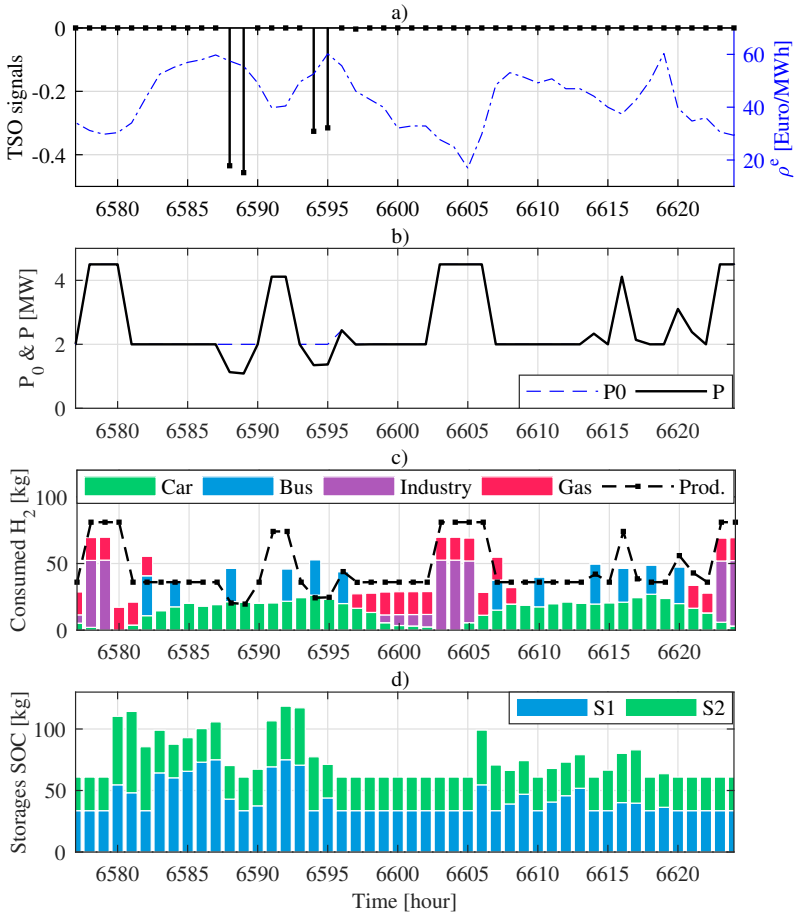

Figure 5.7: Case 5- a) mFRR-U TSO signals, b) Electrolyser power, c) Produced H_2 vs. consumed H_2 in various sectors, d) State of charge of storage units.

Fig. 5.7 depicts the scheduling curves in Case 5. The situation is more or less the same as Case 4 with a difference that mFRR-Up is activated less frequently with lower signal values than the ones for aFRR-Up. Hence, the electrolyser works at a baseline load at most of the hours and the activation remuneration for this service could be less than other services, which might not be high enough to cover the electricity costs originated from working at a baseload around 2 MW at hours with high electricity prices.

Subfigures (c) and (d) in Figs. 5.5- 5.7 tell the same story as already shown for Cases 1 and 2. In case of having surplus hydrogen production at hours with low electricity prices, or when the electrolyser has to increase the electricity demand to provide grid services, the storage tanks, industrial loads and the gas grid are prioritised to be supplied. On the contrary, if hydrogen demand exceeds production due to high electricity prices or when the electrolyser should reduce the hydrogen production to provide grid services, the storage partially supplies the dispensers with the previously stored hydrogen. While the level of the stored hydrogen at each hour and for various cases is different mainly due to different demand and setpoints for the electrolyser, the stored hydrogen level in all cases follows a similar trend primarily due to a similar pattern for the hydrogen demand, electricity price and hydrogen flow in the HRS.

5.3.3 Economic evaluation

The obtained monthly revenue provided by the electrolyser under the grid service provision is depicted in Fig. 5.8. The monthly revenue for the reserved capacity and the activated energy is revealed as the blue and green bars, while the weighted average remuneration price for the reserved capacity α and activated energy β can be found as the black and blue dashed lines. As said earlier, while the HRS, as an FCR provider benefits only from capacity revenue, extra revenues from activated energy can be obtained by providing other services. It is noteworthy to mention that aFRR-Down, aFRR-Up and mFRR-Up were activated 7,953, 8,061 and 329 times during the year, respectively. Thus, higher prices for the activation of aFRR-Up along with more frequent and larger activation signals will bring the most revenue for the HRS as an aFRR provider.

The monthly injected hydrogen to the industry as an additional source of revenue and the obtained profits provided by the electrolyser in different cases against the monthly average electricity prices are depicted in Fig. 5.9(a) and (b), respectively. The least injection to the industry is obtained in September and December due to the influence of the higher electricity prices on the plant performance. The lowest electricity prices let the maximum injection into the industrial pipeline in April and May. Accordingly, the total profits follow the same trend as the costs of bought electricity has a high share in total costs. While the monthly added profits in Cases 2-5 compared to Case 1 are variable from the minimum of €$-$7,463 in September (FCR) to the maximum of €44,098 in January (mFRR-Up), the average added profit amounts to €11,433. The negative value for the added profit of FCR in September shows that FCR provision is not profitable in all months.

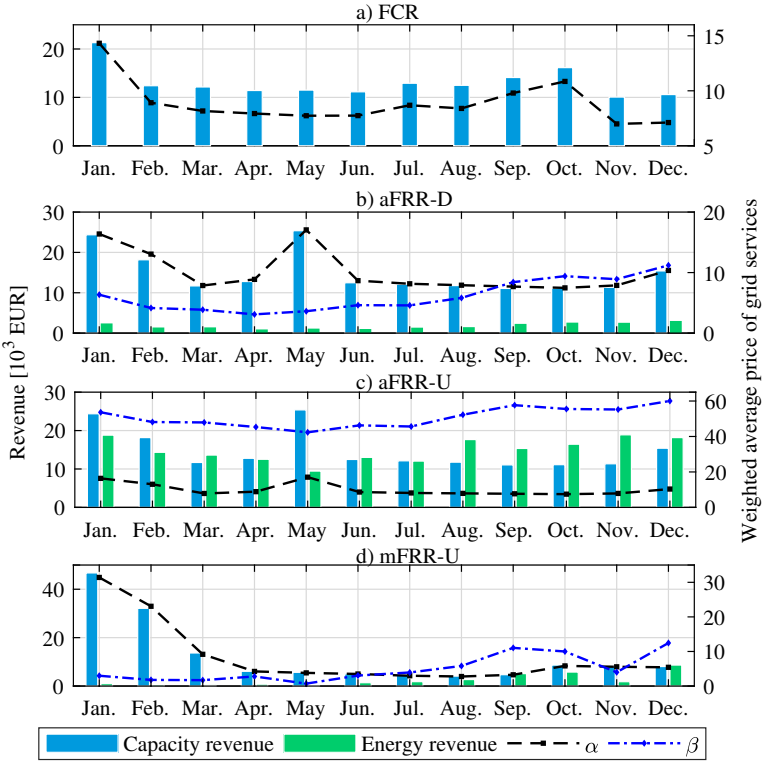

Figure 5.8: Monthly obtained revenues vs. monthly average capacity and activation remuneration prices in different FAS.

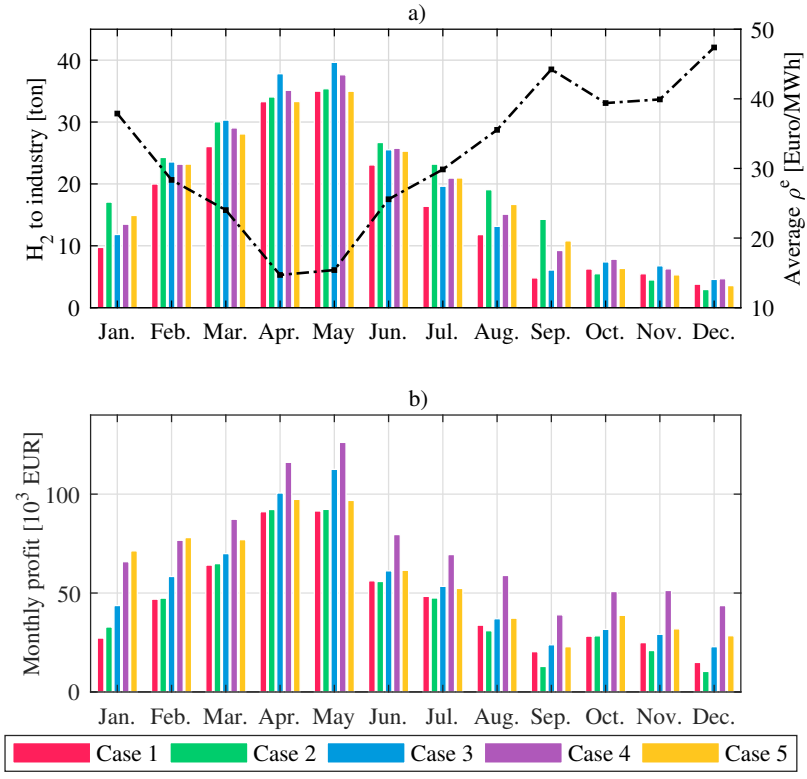

Figure 5.9: a) Monthly total profits in different FAS vs. monthly average electricity prices, b) Monthly injection to the industry.

Table 5.3: Annual costs, revenues and profits for different cases (€)

	No FAS	FCR	$\text{aFRR}_{\text{Down}}$	aFRR_{Up}	mFRR_{Up}
IC	467,258	597,766	591,231	501,807	472,668
EC	745,866	910,284	785,588	846,933	877,438
FASR	0	163,563	199,138	358,057	177,556
IR	391,247	473,842	452,451	456,601	446,831
GR	0	77,724	0	29,370	49,872
AP	547,478	576,434	644,125	864,643	693,508
ρ_a^{be} (€/kg)	4.56	4.40	4.03	2.80	3.75
ρ_b^{be} (€/kg)	4.33	4.19	3.80	2.66	3.57

After all, the revenues obtained against the investment and electricity costs under the proposed algorithm are reported in Table 5.3. Investment, operation and replacement costs (IC) account for 35-43% of the total annual costs, while costs linked to electricity (EC) are considerably high, varying from 57% of total annualised costs in Case 3 to 65% in Case 5. A 24, 13, 11, and 11% increase in the total costs is observed when participating in the FCR, aFRR-Down, aFRR-Up, and mFRR-Up, respectively. This can be explained by the increase in EC and IC due to different ratings for the electrolyser and the requirement of regulation services.

Revenue from the mobility sector amounts to €1,369,355, out of which €974,017 obtained by selling hydrogen to cars and €395,338 by selling hydrogen to buses. The contribution to the total revenue from participation in FAS (FASR) is important (ranging from 8% in Case 2 to 16% in Case 4), while the contribution from the industry (IR) ranges from 21% in Case 4 to 23% in Case 2. Contribution from injection into the natural gas network (GR) can go up to 4% in Case 2. It is also noteworthy that the total annual profits (TAP) can be increased from 5% in Case 2 to 58% in Case 4 compared to Case 1. As mentioned in Section 5.3.1, it is even possible to provide aFRR-Up without changing the size of the electrolyser obtained in Case 1. However, it causes a slight decrease in the total profits to €831,471.

The hydrogen break-even price, i.e., the price at which the total profits come to zero, is used as an economic metric to show at which hydrogen selling prices, investment in the HRS will be feasible. The last two rows of Table 5.3 illustrate the hydrogen break-even price for selling hydrogen to buses ρ_b^{be} and passenger cars ρ_a^{be}. The combined effect of participation in FAS markets, and selling extra produced hydrogen to the industry and gas sectors will make the HRS more economically effective with lower hydrogen break-even prices.

5.3.4 Sensitivity analysis

A sensitivity analysis has been conducted to show the effect of hydrogen selling price variation in different sectors on the ratings of the system and the HRS profitability of the investment. This helps investors to decide whether to invest in an HRS or not based on their predictions of the hydrogen price in different sectors. Variation of the hydrogen selling price in the mobility sector affects only and proportionally the obtained revenues from the mobility sector. Such variation does not have a notable effect on the ratings of the electrolyser and compressors 1 and 2 as they will be sized according to the mobility demand.

The results of Table 5.4, related to Case 5, illustrate that a 20% increase of hydrogen selling price to the industry ρ_i would significantly affect the size of the electrolyser and compressor 3 to produce more hydrogen for injection to the industry at the almost double amount of profits. This significant increase occurs for the size of the electrolyser and compressor 4 when the price of selling hydrogen to the gas sector ρ_g increases 40%. As the conducted sensitivity analysis for other cases showed the same trend, without the loss of generality, only the results related to mFRR-Up are reported.

Moreover, a set of simulations were conducted to highlight the trade-

Table 5.4: Sensitivity to the variation of ρ_i & ρ_g

ρ_i	0.6X	0.8X	1.0X	1.2X	1.4X
E (MW)	4.5	4.5	4.5	22.5	33
C_3 (kg)	25	55	65	335	500
AP (€)	583,875	621,124	693,508	1,317,940	2,609,351
ρ_g	0.6X	0.8X	1.0X	1.2X	1.4X
E (MW)	4.5	4.5	4.5	4.5	30
C_4 (kg)	0	0	10	60	470
TAP (€)	692,233	692,233	693,508	718,415	1,018,569

Table 5.5: Total annual profits considering various combinations of revenue sources (€)

	No FAS	FCR	$\text{aFRR}_{\text{Down}}$	aFRR_{Up}	mFRR_{Up}
MR	444,479	200,297	514,687	730,170	477,779
MR+IR	547,478	533,471	644,125	870,989	692,233
MR+GR	459,640	404,637	540,121	776,540	577,504
MR+GR+IR	547,478	576,434	644,125	864,643	693,508

off to select between different combinations of revenue sources, including mobility (MR), industry (IR) and natural gas (GR). The obtained results given in Table 5.5 confirm how the combination of different revenue sources along with the provision of ancillary services could improve the business case of the HRS. Comparing the values on the second and third rows illustrates significant potential from selling hydrogen to the industry, while for the gas sector the potential is marginal in some cases.

5.4 Summary and conclusions

As a complement to the model proposed in Chapter 4, this chapter, in addition to examining the impact of FCR provision on the investment and operation strategies in an HRS, addressed the implications of providing aFRR and mFRR as well. The uncertain behaviour of hydrogen demand and capacity market prices were also taken into account.

A novel methodology was developed to evaluate the techno-economic feasibility of an HRS intended to provide grid services in different modes of operation. The model optimised the size of all subcomponents and defined the optimal operation plans considering an overall arbitrage trading of electricity, industry, gas, mobility and ancillary service markets. It was observed that the electrolyser is mainly sized according to the maximum hydrogen demand from the mobility sector and the amount of contracted capacity for providing ancillary services. Moreover, the results of the sensitivity analysis showed how the variation of hydrogen prices in gas and industrial sectors affects the size of the electrolyser and compressors.

According to the obtained results, increasing the size of the electrolyser only for FCR provision is marginally profitable with the hypotheses adopted in this research. Provision of aFRR-Down, like FCR, increased the investment costs due to the large size of the electrolyser. The results in Cases 4 and 5 showed that an increase in capacity payment revenue and additional revenue for energy activation could compensate for the higher investment costs. Prioritising mFRR-Up over arbitrage trading also results in even higher revenues, but lower compared to the aFRR-Up product. This also leads to the conclusion that the production of hydrogen in this concept is not only dependent on the price of electricity but also the remuneration price of frequency ancillary services and their activation signals. A comparative analysis of the cost and revenue streams showed that the total annual profit could be increased significantly in the aFRR-Up program compared to Case 1. Thus, the HRS operator has to prioritise aFRR-Up provision over other grid services to increase investment profitability. In conclusion, the stacked benefit from the ancillary service markets and the hydrogen sale

to different sectors enhances the economic viability of the plant and lowers the hydrogen break-even price. Therefore, the proposed model presents new opportunities for the proliferation of HRSs, thereby further inspiring the investment in such plants.

It is noteworthy that while the test system and input data are provided by manufacturers, industrial partners and market operators in Central Europe, the optimisation model is scalable and general enough to consider various types of grid services with different remuneration coefficients and activation signals. With some slight modifications, it can be used for small- and large-scale power-to-hydrogen plants located around the world. Modifications could be either the modelling changes, such as the inclusion of voltage control ancillary service, or change in the test system and respective parameters to include wind and solar farms, together with fuel cells and hydrogen-powered gas turbines to support the grid flexibility.

References

[1] A. Dadkhah, D. Bozalakov, J. D. M. De Kooning, and L. Vandevelde. *Optimal Sizing and Economic Analysis of a Hydrogen Refuelling Station Providing Frequency Containment Reserve*. In 2020 IEEE International Conference on Environment and Electrical Engineering and 2020 IEEE Industrial and Commercial Power Systems Europe (EEEIC/I&CPS Europe), 2020.

[2] A. Dadkhah, D. Bozalakov, J. D. M. De Kooning, and L. Vandevelde. *Techno-Economic Analysis and Optimal Operation of a Hydrogen Refueling Station Providing Frequency Ancillary Services*. IEEE Transactions on Industry Applications, 58(4):5171–5183, 2022.

[3] J. Li, J. Lin, H. Zhang, Y. Song, G. Chen, L. Ding, and D. Liang. *Optimal investment of electrolyzers and seasonal storages in hydrogen supply chains incorporated with renewable electric networks*. IEEE Transactions on Sustainable Energy, 11(3):1773–1784, 2019.

[4] M. Bailera, P. Lisbona, L. M. Romeo, and S. Espatolero. *Power to Gas projects review: Lab and demo plants for storing renewable energy and CO_2*. Renewable and Sustainable Energy Reviews, 69:292–312, 2017.

[5] N. Mendis, K. M. Muttaqi, S. Perera, and S. Kamalasadan. *An effective power management strategy for a wind–diesel–hydrogen-based remote area power supply system to meet fluctuating demands under generation uncertainty*. IEEE Transactions on Industry Applications, 51(2):1228–1238, 2014.

[6] *Key indicators to track clean energy progress on hydrogen*. [Online, Accessed May. 2021]: `https://www.iea.org/reports/hydrogen`.

[7] *Hydrogen Insights, A perspective on hydrogen investment, market development and cost competitiveness*. [Online, Accessed Dec. 2021]: `https://hydrogencouncil.com/wp-content/uploads/2021/02/Hydrogen-Insights-2021-Report.pdf`, Feb. 2021.

[8] *Path to hydrogen competitiveness, A cost perspective*. [Online, Accessed Dec. 2021]: `https://hydrogencouncil.com/wp-content/uploads/`

2020/01/Path-to-Hydrogen-Competitiveness_Full-Study-1.pdf, Jan. 2020.

[9] F. Grueger, O. Hoch, J. Hartmann, M. Robinius, and D. Stolten. *Optimized electrolyzer operation: Employing forecasts of wind energy availability, hydrogen demand, and electricity prices*. International Journal of Hydrogen Energy, 44(9):4387–4397, 2019.

[10] X. Wu, H. Li, X. Wang, and W. Zhao. *Cooperative Operation for Wind Turbines and Hydrogen Fueling Stations with on-site Hydrogen Production*. IEEE Transactions on Sustainable Energy, 11(4):2775–2789, 2020.

[11] D. Apostolou, P. Enevoldsen, and G. Xydis. *Supporting green Urban mobility–The case of a small-scale autonomous hydrogen refuelling station*. International Journal of Hydrogen Energy, 44(20):9675–9689, 2019.

[12] M. Nedd, J. Browell, K. Bell, and C. Booth. *Containing a credible loss to within frequency stability limits in a low-inertia GB power system*. IEEE Transactions on Industry Applications, 56(2):1031–1039, 2019.

[13] *Grid-Forming Capabilities: Towards System Level Integration*. [Online, Accessed Jun. 2021]: https://eepublicdownloads.entsoe.eu/clean-documents/RDC%20documents/210331_Grid%20Forming%20Capabilities.pdf, Mar. 2021.

[14] T. Ku, C. Lin, C. Hsu, C. Chen, Z. Liao, S. Wang, and F. Chen. *Enhancement of Power System Operation by Renewable Ancillary Service*. IEEE Transactions on Industry Applications, 56(6):6150–6157, 2020.

[15] Q. Zhang, Y. Li, Z. Ding, W. Xie, and C. Li. *Self-adaptive secondary frequency regulation strategy of micro-grid with multiple virtual synchronous generators*. IEEE Transactions on Industry Applications, 56(5):6007–6018, 2020.

[16] Y. Cui, Z. Hu, and H. Luo. *Optimal day-ahead charging and frequency reserve scheduling of electric vehicles considering the regulation signal uncertainty*. IEEE Transactions on Industry Applications, 56(5):5824–5835, 2020.

[17] F. Teng, Z. Ding, Z. Hu, and P. Sarikprueck. *Technical Review on Advanced Approaches for Electric Vehicle Charging Demand Management, Part I: Applications in Electric Power Market and Renewable Energy Integration*. IEEE Transactions on Industry Applications, 56(5):5684–5694, 2020.

[18] J. Kim, V. Gevorgian, Y. Luo, M. Mohanpurkar, V. Koritarov, R. Hovsapian, and E. Muljadi. *Super capacitor to provide ancillary services with control coordination*. IEEE Transactions on Industry Applications, 55(5):5119–5127, 2019.

[19] X. Wang and J. Wang. *Economic assessment for battery swapping station based frequency regulation service*. IEEE Transactions on Industry Applications, 56(5):5880–5889, 2020.

[20] *The world's largest-class hydrogen production, Fukushima Hydrogen Energy Research Field (FH2R) now is completed at Namie town in Fukushima.* [Online, Accessed Dec. 2021]: `https://www.nedo.go.jp/english/news/AA5en_100422.html`.

[21] F. Yamane. *Fukushima Hydrogen Energy Research Field (FH2R)*. Toshiba Energy Systems & Solutions Corporation, Tech. Rep., Oct. 2019.

[22] X. Ma, H. Zhou, and Z. Li. *Optimal Design for Interdependencies between Hydrogen and Power Systems*. IEEE Transactions on Industry Applications, 2021.

[23] Z. Zhang, C. Wang, H. Lv, F. Liu, H. Sheng, and M. Yang. *Day-ahead Optimal Dispatch for Integrated Energy System Considering Power-to-Gas and Dynamic Pipeline Networks*. IEEE Transactions on Industry Applications, 2021.

[24] J. Baetens, J. D. M. De Kooning, G. Van Eetvelde, and L. Vandevelde. *A Two-Stage Stochastic Optimisation Methodology for the Operation of a Chlor-Alkali Electrolyser under Variable DAM and FCR Market Prices*. Energies, 13(21):5675, 2020.

[25] A. Samani, A. D'Amicis, J. D. M. De Kooning, D. Bozalakov, P. Silva, and L. Vandevelde. *Grid balancing with a large-scale electrolyser providing primary reserve*. IET Renewable Power Generation, 14(16):3070–3078, 2020.

[26] L. Allidières, A. Brisse, P. Millet, S. Valentin, and M. Zeller. *On the ability of PEM water electrolysers to provide power grid services*. International Journal of Hydrogen Energy, 44(20):9690–9700, 2019.

[27] A. Dadkhah, D. Bozalakov, J. D. M. De Kooning, and L. Vandevelde. *On the optimal planning of a hydrogen refuelling station participating in the electricity and balancing markets*. International Journal of Hydrogen Energy, 46(2):1488–1500, 2021.

[28] N. A. El-Taweel, H. Khani, and H. E. Z. Farag. *Hydrogen storage optimal scheduling for fuel supply and capacity-based demand response program under dynamic hydrogen pricing*. IEEE Transactions on Smart Grid, 10(4):4531–4542, 2018.

[29] H. Khani, N. A. El-Taweel, and H. E. Z. Farag. *Supervisory scheduling of storage-based hydrogen fueling stations for transportation sector and distributed operating reserve in electricity markets*. IEEE Transactions on Industrial Informatics, 16(3):1529–1538, 2019.

[30] M. Kermani, E. Shirdare, A. Najafi, B. Adelmanesh, D. L. Carnì, and L. Martirano. *Optimal Self-scheduling of a real Energy Hub considering local DG units and Demand Response under Uncertainties*. IEEE Transactions on Industry Applications, 57(4):3396–3405, 2021.

[31] G. Matute, J. M. Yusta, and L. C. Correas. *Techno-economic modelling of water electrolysers in the range of several MW to provide grid services while generating hydrogen for different applications: A case study in Spain applied to mobility with FCEVs*. International Journal of Hydrogen Energy, 44(33):17431–17442, 2019.

[32] L. Baudouin. *Overview of current electrolysis technologies*. [Online, Accessed Jan. 2021]: `https://www.ie-net.be/sites/default/files/Presentatie%205_Baudouin%20de%20Lannoy.pdf`, 2020.

[33] F. Grüger, L. Dylewski, M. Robinius, and D. Stolten. *Carsharing with fuel cell vehicles: Sizing hydrogen refueling stations based on refueling behavior*. Applied Energy, 228:1540–1549, 2018.

[34] N. A. El-Taweel, H. Khani, and H. E. Farag. *Analytical size estimation methodologies for electrified transportation fueling infrastructures using public–domain market data*. IEEE Transactions on Transportation Electrification, 5(3):840–851, 2019.

[35] *Hydrogen Belgium Brochure*. [Online, Accessed May. 2021]: https://www.fch.europa.eu/sites/default/files/file_attach/Brochure%20FCH%20Belgium%20%28ID%209473032%29.pdf.

[36] C. B. Smith and K. E. Parmenter. *Energy management principles: Applications, benefits, savings*. Elsevier, 2013.

[37] *FCR design note*. [Online, Accessed Jun. 2021]: https://tinyurl.com/yx3vu5z7, Apr. 2019.

[38] *Separated procurement of FCR and aFRR products*. [Online, Accessed Apr. 2021]: https://www.elia.be/-/media/project/elia/elia-site/public-consultations/20181009_consultation_document_2_separated_procurement_of_fcr_and_afrr_products_en.pdf?la=en, Dec. 2019.

[39] *Study on paid-as-cleared settlement for aFRR and mFRR activated energy*. [Online, Accessed Jan. 2021]: https://tinyurl.com/ytkje6vp, Dec. 2017.

[40] *EPEX spot market*. [Online, accessed 17 December 2019]: https://www.epexspot.com/en.

[41] *Activated energy volumes and energy prices*. [Online, Accessed Jan. 2021]: https://www.elia.be/en/grid-data/balancing/energy-activated-volumes-and-prices-15-min.

[42] J. Kurtz, T. Bradley, E. Winkler, and C. Gearhart. *Predicting demand for hydrogen station fueling*. International Journal of Hydrogen Energy, 45(56):32298–32310, 2020.

[43] *Next Generation Hydrogen Station Composite Data Products: Retail Stations*. [Online]: https://www.nrel.gov/docs/fy21osti/79141.pdf, 2021.

[44] D. Thomas, D. Mertens, M. Meeus, W. van der Laak, and I. Francois. *Power-to-Gas Roadmap for Flanders*. [Online, Accessed Dec. 2019]: https://www.waterstofnet.eu/_asset/_public/powertogas/P2G-Roadmap-for-Flanders.pdf, 2016.

[45] *ZTP spot market*. [Online, Accessed Dec. 2021]: https://my.elexys.be/MarketInformation.aspx.

6

Flexibility of supply- & demand-side to support the system reliability

Chapters 4 and 5 explored the role of large responsive electrolysers to provide FASs while looking at the potential effects on the investment and operational strategies from the electricity consumer point of view. However, the role of generation-side flexibility and implementation of demand response programs (DRP) in the reliability of power systems still needs to be considered. Power production plants must match the energy demand at a minimum cost and ensure system reliability. The reliability of power systems can also be improved by optimally provisioning grid balancing from the demand side. Responsive loads such as electrolysers and electric vehicles (EV) are more than clean technologies; they are a powerful resource for consumers and power sector actors. It is critical, therefore, to draw the most value from scheduling such devices through so-called smart scheduling. Smart scheduling means flexibly adjusting consumption of these devices to lower costs for consumers and grid operators, to accommodate the integration of renewable energy sources and to minimise collective impact of new technologies on the power system.

Assuming a basic level of quality and reliability of the power system, where power is considered a commodity and not as a luxury, flexibility is a resource owned by the customer that should be bought back. However, there is also a need for goodwill. Although the technologies already exist, goodwill appears to be the most uncertain parameter for developing flexibility in consumption. Moreover, empowering consumers to make an informed choice and improving rewards for consumer flexibility seem to be necessary for exploiting the maximum flexibility from the consumption side.

In this context, this chapter studies the role of two DR schemes in ensuring power systems reliability while minimising the daily operation costs of the system. Different constraints including those related to the system, units, transmission system, and DRPs as well as security constraints are taken into consideration. The proposed methodology introduces a DR model based on price elasticity of demand considering the comfort and flexibility level of consumers. The proposed approach is practiced over the IEEE 24-bus reliability rest system (RTS). Obtained results demonstrate that with proper deployment of DRPs and optimal design of real-time prices and incentives the operation cost will be reduced while the security of the system is guaranteed.

The rest of this chapter is structured as follows: Section 6.1 reviews the literature and presents the novelty of this chapter to cover the research gap. Section 6.2 defines the proposed method and problem formulation. Section 6.3 describes the test system information. Then, the numerical studies and simulation results for different cases are presented in Section 6.4. Finally, Section 6.5 describes conclusions. The content of this chapter has been published in [1, 2].

Optimal price-based and emergency demand response programs considering consumers preferences

Akbar Dadkhah, Navid Bayati, Miadreza Shafie-khah,
Lieven Vandevelde and João P.S. Catalão

Published in International Journal of Electrical Power
& Energy Systems, 2022
DOI: 10.1016/j.ijepes.2021.107890

Abstract: *This chapter presents a pricing optimisation framework for energy, reserve, and load scheduling of a power system considering demand response. The proposed scheduling framework is formulated as a reliability-constrained unit commitment program to minimise the power system operation costs by finding optimal electricity prices and optimal incentives while guaranteeing the reliability of the system during contingencies. Moreover, attitude of customers toward the electricity price and incentive adjustment and the effect of their preferences on load scheduling and operation of the system are investigated in various DR programs. The proposed scheme is implemented on an IEEE test system, and the scheduling process with and without DR implementation is discussed in detail by a numerical study. The proposed method helps both the system operators and customers to reliably schedule generation and consumption units and select the proper DR program according to defined prices and incentives in the case of an emergency.*

Nomenclature

Indices

b, b'	Index of buses
c	Index of components
f	Index for segments of linearised fuel cost
g	Index of generators
i, j	Index of times
l	Index of transmission lines
s	Index of scenarios

Parameters

B Number of buses

C Number of components

d_{bi}^{0} Baseline consumption of bus b at hour i (MW)

$\overline{DR_b}$ Maximum consumers' reply to DR signals at bus b

$\overline{EDNS}$ Maximum amount of EDNS (MW)

E_{ij} Elasticity of demand

F Number of segments in piece-wise linearised fuel cost

$\underline{FC_g}$ Minimum fuel cost of generator g (\$/h)

G Number of generators

G_b Number of generation units at bus b

H Number of hours

K_g Start-up cost of generator g (\$/MWh)

L Number of transmission lines

$\overline{M_{fg}}$ Maximum production of segment f for generator g (MW)

$\overline{P_g}, \underline{P_g}$ Maximum/minimum production of generator g (MW)

$\overline{P_l}$ Maximum power on line l (from bus b to b') (MW)

S Number of scenarios

T Spinning reserve market lead time (min)

V_{bi}^{Sh} Penalty for not-served load at bus b, hour i (\$/MWh)

$X_{bb'}$ The line reactance (from bus b to b')

α_s Probability of scenario s

β_{fg} Slope of segment f in cost curve of generator g (\$/MWh)

ψ Loss-gain coefficient

ρ_{bi}^{0} Baseline rate at bus b and hour i (\$/MWh)

Variables

I_{gi} Off/On status of generator g at hour i

SUC_{gi} Start-up cost of generator g at hour i (\$)

SRC_{gi}^{U} Up-spinning reserve cost of generator g at hour i (\$/MW)

SRC_{gi}^{D} Down-spinning reserve cost of generator g at hour i (\$/MW)

P_{gi} Production of generator g at hour i (MW)

R_g^D Ramp-down of generator g (MW/h)

R_g^U Ramp-up of generator g (MW/h)

P_{gi}^f Generation of segment f in fuel cost curve (MW)

A_{bj} Incentive in EDRP at bus b and hour j ($/MWh)

FC_{gi} Fuel cost of generation unit g at hour i ($)

SR_{gi}^U Up-spinning reserve of generator g at hour i (MW)

SR_{gi}^D Down-spinning reserve of generator g at hour i (MW)

SR_{gis}^U Up-spinning reserve of generator g at hour i in scenario s (MW)

SR_{gis}^D Down-spinning reserve of generator g at hour i in scenario s (MW)

Θ_{bis} Voltage angle at bus b and hour i in scenario s (rad)

$P_{bb'i}$ Active power of line from bus b to b' at hour i (MW)

d_{bi} Customers' consumption at bus b and hour i (MW)

L_{bis}^{Sh} Load curtailment at bus b, hour i, scenario s (MW)

σ_{gi} Reserve condition of generator g at hour i

CP_i Customers payment at hour i ($)

ρ_{bi} Electricity price at bus b and hour i ($/MWh)

6.1 Introduction

Demand response (DR) is a significant way to help network operators to control the electrical energy consumption during emergency conditions [3, 4]. DR implementation in modern electricity grids with modified pricing methods influences the comfort and payments of consumers [5]. The economic consequence of DR is at the heart of attraction in most DR-related studies, especially in the United States and Europe. In [6], the authors have presented a bi-level model to minimise the total costs of an isolated microgrid and maximise the revenues of a storage system using a DR scheme. Mathematical optimisation models in a real energy hub considering demand response under uncertainties have been proposed in [7, 8] to minimise the operation costs. Linear and nonlinear optimisation models have been proposed in [9, 10] to assess the economic feasibility of providing DR programs by hydrogen production units and their effect on power system flexibility. An experimental methodology has been introduced in [11]

to identify the flexibility of customers in response to financial incentives. The authors have examined the relationships of home appliance usage, energy consumption, and participation in incentive-based DR programs (IBDRPs) for peak load reduction in [12]. The impact of a time-of-use (TOU) program on consumption patterns of the residential consumers has been studied in [13]. Although TOU design has been employed as a powerful approach to change customers electricity consumption, current TOU programs are not as effective as required in many developed countries due to the complexity of human behaviour. Some metrics have been used in [14] to assess the DR flexibility of heat pumps. A control algorithm for the load aggregation has been presented by using an energy consumption tool. Compared to [14], it is also possible to examine the total consumption at each bus rather than modelling of the individual consumption pattern for residential loads. In this manner, DR programs let the system operator plan a proper production capacity. In [15], the influence of customers participation level in an emergency DR program (EDRP) and the effect of incorrect incentives on the microgrid performance have been studied. In the abovementioned studies, TOU or IBDRPs have been used without considering reliability standards and different types of consumers whose comfort preferences have not been examined when participating in such programs.

Apart from the economic point of view, DR programs have also been employed in several studies for enhancing the reliability of the network by considering renewable energy penetration and unforeseen events [16, 17]. In [18], a new formulation of reliability indices has been proposed considering the outages of generation units where the customers participate in both energy and reserve scheduling through DR. However, the hourly price of electricity and incentives have not been calculated. Transmission switching has been deployed in a unit commitment (UC) problem in [19, 20] to improve grid flexibility. However, demand-side activities have been overlooked. In [21], the authors have proposed a method that evaluates DR penetration to support the reliability of electricity grids. A probabilistic modelling strategy to maximise reliability through DR in emergency conditions has been offered in [22]. However, only the EDRP and incentives have been considered in [21, 22], where consumer behaviour and electricity price design were not taken into account. Several flexible resources such as a DR program and energy storage units to provide the grid with enough flexibility have been considered in [23]. However, outages of generation units or transmission lines have not been examined. Besides, the proposed model has mainly focused on the generation-side scheduling and ramp products, where the calculation of optimal electricity rates considering consumers role for scheduling of the demand side has not been studied.

Information gap decision theory (IGDT) based models have been proposed in [24, 25] to solve the UC problems integrated with DR considering electric vehicles (EV) and wind power uncertainties. However, contingencies as a result of network component outages and customers behaivour have not been taken into account for an ideal price design. In [26], a security-constrained unit commitment (SCUC) model linked with DR plans has been used in an islanded microgrid to maximise the expected benefits of the operator considering the uncertainties of loads and renewable energy sources. For the optimal scheduling of a virtual power plant considering DR and the influence of the risk on decision making, a stochastic framework has been presented in [27]. The authors have foreseen electricity market prices in price-based DR programs (PBDRP). However, the calculation of incentives in EDRPs and the behaviour and comfort indices of consumers have not been taken into account in the optimisation model in [26, 27].

A data-driven UC method considering load and renewable production uncertainties has been implemented in [28] to minimise total operating costs while ensuring system safety. A flexible uncertainty set strategy has been introduced in [29] to deal with the uncertain production of renewable energy sources in UC, where DR has been applied to overcome the risk of load shedding and renewable energy curtailment. A set of reserve limits have been elaborated in [30], considering the activation cost of reserves in high renewable-penetrated power systems. A SCUC model considering the coordinated performance of DR and hydrogen storage systems in the presence of wind energy has been presented in [31]. In [32], a scenario-based SCUC model has been introduced considering uncertain wind power generation with the Weibull distribution function. The integration of the aggregated EV fleets and DR into power systems has been studied in [33] using the SCUC to minimise total operating costs and examine the reliability of power systems. The presented UC model in [34] has analysed the frequency dynamics of the power system where the impact of wind turbines, PEVs and DR have been investigated. While the above-mentioned studies have looked at different aspects of integrated UC and DR models, the behaviour and comfort indices of consumers have not been taken into account in the proposed optimisation models.

According to the literature review, the consequences of outages are reduced by DR, and responsive loads, by adjusting their consumption, help the operators to improve the reliability level. Electricity consumers also desire to minimise their electricity bills by participating in DR programs and appropriate load scheduling. However, participation in DR programs has a great impact on consumers comfort [35]. If consumers perceive difficulty more than the achievable financial compensation, they might refuse a DR

program. Moreover, without considering the impacts of human behaviour and comfort, unacceptable errors arise in evaluating the effectiveness of DR strategies. In [36], the authors have suggested a DR algorithm to study the eagerness of customers to participate in a DRP. However, the price design for optimal supply-side scheduling considering network flexibility has not been examined. A DR model in which residential loads are sorted into several categories according to various DR programs has been presented in [37]. However, consumers comfort index, optimum incentives, and reliability measures were not considered. In [38], a multi-objective algorithm has been applied to solve the scheduling problem. User preference has been evaluated from historical usage patterns. A comfort model, which includes psychological aspects and predicts the rate of unsatisfied residents has been presented in [39]. While consumer comfort and bill reduction at the residential level is the point of focus in [38, 39], calculation of prices and incentives and reliability constraints have not been included in the model.

System operators or utilities persuade the clients by proposing cost drops as a result of reducing energy consumption or with greater incentives in peak hours, which is more acceptable by customers with less operational restrictions on their loads. While comprehensive models have been offered in literature regarding the dynamic electricity pricing, a wide range of customer viewpoints regarding the fluctuations of prices and incentives has remained unexplored, where their satisfaction and behaviour have not been addressed thoroughly. Hence, customer behaviour and comfort as fundamental principles must be included in the optimal scheduling of demand units to improve the reliability and efficiency of DR programs [35].

The main aim of this work is to define an accurate model of DR considering customer behaviour and the effect of customer preferences on the optimal power system operation. Instead of focusing on individual consumption pattern modelling in the residential sector and at the distribution level, the introduced approach focuses on total consumption at the transmission level. This chapter further develops a pricing algorithm to find the optimal electricity prices and incentives to guarantee network reliability and comfort of customers, while minimising system operation costs in the presence of uncertainties. Two types of consumers are used for modelling the involvement of users in DR. In the employed EDRP, a factor that shows the value of the incentive payment perceived by the customers is used. Several cases are considered to model the effect of the outage of generators or transmission lines and behaviour of customers on power systems operation.

6.2 Methodology

This part explains the proposed strategy to combine UC and DRPs, considering network constraints and reliability measures. Contingencies are included in a two-stage SCUC problem by using a probabilistic mixed-integer linear program (MILP) model, and the performance of both supply- and demand-sides are optimised concurrently. The first stage decision variables, which are linked to market-clearing, are given before the scenarios occur. These variables include start-up and shut-down costs, power generation, up and down reserve of each unit, and DR decisions. The second stage variables associated with uncertainties and the real performance of the system consider the values of up and down spinning reserves and the quantity of unintentional load shedding in all scenarios.

6.2.1 DR formulation

Electricity consumption, like many products, is sensitive to the price. When the electricity price drops, the customers show elasticity and might have the intention to increase the demand. On the other hand, by an increase in the electricity price, consumers try to reduce their consumption. To model this sensitivity, the concept of elasticity of demand is used in this chapter.

The elasticity of demand, which is shown in (6.1), is defined as the electricity demand change at h^{th} interval Δd_h concerning the variation of electricity price at h'^{th} period $\Delta\rho_{h'}$. The elasticity matrix contains self and mutual elasticity elements (see (6.1)). $\rho^0_{h'}$ and d^0_h are the baseline price and demand at hours h' and h, respectively.

$$E_{hh'} = \frac{\rho^0_{h'}\Delta d_h}{d^0_h \Delta\rho_{h'}} \quad \begin{cases} \leq 0, & \text{if} \quad h = h' \\ \geq 0, & \text{if} \quad h \neq h' \end{cases} \tag{6.1}$$

6.2.1.1 Customers rationality

A crucial point in describing the behaviour of consumers relates to the time range of their rationality. The price elasticity matrix (PEM), which measures the sensitivity of consumers to the price, will have non-zero records only within a time range covered by the perception of consumers. Considering the time range, customers could be classified into five different types. The first type is the *short-range consumers* (SRCs) who do not optimise their consumption and think only about the price at the current time interval. They could, therefore, be represented by a diagonal PEM. The ideal

Table 6.1: A section of PEM for LRCs.

h	7	8	9	10	11	12	13
2	0.01	0.01	0.01	0.012	0.012	0.013	0.013
...	...	...	...	...	...	...	...
7	−0.01	0.017	0.018	0.019	0.02	0.022	0.021
8	0	−0.01	0.015	0.016	0.018	0.019	0.019
9	0	0	−0.02	0.015	0.017	0.018	0.016
10	0	0	0	−0.05	0.015	0.016	0.017
11	0	0	0	0	−0.1	0.02	0.016
12	0	0	0	0	0	−0.16	0.02

consumers are defined to be the ones who take a long-range outlook in decision making. In that way, the *long-range consumers* (LRCs) choose how to shift and optimise their consumption over a wide range of hours following variations in prices. The PEM of the LRCs might have non-zero coefficients anywhere during the 24 hours. The third type covers deferring consumers who pay attention to the current and future prices only. These consumers, unlike LRCs who optimise their load throughout the day, change their consumption over a shorter range of hours into the future. On the other hand, the behaviour of advancing customers is affected by current and past prices. The PEMs of these consumers would be similar to deferring consumers except that there will be non-zero elements on and above the diagonal indicating their insight into current and past periods. Finally, *mixed consumers* (MCs) whose electricity demand is influenced by past, present and future electricity rates. The elasticity values for LRCs in [1] are used along with new elasticity coefficients for MCs depending on the rationalities explained above. A mixture of postponing, advancing, and short-range consumers is taken into account here. It is assumed that the awareness of MCs goes into six earlier and forthcoming hours. Non-zero elements will be on both sides of the diagonal in the PEM of MCs. Tables 6.1 and 6.2 show the PEM sections for LRCs and MCs, respectively.

Another notable point is that the behaviour of customers in PBDRPs, where real-time (RT) prices are applied, is different than their behaviour in EDRPs. Losses have a greater impact than the effect of benefits on the customers preferences. In PBDRPs, where the highest prices are set for the peak hours, consumers perceive any load shift to the off-peak hours as a loss. On the other hand, in an EDRP, customers see the obtained remunerations by load reduction and/or load shifting as profits. Hence, while the implementation of both programs needs the same action, customers perceive the results as penalties and rewards, which have opposite effects on their

Table 6.2: A Section of PEM for MCs.

h	16	17	18	19	20	21	22
16	−0.04	0.025	0.025	0.02	0.017	0.015	0.014
17	0	−0.16	0.1	0.08	0.025	0.02	0.017
18	0	0	−0.45	0	0	0	0
19	0	0	0.019	−0.25	0	0	0
20	0	0	0.02	0.019	−0.22	0	0
21	0	0	0.03	0.025	0.02	−0.2	0
22	0	0	0.033	0.027	0.021	0.022	−0.18

decision making. In this concept, the perceived effect of penalties or losses is steeper than perceived values of rewards and gains [40, 41]. Thus, the experienced value by consumers, which they respond to, is not the same as the given value of the imposed prices or offered incentives. ψ is a weighting factor representing the value perception of the incentive remunerations.

Considering the above-mentioned points, the proposed method modifies the general economic model of DR presented in [42] by considering the loss-gain factor and adding constraints related to consumers payment and consumption way to contemplate the behavioural aspects and preferences of consumers. Accordingly, optimal electricity prices in PBDRPs and incentives in EDRPs are calculated to manage the consumption.

So, the term $\psi A_{bh'}$ is included in the DR model to compare the results of PBDRPs and EDRPs. The relation between power price $\rho_{bh'}$ and the electricity consumption level at each bus d_{bh} is clarified in (6.2) as the increase of tariff and reward $A_{bh'}$ at each bus and hour can flatten the consumption profile in the peak hours, however, the degree of load decline is not identical. $\rho^0_{bh'}$ and d^0_{bh} are the baseline price and demand at bus b and hours h' and h, respectively.

$$d_{bh} = d^0_{bh}\left[1 + \frac{\sum_{h'=1}^{24} E_{hh'}(\rho_{bh'} - \rho^0_{bh'} + \psi A_{bh'})}{\rho^0_{bh'}}\right] \tag{6.2}$$

Fig. 6.1 shows the process of calculating RT rates and incentives for PBDRPs and EDRPs considering the objective function and given constraints. The goal is to determine the incentives and the price deviations $\Delta\rho_{bh}$ from the base line price $\rho^0_{bh'}$ to minimise the net operation costs and ensure system reliability. First, the conventional UC is performed to find the flat rate, and consequently, RT prices in PBDRPs and incentives during peak hours in EDRPs for all buses are obtained. After calculating RT rates and incentives at each load bus and time, the modified demand profile is entered as an

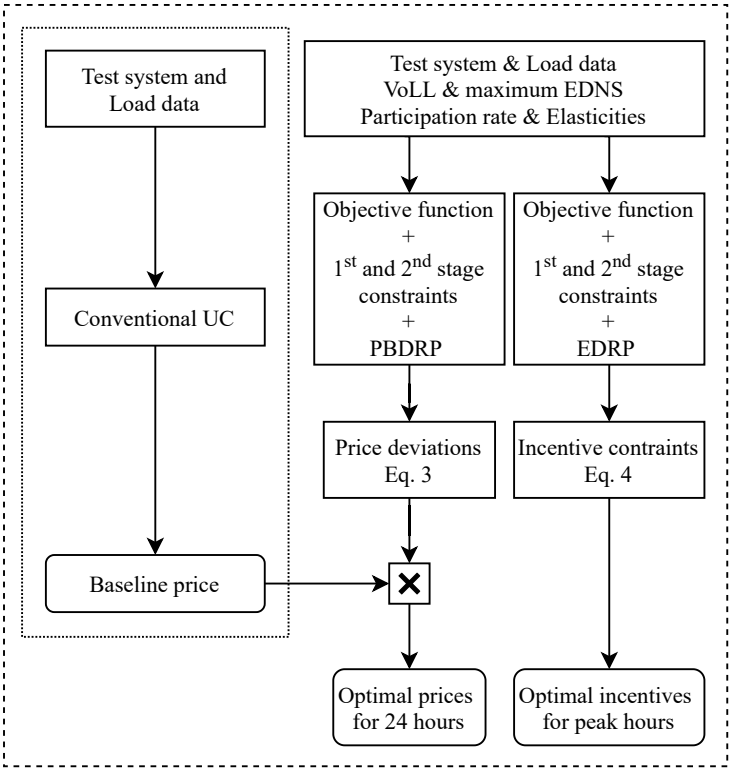

Figure 6.1: Method to find real-time prices and incentives.

input to the supply-side scheduling section. This link between supply and demand sides could ensure a flexible and efficient power system operation.

6.2.1.2 DR constraints

Several constraints must be considered to find a suitable pricing programme. It is acceptable to allocate the lowest price to the period with minimum consumption level, fifth period here [43]. Consequently, the electricity price ρ_{bh} compared to the the baseline rate ρ^0_{bh} should raise according to the electricity demand at each hour. Twenty-four limitations for change in prices are considered (see (6.3)). The larger the consumption of hour h is, the larger $\Delta\rho_{bh}$ should be set for that hour. This variable is negative for (h= 2-8), which suggests lower rates than the flat rate. $\Delta\rho_{bh}$ assumed as a free variable for (h= 1, 9, 14-16, 23-24) and as a positive variable for the remaining hours, which means consumers are charged with higher rates than the flat rate.

$$\Delta\rho_{bh} = \frac{\rho_{bh} - \rho^0_{bh}}{\rho^0_{bh}} \tag{6.3}$$

In addition to the PBDRP, as mentioned before, an EBDRP is also analysed along with the SCUC problem. By dividing the peak hours into three peak periods, it is acceptable to designate the higher incentive values to the periods with more consumption. To have a suitable incentive scheme, inequality (6.4) has been considered to define the logical range of incentives in peak hours. TLP represents the hours with lower peaks (h = 10-13, 17, 21-22), TMP represents the hours with medium peaks (h = 19, 20) and THP represents the peak period with the highest consumption, h = 18.

$$0 \leq A^{\text{TLP}}_b \leq A^{\text{TMP}}_b \leq A^{\text{THP}}_b \tag{6.4}$$

The maximum available demand at each bus, which can be changed at different hours, is shown in (6.5). $\overline{\text{DR}_b}$ is the maximum reply of consumers to DR signals at bus b. Consulting the values reported in [44–46], the maximum DR potential for demand modification is assumed to be 15% at all load buses, which guarantees a load increase at low-load or off-peak hours does not create a larger peak for the system.

$$-\overline{\text{DR}_b} d^0_{bh} \leq \Delta d_{bh} \leq \overline{\text{DR}_b} d^0_{bh} \tag{6.5}$$

As mentioned before, if the proposed method ignores the preferences of customers, the optimum points can make an undesirable load shifting and affect the comfort of customers. Consumption way and payment indices are used in this work to quantify consumers satisfaction. The constraints for consumption way index (CWI) and the payment index (PI) are formulated as (6.6) and (6.7), respectively. Customers ideally prefer not to change their consumption or minimise it. Thus, smaller Δd_h and larger CWI show that consumers face less discomfort. Undeniably, a larger PI will reduce customer payment CP_h overall and bring more satisfaction. ΔCP_h is the change in the payment of consumers at hour h. Lower bounds for CWI and PI are extracted from [47]. Moreover, to guarantee users convenience, it is ensured by (6.8) that the overall energy usage at every bus remains unchanged during the DR exertion. The average consumption delay index (CDI) (6.9) is also considered to show the average time that consumers shift the usage time of one MW electricity while participating in DR programs compared to the situation without demand response implementation. $\Delta d_{hh'}$ is the exchanged demand between hours h and h'.

$$\text{CWI} = \frac{\sum_{h=1}^{24} d_h^0 - |\Delta d_h|}{\sum_{h=1}^{24} d_h^0} \geq 0.95 \tag{6.6}$$

$$\text{PI} = \frac{\sum_{h=1}^{24} \text{CP}_h - \Delta\text{CP}_h}{\sum_{h=1}^{24} \text{CP}_h} \geq 1.02 \tag{6.7}$$

$$\sum_{h=1}^{H} \Delta d_{bh} = 0 \tag{6.8}$$

$$\text{CDI} = \frac{\sum_{h'=1}^{24} \sum_{h=1}^{24} |\Delta d_{hh'}||h - h'|}{\sum_{h=1}^{24} |\Delta d_h|} \tag{6.9}$$

6.2.2 Objective function

The proposed model aims to schedule the units at minimum production costs without jeopardising system security when the system encounters contingencies. The objective function (see (6.10)) covers seven terms, among which terms 1–4 are linked to first-stage choices, and terms 5–7 are associated with the second stage. The first-stage choices are made before the realisation of scenarios in contingencies. Hence, a conventional UC problem is performed in the first stage to define the commitment status of generators and their programmed energy and reserve capacity. The reliability limits of the system are examined after the realisation of scenarios in the second stage. A DC optimal power flow (DC-OPF) is performed in the second stage to optimise the volume of deployed down- and up-spinning reserves and load curtailment in each scenario[1] [49]. In this manner, system security will be guaranteed based on the desired maximum expected demand not served (EDNS) value set by the system operator.

Precisely, the first and second terms handle the energy costs and the start-up costs of generators, third and fourth terms calculate the costs of scheduling down- and up-spinning reserves, fifth and sixth terms define the costs associated with the deployment of down-and up-spinning reserves in scenarios, and the last term is the costs of load shedding. So, the stage two in the proposed model includes the costs of providing supply-load balance in scenarios.

[1]DC–OPF is a fast method used mainly to solve market clearing problems, can be applied to large models and is accurate enough to address the issues in this chapter. The other method, AC–OPF, is primarily used for optimal operation and control actions. Continuous efforts are being made to reduce computation time and increase the system size in the AC–OPF models [48].

$$\text{OF} = \sum_{h=1}^{H}\sum_{g=1}^{G}\Big[\text{FC}_{gh}I_{gh} + \text{SUC}_{gh} + \text{SRC}^{D}_{gh}\text{SR}^{D}_{gh} + \text{SRC}^{U}_{gh}\text{SR}^{U}_{gh}\Big] + \sum_{s=1}^{S}\alpha_s\Bigg[\sum_{h=1}^{H}\sum_{g=1}^{G}\Big(\text{SRC}^{D}_{gh}\text{SR}^{D}_{ghs} + \text{SRC}^{U}_{gh}\text{SR}^{U}_{ghs}\Big) + \sum_{h=1}^{H}\sum_{b=1}^{B}V^{\text{Sh}}_{bh}L^{\text{Sh}}_{bhs}\Bigg] \tag{6.10}$$

Looking at (6.10), H, G, S, and B are the number of scheduling hours, generating units, scenarios, and buses, respectively. FC_{gh}, I_{gh}, and SUC_{gh} are the fuel cost, the commitment state, and the startup cost of unit g at hour h, respectively. SRC^{D}_{gh} and SR^{D}_{gh} are the down-spinning reserve cost and the down-spinning reserve of production unit g at hour h. Similarly, SRC^{U}_{gh} and SR^{U}_{gh} are the up-spinning reserve cost and the up-spinning reserve of generator g at hour h. α_s is the probability of scenario s. SR^{D}_{ghs} and SR^{U}_{ghs} are the deployed down- and up-spinning reserve of unit g at hour h in scenario s, respectively. V^{Sh}_{bh} is the value of lost load in bus b at time h, and L^{Sh}_{bhs} is the load shedding in bus b at time h in scenario s.

In case of the EBDRP, IC which calculates the amount of incentive payed to the customers will be added to the objective function. This term has been linearised using [50] in order to fit in the linear model of this study.

$$\text{IC} = \sum_{h=1}^{H}\sum_{b=1}^{B}A_{bh}(d^{0}_{bh} - d_{bh}) \tag{6.11}$$

The following assumptions have been considered:

- It is assumed that shut down costs are negligible compared to other expenses such as startup costs.
- Losses over transmission lines are ignored.
- Piece-wise linear approximation is adopted for the incremental cost function of thermal units to facilitate reaching a real-time solution without a notable impact on the accuracy.
- Outage of a generator or a transmission line is taken into account in contingency events as multiple outages have approximately low possibilities while adding more computational complexity.

6.2.2.1 First stage constraints

The first stage constraints are given in this section. The costs of generation units are defined as an incremental cost function in a linear piece-wise form. The generation cost of generator g at hour h is given by (6.12).

$$\begin{aligned} \mathrm{FC}_{gh} &= \underline{\mathrm{FC}_g} I_{gh} + \sum_{f=1}^{F} \beta_{fg} P_{gh}^{f} \\ \text{where} \qquad & 0 \le \mathrm{P}_{\mathrm{gh}}^{\mathrm{f}} \le \overline{\mathrm{M}_{\mathrm{fg}}} \end{aligned} \tag{6.12}$$

$\underline{\mathrm{FC}_g}$ is the minimum fuel cost of generator g and F is the number of segments in piece-wise linearised fuel cost. β_{fg}, P_{gh}^{f}, and $\overline{M_{fg}}$ are the slope, the generation, and the maximum production of segment f in cost curve of the generator g, respectively.

The linear relation of the total scheduled power of the generation unit P_{gh} is defined by (6.13). $\underline{P_g}$ is the minimum production of generator g.

$$P_{gh} = \underline{P_g} I_{gh} + \sum_{f=1}^{F} P_{gh}^{f} \tag{6.13}$$

- Start-up cost constraints of generation units

$$0 \le \mathrm{SUC}_{gh} \le K_g (I_{gh} - I_{g,h-1}) \tag{6.14}$$

where SUC_{gh} is the startup cost of unit g at hour h, K_g is the start-up cost of generator g, and I_{gh} is the commitment status of generator g at hour h.

- Constraints of spinning reserves

Constraints of down- and up-spinning reserves are shown in (6.15) and (6.16). $\overline{P_g}$ is the maximum production of generator g. SR_{gh}^{D} and SR_{gh}^{U} are the down- and up-spinning reserves of generator g at hour h. R_g^D and R_g^U are ramp-down and ramp-up of generator g. T is the spinning reserve market lead time.

$$P_{gh} + \mathrm{SR}_{gh}^{U} \le \overline{P_g} I_{gh}, \quad P_{gh} - \mathrm{SR}_{gh}^{D} \ge \underline{P_g} I_{gh} \tag{6.15}$$

$$0 \le \mathrm{SR}_{gh}^{U} \le R_g^U T, \quad 0 \le \mathrm{SR}_{gh}^{D} \le R_g^D T \tag{6.16}$$

- Up and down constraints of generation units

$$P_{gh} - P_{g,h-1} \leq R_g^U I_{gh} + \underline{P_g}(1 - I_{g,h-1}) \tag{6.17}$$

$$P_{g,h-1} - P_{gh} \leq R_g^D I_{g,h-1} + \underline{P_g}(1 - I_{gh}) \tag{6.18}$$

- Time constraints of generation units

$$\sum_{h'=h+2}^{h+T_g^+} (1 - I_{gh'}) + T_g^+(I_{gh} - I_{g,h-1}) \leq T_g^+ \tag{6.19}$$

$$\sum_{h'=h+2}^{h+T_g^-} I_{gh'} + T_g^-(I_{g,h-1} - I_{gh}) \leq T_g^- \tag{6.20}$$

- Ramp-down and ramp-up constraint

$$P_{gh} - P_{g,h+1} \leq R_g^D, \quad P_{g,h+1} - P_{gh} \leq R_g^U \tag{6.21}$$

- Active power equilibrium

The power balance between loads and generation units on each bus is ensured by (6.22). P_{gh} and $P_{bb'h}$ are the production of generator g and the active power of the transmission line from bus b to bus b' at hour h, respectively. $X_{bb'}$ and Θ_{bh} are the line reactance from bus b to bus b' and the voltage angle at bus b and hour h, respectively.

$$\begin{gathered} \sum_{g=1}^{G_b} P_{gh} - d_{bh}^0 - \Delta d_{bh} = \sum_{b'=1}^{B} P_{bb'h} \qquad b' \neq b \\ \text{where} \quad P_{bb'h} = \frac{1}{X_{bb'}}(\Theta_{bh} - \Theta_{b'h}) \end{gathered} \tag{6.22}$$

6.2.2.2 Second stage constraints

The outage scenarios are taken into account by the equations of stage 2, which are given hereafter. Examining reliability measures in scenarios depends on the determination of contingencies, which could be done by enumeration techniques. Once the set of contingencies are determined, one must focus on analysing their possibility. The forced outage rate (FOR) of components in each contingency is employed to calculate the failure possibility α_s (see (6.23)). c' is the failed component, c is the index of components, and C is the number of components.

$$\alpha_s = \text{FOR}_{c'} \prod_{\substack{c \in C \\ c \neq c'}} (1 - \text{FOR}_c) \tag{6.23}$$

FOR is calculated based on the statistical data of that component using (6.24), where MTTR and MTTF stand for mean time to repair and mean time to failure, respectively.

$$\text{FOR} = \frac{\text{MTTR}}{\text{MTTR} + \text{MTTF}} \tag{6.24}$$

- Active power equilibrium considering scenarios

Frequency stability issues as a result of contingency events are one of the main concerns of system operators. However, the balance between generations, losses and loads ensures frequency stability throughout the system. In contingency events, power balance at each bus is ensured by loads and generators. So, the DC power flow equation applied to the system is shown in (6.25). τ and υ present the availability condition of transmission lines and generation units, respectively. During the component outages, they are set to 0 while they are 1 otherwise.
SR^U_{ghs} and SR^D_{ghs} are the up- and down-spinning reserves of generator g at hour h in scenario s. L^{Sh}_{bhs} represents the amount of load curtailment at bus b. P_{lhs} is the active power of transmission line l at hour h from bus b to b' in scenario s, while $\overline{P_l}$ is the maximum allowable power on line l.

$$\begin{gathered} \sum_{g=1}^{G_b} \upsilon [P_{gh} + \text{SR}^U_{ghs} - \text{SR}^D_{ghs}] - d_{bh} - L^{\text{Sh}}_{bhs} = \sum_{l \in L_b} \tau P_{lhs} \\ \text{where} \quad -\overline{P_l} \leq P_{lhs} = \frac{1}{X_{bb'}} (\Theta_{bhs} - \Theta_{b'hs}) \leq \overline{P_l} \end{gathered} \tag{6.25}$$

- Constraints of spinning reserves in contingencies

The reliability of the system is secured by down- and up-spinning reserves together with DR plans when the system operator monitors changes in demand-side behaviour or the component availability status. The relationship between the first- and the second-stage spinning reserve variables is specified in (6.26).

$$0 \leq \mathrm{SR}^{U}_{ghs} \leq \sigma_{ghs}\mathrm{SR}^{U}_{gh}, \quad 0 \leq \mathrm{SR}^{D}_{ghs} \leq \sigma_{ghs}\mathrm{SR}^{D}_{gh} \tag{6.26}$$

where σ_{ghs} is the reserve state of generator g at hour h in scenario s, which is 0 if the unit outage has occurred and otherwise it is considered 1. It ensures that only available production units in scenarios would provide spinning reserves.

- Load shedding constraint

The generation shortage may cause involuntary load shedding to ensure the system security. Eq. (6.27) guarantees that the amount of load shedding in each scenario at each bus remains less than the electricity consumption of the respective bus.

$$0 \leq L^{\mathrm{Sh}}_{bhs} \leq d_{bh} \tag{6.27}$$

6.2.3 Reliability assessment

Using [51], to measure the reliable scheduling this work employs an expected demand not served (EDNS) index, which is achievable by multiplying the value of load shedding and the likelihood of the component failure in each scenario s at bus b and hour h (see (6.28)). As shown in (6.28), the continuous power generation and consumption are guaranteed by the highest permitted amount of EDNS, which is set by the system operator.

$$\mathrm{EDNS}_h = \sum_{b=1}^{B}\sum_{s=1}^{S} \alpha_s L^{\mathrm{Sh}}_{bhs} \leq \overline{\mathrm{EDNS}} \tag{6.28}$$

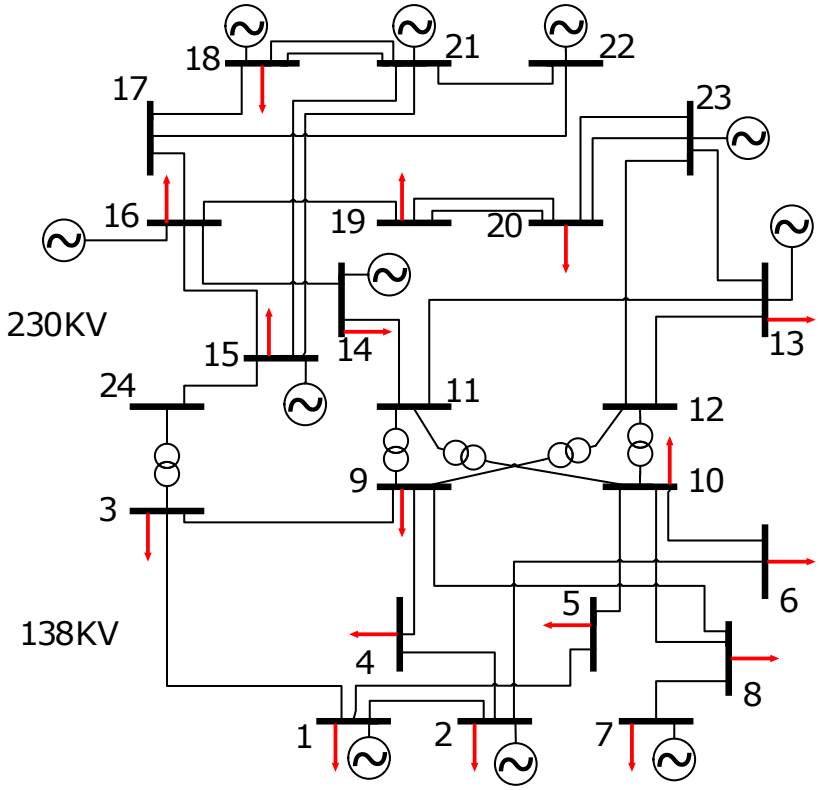

Figure 6.2: Schematic of the 24-bus reliability test system

6.3 Test system

Fig. 6.2 shows the IEEE 24-bus test system with overall generation and load capacity of 3,405 MW and 2,850 MW, respectively. The generation and consumption data, ramp rates, reliability factors, cost coefficients etc., are taken from [43]. The load profile is divided into three sections, including low consumption (2-8), off-peak (1, 9, 14-16, 23-24) and peak (10-13, 17-22) hours. The value of lost load (VoLL) is set to 150, 300 and 450 $/MWh for low-load, off-peak and peak periods, respectively. The maximum amount of EDNS is assumed 7 MW to ensure the reliability.

6.4 Results and discussion

The electricity generation planning without and with implementing DR are studied hereafter. First, the total system operating cost of $701,202 was obtained in the absence of contingency events and DRPs. By analysing component contingencies using the N – 1 criterion and under a flat rate price scheme, the system operator has to provide the required flexibility by optimal supply-side scheduling. As a result, a UC is obtained with the total operation cost of $831,991. This 18.7% increase in operating cost compared to the condition without contingencies is because of the extra costs due to the provision of reliability as at such times, the peak load production units should be started up and run at a non-economic point.

The proposed model is also applied to the system once without considering reliability constraints, where the maximum EDNS is ignored, and the influence of a contingency event on the system functioning is taken into account. As a result of ignoring the upper limit of 7 MW for EDNS, the average amount of calculated compulsory load shedding is higher (40.8 MW) compared to other cases, which implies this limit brings more consumers dissatisfaction resulting the total operation costs of $757,650.

Then, in the absence of DR, but by considering the maximum amount of EDNS as the reliability constraint $831,991 and 4.98 MW are found as the total calculated operation cost and the average amount of EDNS, respectively. The $74,341 increase in the operating cost compared to the case without limit for EDNS should be spent to supply the reliability necessities in case of contingency events.

To study the effect of DR programs on system reliability in case of component contingencies, price- and incentive-based DR programs are investigated in 2 cases. In the first case, where the total daily energy consumption should remain constant (see (6.8)), the proposed model aims to ensure reliable and flexible operation of the system by finding optimal hourly electricity prices. To guarantee the reliability, the EDNS should be below 7 MW at all buses and each hour. In the second case, constraints of energy, consumption way, and payment are neglected, and the target of implementing EDRP and PBDRP is the reduction of peak loads where the calculated hourly rates from the first case and incentives are applied.

In the following sections, two cases are examined in which LRCs and MCs are modelled by allocating DR patterns come from their PEMs. Besides, a behavioural factor is considered to show the various response of customers to incentives and punishments. The optimal hourly electricity prices in PBDRPs and optimum incentives at peak hours in EDRPs are calculated to minimise the system operational cost and ensure the reliability.

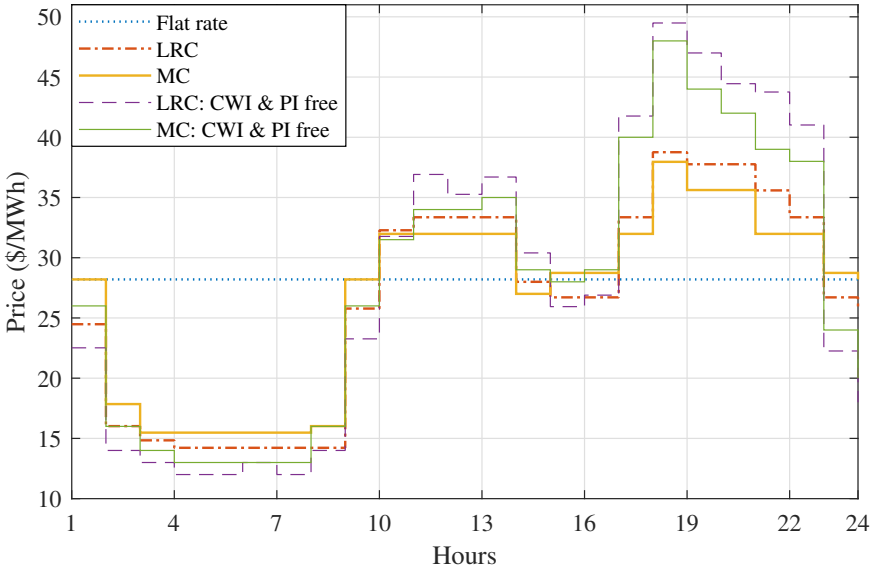

Figure 6.3: RT rates at each hour in Case 1

6.4.1 Case 1: DR with constant total energy consumption

In addition to the generation side scheduling, both reliability constraints and demand-side response are integrated into the problem in this case. Consequently, the load profile is modified according to the consumers response to the electricity rates. Fig. 6.3 gives the average RT tariffs for different types of customers. LRCs, compared to MCs, face prices with more deviation at low-load and peak hours. While the average and the standard deviation of the electricity price for LRCs are 26.4 and 8.8, respectively, the resulting values are 26.8 and 7.5 for MC consumers. This illustrates the ability of DR to decrease the average electricity prices for consumers.

Fig. 6.4 shows the influence of applying optimised RT rates on the load profile. During the peak hours, because of the higher rates, electricity consumption is reduced and shifted to the low-load hours, where electricity prices are much lower. Notably, compared with MCs, LRCs have a flatter load profile because of stronger price deviation where they face lower rates at low-load hours and higher rates at peak hours.

The results of applying the PBDRP in Case 1 are summarised in Table 6.3. The operational costs when LRCs and MCs participate in DR are reduced by 3.2% and 2.9%, respectively. Despite the reduction of operation cost, energy consumption remains invariable for all customers. The role of

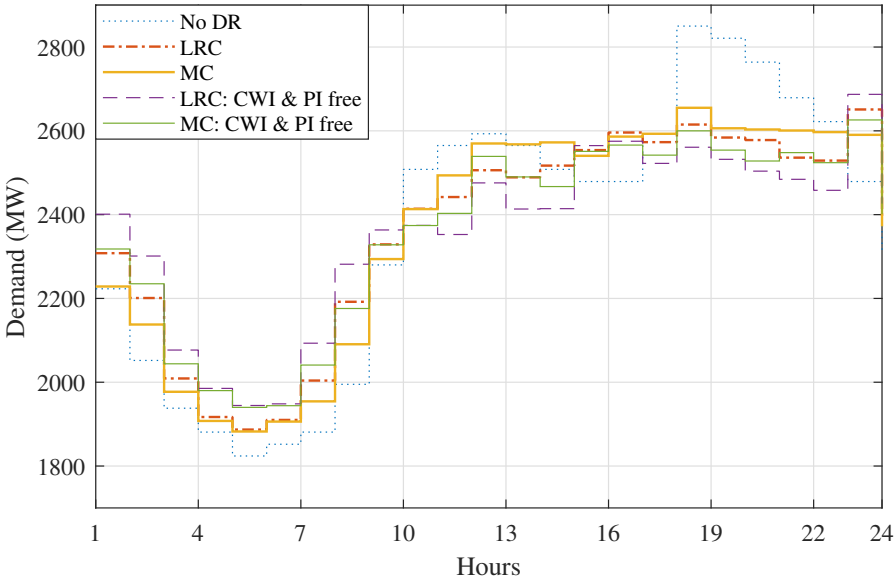

Figure 6.4: Demand profiles in Case 1

DR in decreasing consumers payments is also confirmed by the given results. Given CWI, PI, and the average EDNS indices in Table 6.3 show that the proposed method meets all the reliability and customers satisfactory constraints. Although LRCs change their load more than MCs and have lower CWI, higher PI shows the lower cost they should pay. Compared to MCs, the larger value for the average consumption delay index CDI between LRCs makes them more competent to shift their loads and reduce the average peak and EDNS values. The calculated values for EDNS confirm the efficiency of DR implementation to ensure the system reliability. As it is depicted in Fig. 6.5, the value of EDNS in all hours is always less than 7 MW, and generally decreases after using DR programmes compared with the base case without (w/o) DR implementation.

The rates have also been calculated for a situation that ignores the limits of CWI and PI. As a result of neglecting the CWI limit, the model reduces the load as much as possible during a contingency event to reduce the costs of the generation side by minimising the start-up and generation costs of expensive units, which is not close to real situations. On the other hand, by neglecting the limit for PI, the model changes the loads in a way to increase the CWI and decrease the EDNS. As a result, the customers payment will increase, which causes monetary dissatisfaction for consumers. For a sit-

Table 6.3: Results of the PBDRP implementation.

	Operation cost ($)	Consumers payment ($)	$\mathrm{Peak}_{\mathrm{avg}}$ (MW)	PI	CWI	CDI (Hour)	$\mathrm{EDNS}_{\mathrm{avg}}$ (MW)
w/o DR	831,991	1,600,100	2,656	1	1	0	4.98
Long-range customers	805,209	1,559,200	2,527	1.03	0.95	6.1	2.05
	96.78%	97.44%	95.14%				
Mixed customers	807,697	1,575,900	2,570	1.02	0.97	3.9	2.16
	97.08%	98.49%	96.74%				
Long-range customers	790,008	1,620,530	2,468	0.99	0.93	6.6	2.05
(w/o CWI & PI limits)	94.95%	101.28%	92.92%				
Mixed customers	797,605	1,625,804	2,510	0.98	0.94	4.3	2.16
(w/o CWI & PI limits)	95.87%	101.61%	94.50%				

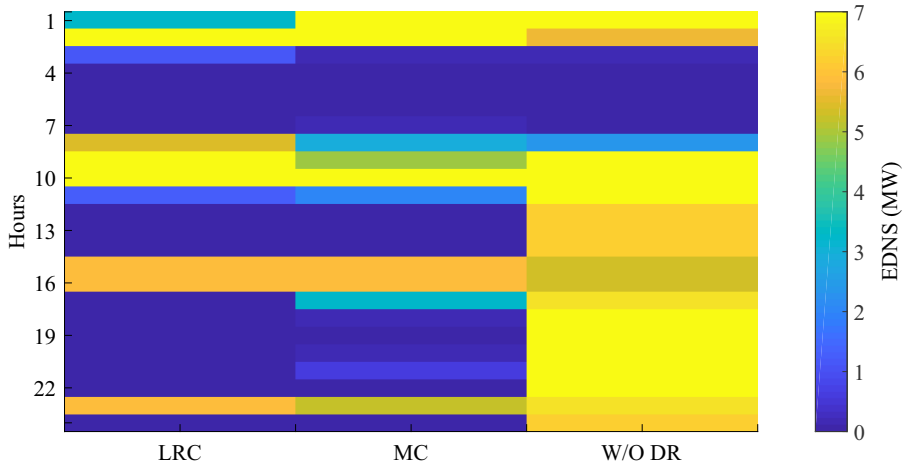

Figure 6.5: Calculated hourly EDNS values in different situations

uation that ignores the limits of CWI and PI, the prices (see Fig. 6.3) and electricity demand (see Fig. 6.4) change more violently, new peaks have emerged, and CWI and PI got worse (see Table 6.3) compared to the cases where a limit for those indices was set. The results show that operation costs in such a situation decrease, while customers experience an increase in their payments. Such a scenario would reduce customer satisfaction, reflected in a 2.5% and 4% decrease in CWI and PI, respectively.

Fig. 6.6 shows how DR programs could affect the generation mix. The legend shows bus numbers. In contingency events and without DR implementation, the system operator must commit expensive units, located at Buses 1, 2, 7, and 13 to secure the system reliability. When DR is implemented, i.e., the load can shift between periods, expensive units are committed for fewer hours at peak period compared to the situation without DR implementation.

Fig. 6.6 shows that the proposed method decreases the generated power of units located at mentioned buses in peak and off-peak hours. In the case of LRCs, the mentioned units are committed for fewer peak hours compared to the MCs. Therefore, the operation costs of the mentioned units are reduced and then decrease the total operating costs of the system, as given in Table 6.3.

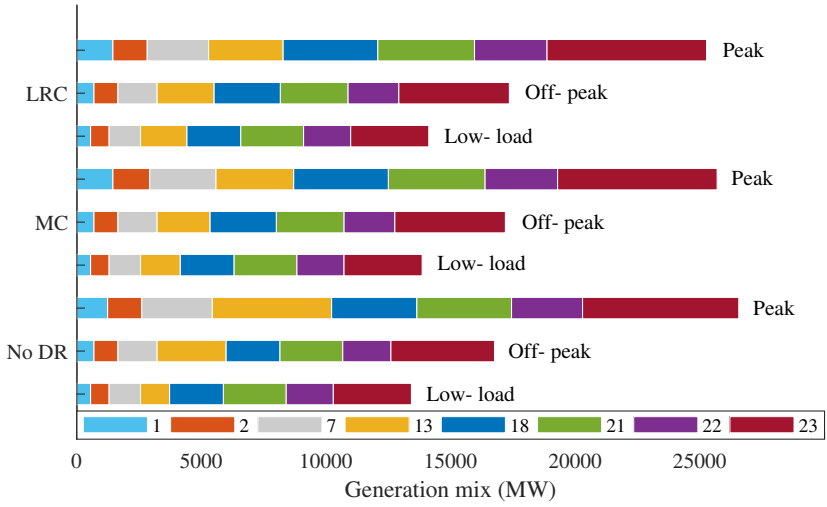

Figure 6.6: Effect of DR programs on the generation mix

6.4.2 Case 2: DR without energy constraint

EDRPs are also run for two types of consumers with different response characteristics. In this case, the energy consumption, consumption way and payment constraints are neglected, and it is assumed that the system operator aims to reduce electrical energy consumption during the peak period. So, in addition to the PBDRP, two options for the EDRP are studied. EDRP1 is an option without considering the loss-gain factor ($\psi = 1$). EDRP2 is the other choice that the loss-gain parameter changes in a range ($\frac{1}{8} \leq \psi \leq 1$). As explained before in Section 6.2, the loss-gain factor interprets a behavioural tendency where people are afraid of losses, and hate losing more than they like winning. Thus, losses appear to be be more than the earnings even though the value in monetary terms may be equal. For example, for $\psi = \frac{1}{4}$, it is assumed that loss of every dollar has the forth value of every dollar gained and so on.

The calculated incentives would cause a reduction in the peak hours demand, which reduces the burden on the generation side and the operation costs. On the other hand, the calculated incentives add costs to the system operator side due to the reward payments to the customers, which will be added to the objective function for this case.

It is acceptable to consider the highest incentive value for the period with a maximum consumption level. Consequently, the incentive values should decrease according to the electricity demand decrease at each peak

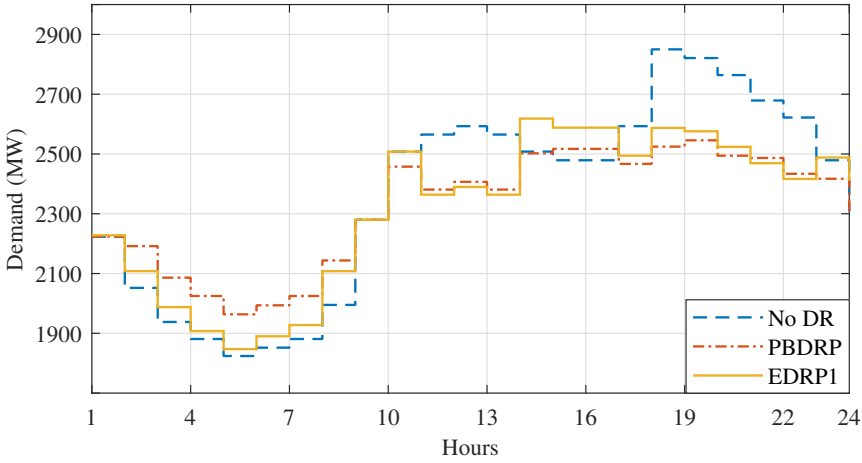

Figure 6.7: Demand profiles for mixed customers in Case 2

hour. Thus similar to the procedure of finding the optimal prices in Case 1, the incentives for peak hours would be calculated. The calculated average rewards per MWh demand reduction, compared to the baseline demand, in EDRPs, are given in Table 6.4. Accordingly, the load profiles are modified according to the consumers response to the incentives. Obtained incentives show that LRCs expect lower remuneration than MCs in peak hours. Fig. 6.7 and Fig. 6.8 illustrate the influence of applying planned RT tariffs and rewards on the load profile for MCs and LRCs.

According to the results shown in Table 6.5 and Fig. 6.9, both the EDRP and the PBDRP reduce the peak demand, and as a result, the operation costs, which are favourable for the system operators. On the other hand, the amount customers have to pay and, consequently, the utility revenue will decrease. The obtained results for CWI and PI show how ignoring their related constraints in Case 2 could affect the electricity bill of customers and the demand change. From the utility point of view, as long as $\psi \geq \frac{1}{3}$, the utility achieves its target better with EDRP, losing less revenue compared to PBDRP. On the other hand, taking the loss-gain factor $\psi \leq \frac{1}{4}$

Table 6.4: Calculated A_h ($/MWh)

Hour	10-13	17	18	19,20	21,22
MC	12.2	9.0	15.0	14.3	12.1
LRC	12.0	9.0	14.7	14.0	12.0

Table 6.5: Results of PBDRP, EDRP1, and EDRP2 for $\psi = \frac{1}{4}$

	Scenario	Peak_{avg} (MW)	Payment ($)	CWI	PI	CDI (Hour)
Mixed consumers	PBDRP	2,459 (-7.4%)	1,544,745	94.22%	1.03	2.5
	EDRP1	2,486 (-6.4%)	1,585,900	94.02%	1.01	1.2
	EDRP2 ($\psi = \frac{1}{4}$)	2,405 (-9.5%)	1,542,985	93.91%	1.04	1.3
Long-range consumers	PBDRP	2,367 (-10.8%)	1,527,847	92.46%	1.05	3.3
	EDRP1	2,430 (-8.5%)	1,568,439	91.87%	1.02	1.6
	EDRP2 ($\psi = \frac{1}{4}$)	2,309 (-13.0%)	1,516,647	91.60%	1.06	1.7

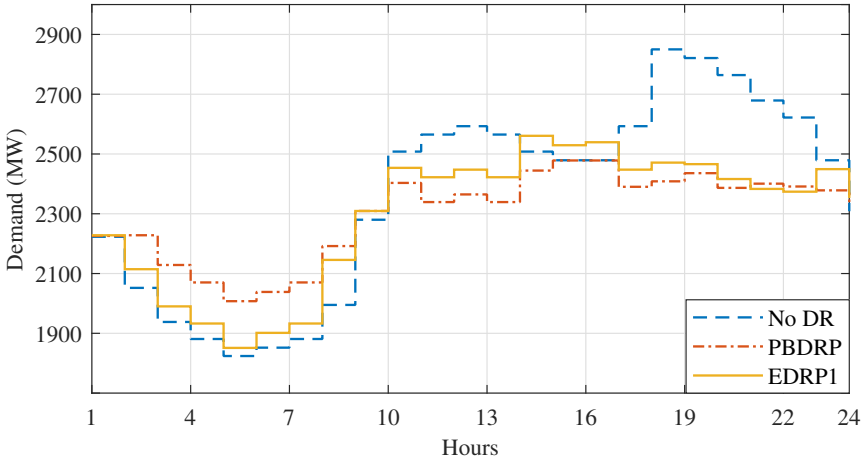

Figure 6.8: Demand profiles for long-range customers in Case 2

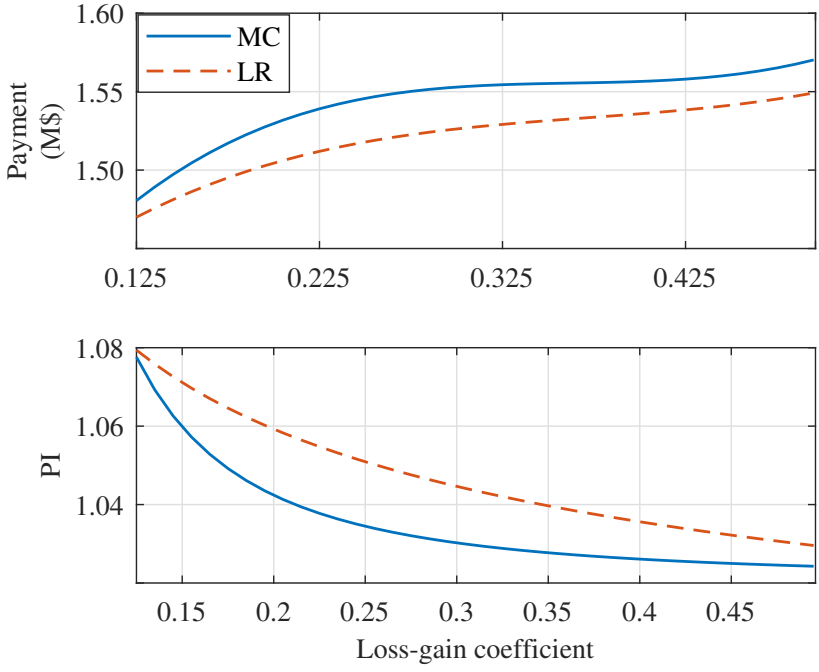

Figure 6.9: Results for $0.125 \leq \psi \leq 0.5$

into account, PBDRP outperforms EDRP. It is clear that when the loss-gain parameter changes in the range of ($\frac{1}{8} \leq \psi \leq 1$), the amount of ψA_h should be constant to get comparable change in the peak load. So, optimal incentive values should be offered to each type of customers during peak hours. The values of ψA_h, which are given in Table 6.4 illustrate the reliance of the offered incentives on the reward weighting factor ψ.

6.4.3 Computational complexity and implementation issues

To solve the proposed mixed-integer programming model CPLEX as a high-performance solver is used. CPLEX optimisers have been widely used by researchers to solve large and complex problems swiftly and with minimum user interference [49, 50, 52]. Each case has been run in less than 5 minutes on a 2.11 GHz Windows-based system with 16 GB of RAM. Thus, the proposed optimisation problem can be solved nearly in real-time, providing a fast response to changes in power system situations, electricity prices, or electricity demand.

With an increase in problem size, the run time could increase exponentially, which brings significant burdens for solving scheduling problems. However, to analyse a system with a large number of buses, lines, and scenarios some possible solutions are available. One of the most practised approaches to overcome computational complexity of large MILP models originates from the idea of decomposition, which divides a large problem into smaller non-complex subproblems. Reducing the number of scenarios and using supercomputers and methods to simplify the network are other available options to cope with computational complexity while considering larger systems in case studies.

6.5 Summary and conclusions

This chapter introduced a probabilistic day-ahead security-constrained scheduling problem with various integrated demand response programs considering consumers rationality for managing the contingency events. DR has been formed as a responsive shiftable/curtailable demand bidding mechanism that moves the consumption from peak hours to off-peak or low-load hours and ensures social welfare. This work emphasised the influence of consumers representation on the power system performance. The offered model studied the constraints of customers preferences in addition to the constraints of the traditional unit commitment algorithms.

The offered probabilistic model was formulated as a mixed-integer linear programming problem that deals with the SCUC. Both incentives and

hourly electricity prices were calculated in emergency and price-based demand response programs. The electricity consumption was adjusted by DR to control the outages in the power grid, and hence, the modified demand profile helped the system operator to reduce the start-up and reserve costs of generation units. The achieved results validated the ability of the suggested approach in decreasing the operational costs of the system, customers payment, and peak load by optimal scheduling of generation units and optimal use of the demand response potential without bringing notable discomfort to the customers.

The results also showed that consideration of different demand response programs, different types of consumers and comfort constraints have a significant impact on power system reliability and minimising daily operation cost. Overall, meaningful insight into system performance with real-time prices and incentives was obtained. Results suggested that system behaviour depends not only on the degree of elasticity but also on the time range of customers rationality. The implementation of optimal system dispatch necessitates the modelling of time-dependent elasticity to find the optimal scheduling solutions at different hours.

The impact of the loss-gain factor on the results of the demand response programs for peak reduction showed that when people are in a position where both earnings and losses are likely, they normally favour less risky options. If possible losses could be destructive or threaten customer lifestyle, they will generally reject the choice of participation in demand response programs that bring losses and discomfort. This is one reason for system operators to optimise the prices for reducing the consumer losses at peak-price periods, while they make sure that it can minimise the system operation costs. By limiting potential losses and maximising profits, current consumers will continue providing demand response and new consumers might join the demand response programs too.

Hence, the explained method could be used to determine optimal scheduling plans, and grid operators together with consumers could benefit from the offered method to schedule the generations units and loads in a way that meets the customers demand while the network reliability and consumers comfort are guaranteed.

References

[1] A. Dadkhah, B. Vahidi, M. Shafie-khah, and J. P. S. Catalão. *Power system flexibility improvement with a focus on demand response and wind power variability*. IET Renewable Power Generation, 14(6):1095–1103, 2020.

[2] A. Dadkhah, N. Bayati, M. Shafie-khah, L. Vandevelde, and J. Catalão. *Optimal price-based and emergency demand response programs considering consumers preferences*. International Journal of Electrical Power & Energy Systems, 138:107890, 2022.

[3] O. Sadeghian, M. Nazari-Heris, M. Abapour, S. Taheri, and K. Zare. *Improving reliability of distribution networks using plug-in electric vehicles and demand response*. Journal of Modern Power Systems and Clean Energy, 7(5):1189–1199, 2019.

[4] B. Vahidi and A. Dadkhah. *New demand response platform with machine learning and data analytics*. In Demand Response Application in Smart Grids, pages 113–137. Springer, Cham, 2020.

[5] F. Wang, H. Xu, T. Xu, K. Li, M. Shafie-Khah, and J. Catalão. *The values of market-based demand response on improving power system reliability under extreme circumstances*. Applied Energy, 193:220–231, 2017.

[6] Y. Li, Z. Yang, G. Li, Y. Mu, D. Zhao, C. Chen, and B. Shen. *Optimal scheduling of isolated microgrid with an electric vehicle battery swapping station in multi-stakeholder scenarios: A bi-level programming approach via real-time pricing*. Applied Energy, 232:54–68, 2018.

[7] M. Kermani, E. Shirdare, A. Najafi, B. Adelmanesh, D. L. Carnì, and L. Martirano. *Optimal Self-scheduling of a real Energy Hub considering local DG units and Demand Response under Uncertainties*. IEEE Transactions on Industry Applications, 57(4):3396–3405, 2021.

[8] M. Kermani, E. Shirdare, A. Najafi, B. Adelmanesh, D. Luca. Carnì, and L. Martirano. *Optimal Operation of a real Power Hub based on PV/FC/GenSet/BESS and Demand Response under Uncertainty*. In 2020 IEEE Industry Applications Society Annual Meeting, 2020.

[9] A. Dadkhah, D. Bozalakov, J. D. M. De Kooning, and L. Vandevelde. *On the optimal planning of a hydrogen refuelling station participating in the electricity and balancing markets*. International Journal of Hydrogen Energy, 46(2):1488–1500, 2021.

[10] A. Dadkhah, D. Bozalakov, J. D. M. De Kooning, and L. Vandevelde. *Optimal Sizing and Economic Analysis of a Hydrogen Refuelling Station Providing Frequency Containment Reserve*. In 2020 IEEE International Conference on Environment and Electrical Engineering and 2020 IEEE Industrial and Commercial Power Systems Europe (EEEIC/I&CPS Europe), 2020.

[11] M. Vallés, A. Bello, J. Reneses, and P. Frías. *Probabilistic characterization of electricity consumer responsiveness to economic incentives*. Applied Energy, 216:296–310, 2018.

[12] Q. Shi, C. Chen, A. Mammoli, and F. Li. *Estimating the profile of incentive-based demand response (IBDR) by integrating technical models and social-behavioral factors*. IEEE Transactions on Smart Grid, 11(1):171–183, 2019.

[13] L. Zhao, Z. Yang, and W. Lee. *The impact of time-of-use (TOU) rate structure on consumption patterns of the residential customers*. IEEE Transactions on Industry Applications, 53(6):5130–5138, 2017.

[14] L. Zhang, N. Good, and P. Mancarella. *Building-to-grid flexibility: Modelling and assessment metrics for residential demand response from heat pump aggregations*. Applied Energy, 233:709–723, 2019.

[15] M. Imani, P. Niknejad, and M. Barzegaran. *The impact of customers' participation level and various incentive values on implementing emergency demand response program in microgrid operation*. International Journal of Electrical Power & Energy Systems, 96:114–125, 2018.

[16] M. Amini, S. Talari, H. Arasteh, N. Mahmoudi, M. Kazemi, A. Abdollahi, V. Bhattacharjee, M. Shafie-Khah, P. Siano, and J. Catalão. *Demand response in future power networks: panorama and state-of-the-art*. In Sustainable interdependent networks II, pages 167–191. Springer, 2019.

[17] A. Dadkhah and B. Vahidi. *On the network economic, technical and reliability characteristics improvement through demand-response implementation considering consumers' behaviour*. IET Generation, Transmission & Distribution, 12(2):431–440, 2018.

[18] A. Fattahi, A. Nahavandi, and M. Jokarzadeh. *A comprehensive reserve allocation method in a micro-grid considering renewable generation intermittency and demand side participation*. Energy, 155:678–689, 2018.

[19] A. Nikoobakht, J. Aghaei, M. Mardaneh, T. Niknam, and V. Vahidinasab. *Moving beyond the optimal transmission switching: stochastic linearised SCUC for the integration of wind power generation and equipment failures uncertainties*. IET Generation, Transmission & Distribution, 12(15):3780–3792, 2017.

[20] A. Nikoobakht, M. Mardaneh, J. Aghaei, V. Guerrero-Mestre, and J. Contreras. *Flexible power system operation accommodating uncertain wind power generation using transmission topology control: an improved linearised AC SCUC model*. IET Generation, Transmission & Distribution, 11(1):142–153, 2017.

[21] B. Zeng, G. Wu, J. Wang, J. Zhang, and M. Zeng. *Impact of behavior-driven demand response on supply adequacy in smart distribution systems*. Applied Energy, 202:125–137, 2017.

[22] K. Kopsidas and M. Abogaleela. *Utilizing demand response to improve network reliability and ageing resilience*. IEEE Transactions on Power Systems, 34(3):2216–2227, 2018.

[23] E. Heydarian-Forushani, M. E. Golshan, M. Shafie-khah, and P. Siano. *Optimal operation of emerging flexible resources considering sub-hourly flexible ramp product*. IEEE Transactions on Sustainable Energy, 9(2):916–929, 2017.

[24] X. Dai, Y. Wang, S. Yang, and K. Zhang. *IGDT-based economic dispatch considering the uncertainty of wind and demand response*. IET Renewable Power Generation, 13(6):856–866, 2018.

[25] M. Ahrabi, M. Abedi, H. Nafisi, M. Mirzaei, B. Mohammadi-Ivatloo, and M. Marzband. *Evaluating the effect of electric vehicle parking lots in transmission-constrained AC unit commitment under a hybrid IGDT-stochastic approach*. International Journal of Electrical Power & Energy Systems, 125:106546, 2021.

[26] M. Vahedipour-Dahraei, H. Najafi, A. Anvari-Moghaddam, and J. M. Guerrero. *Security-constrained unit commitment in AC microgrids considering stochastic price-based demand response and renewable generation*. International Transactions on Electrical Energy Systems, 28(9):e2596, 2018.

[27] M. Vahedipour-Dahraie, H. Rashidizadeh-Kermani, A. Anvari-Moghaddam, and P. Siano. *Risk-averse probabilistic framework for scheduling of virtual power plants considering demand response and*

uncertainties. International Journal of Electrical Power & Energy Systems, 121:106126, 2020.

[28] C. Duan, L. Jiang, W. Fang, and J. Liu. *Data-driven affinely adjustable distributionally robust unit commitment*. IEEE Transactions on Power Systems, 33(2):1385–1398, 2017.

[29] Y. Du, Y. Li, C. Duan, H. B. Gooi, and L. Jiang. *Adjustable uncertainty set constrained unit commitment with operation risk reduced through demand response*. IEEE Transactions on Industrial Informatics, 17(2):1154–1165, 2020.

[30] K. Bruninx and E. Delarue. *Endogenous probabilistic reserve sizing and allocation in unit commitment models: Cost-effective, reliable, and fast*. IEEE Transactions on Power Systems, 32(4):2593–2603, 2016.

[31] M. Mirzaei., A. Yazdankhah, and B. Mohammadi-Ivatloo. *Stochastic security-constrained operation of wind and hydrogen energy storage systems integrated with price-based demand response*. International Journal of Hydrogen Energy, 44(27):14217–14227, 2019.

[32] A. Salimi, A. Karimi, and Y. Noorizadeh. *Simultaneous operation of wind and pumped storage hydropower plants in a linearized security-constrained unit commitment model for high wind energy penetration*. Journal of Energy Storage, 22:318–330, 2019.

[33] M. Rahmani, S. H. Hosseinian, and M. Abedi. *Stochastic two-stage reliability-based Security Constrained Unit Commitment in smart grid environment*. Sustainable Energy, Grids and Networks, 22:100348, 2020.

[34] S. M. Mousavi-Taghiabadi, M. Sedighizadeh, M. Zangiabadi, and A. Fini. *Integration of wind generation uncertainties into frequency dynamic constrained unit commitment considering reserve and plug in electric vehicles*. Journal of Cleaner Production, 276:124272, 2020.

[35] G. Li, Z. Bie, H. Xie, and Y. Lin. *Customer satisfaction based reliability evaluation of active distribution networks*. Applied Energy, 162:1571–1578, 2016.

[36] I. Ismael, M. Saeed, S. Kaddah, and S. Abdelkader. *Demand response for indirect load control in smart grid using novel price modification algorithm*. IET Renewable Power Generation, 13(6):877–886, 2018.

[37] S. Nan, M. Zhou, and G. Li. *Optimal residential community demand response scheduling in smart grid*. Applied Energy, 210:1280–1289, 2018.

[38] T. Pamulapati, R. Mallipeddi, and M. Lee. *Multi-objective home appliance scheduling with implicit and interactive user satisfaction modelling*. Applied Energy, 267:114690, 2020.

[39] M. Vellei and J. Le Dréau. *A novel model for evaluating dynamic thermal comfort under demand response events*. Building and Environment, 160:106215, 2019.

[40] N. Good. *Using behavioural economic theory in modelling of demand response*. Applied Energy, 239:107–116, 2019.

[41] M. Nicolson, G. Huebner, and D. Shipworth. *Are consumers willing to switch to smart time of use electricity tariffs? The importance of loss-aversion and electric vehicle ownership*. Energy Research & Social Science, 23:82–96, 2017.

[42] H. A. Aalami, H. Pashaei-Didani, and S. Nojavan. *Deriving nonlinear models for incentive-based demand response programs*. International Journal of Electrical Power & Energy Systems, 106:223–231, 2019.

[43] C. Grigg, P. Wong, P. Albrecht, R. Allan, M. Bhavaraju, R. Billinton, Q. Chen, C. Fong, S. Haddad, S. Kuruganty, et al. *The IEEE reliability test system-1996. A report prepared by the reliability test system task force of the application of probability methods subcommittee*. IEEE Transactions on Power Systems, 14(3):1010–1020, 1999.

[44] X. Dai, Y. Wang, S. Yang, and K. Zhang. *IGDT-based economic dispatch considering the uncertainty of wind and demand response*. IET Renewable Power Generation, 13(6):856–866, 2019.

[45] *Survey: Only 14% of utility customers participate in demand response programs*. [Online, Accessed Jan. 2020]: `https://tinyurl.com/yckx5vhr`, 2014.

[46] *Targeting Small Businesses–The Search for 80/20 in the 20/80 World*. [Online]: `https://www.aceee.org/files/proceedings/2016/data/papers/4_727.pdf`, 2016.

[47] Z. Bie, H. Xie, G. Hu, and G. Li. *Optimal scheduling of power systems considering demand response*. Journal of Modern Power Systems and Clean Energy, 4(2):180–187, 2016.

[48] S. Chatzivasileiadis. *Optimal Power Flow (DC-OPF and AC-OPF)*. [accessed Aug. 2022]: http://www.energy-markets-school.dk/documents/2017/Chatzivasileiadis/Optimal%20Power%20Flow%20(DC%20and%20AC%20OPF).pdf.

[49] E. Heydarian-Forushani, M. E. Golshan, and P. Siano. *Evaluating the operational flexibility of generation mixture with an innovative techno-economic measure*. IEEE Transactions on Power Systems, 33(2):2205–2218, 2017.

[50] J. Aghaei, M. Alizadeh, P. Siano, and A. Heidari. *Contribution of emergency demand response programs in power system reliability*. Energy, 103:688–696, 2016.

[51] X. Liu, M. Shahidehpour, Z. Li, X. Liu, Y. Cao, and Z. Bie. *Microgrids for enhancing the power grid resilience in extreme conditions*. IEEE Transactions on Smart Grid, 8(2):589–597, 2016.

[52] H. Karimi, S. Jadid, and H. Saboori. *Multi-objective bi-level optimisation to design real-time pricing for demand response programs in retail markets*. IET Generation, Transmission & Distribution, 13(8):1287–1296, 2018.

7

Conclusions & perspectives

This chapter summarises the conclusions of the individual chapters. Future improvements and applications of this work are also discussed in the perspectives section.

7.1 Conclusions and summary

With a higher integration of variable RES into power systems, an increasing interest in supplying flexibility via responsive loads has emerged in recent years. The contribution of loads in DRPs and providing ancillary services can be beneficial for electrical system operators and responsive consumers.

This thesis contributed to the domain of flexibility in power systems by offering different optimisation approaches to evaluate the techno-economic feasibility of providing different FAS and DRPs. Chapters 2 and 3 introduced the need for flexibility and various present options, while Chapters 4-6 suggested methodologies to examine the importance of various demand side response options for TSOs and consumers. The summary and outcomes stemming from each chapter are briefly described below:

In Chapter 2, the current policies and plans related to the increasing share of RES in the energy mix, together with the challenges of such a large-scale deployment, were presented. It was mentioned that the need for flexibility in energy systems, specifically in power systems, is present today. Hence, a combination of options, including flexibility of supply- and

demand-side, will be essential to meet these needs. Moreover, as energy markets are shifting towards a technology-neutral and competitive design, all market parties, including those on the demand side, can play an active role in supporting the electrical grids.

In Chapter 3, the concepts of grid balancing, frequency stability and FAS were defined. The opportunities for electricity consumers, specifically $P2H_2$ systems, to balance the grid were discussed. $P2H_2$ systems equipped with PEMELs and storage facilities are able to offset the volatile renewable power generation and offer FAS to the grid operators. It was concluded that the operation of a PEMELs to provide FAS while technically viable, might be economically unfeasible. This makes the optimisation of hydrogen production costs and optimal provision of ancillary service more critical.

Chapters 4 and 5 offered methodologies to evaluate the techno-economic feasibility of power-to-hydrogen facilities providing grid services in different modes of operation. While literature sets a precious foundation for this thesis, the size optimisation of a power-to-hydrogen system, together with the optimal hourly provision of FCR, has not been analysed. They also have not employed a detailed model for calculating grid costs; instead, a constant price per MWh consumption has been assumed. Thus, Chapter 4 considered a detailed model of a power-to-hydrogen plant providing FCR, and employed exact models of the electrolyser and grid costs.

As mentioned before, and while the operation of power-to-hydrogen facilities has been studied in literature, an applicable approach for the optimal planning and scheduling of multiple subcomponents considering the provision of FCR, aFRR, and mFRR services has not been adequately examined. Most recent studies have used predefined sizes for subcomponents or estimated the sizes according to the hydrogen demand. Then they looked at additional revenue stemming from the provision of grid services considering an average price for the service throughout the year. However, the average values do not reflect the weekly, daily, nor hourly variation of remuneration prices of FAS.

To employ and compare the potential of the plant in providing different FAS, their impact on both the operation and design of the plant has to be included in the optimisation model. In particular and without loss of generality, Chapter 5 presented a new optimisation model for the performance of a power-to-hydrogen system considering the energy supply to hydrogen-powered vehicles, providing hydrogen as a feedstock for industry and hydrogen injection into the natural gas grid. Detailed operation mechanisms and optimisation constraints of FCR, aFRR, and mFRR were presented to compare all FAS from the techno-economic viewpoint. The uncertainty of the hydrogen demand and the price of grid services were embedded into

the optimisation model to reflect the effect of uncertain parameters on the system operation.

The models proposed in Chapters 4 and 5 optimised the size of all subcomponents and defined the optimal operating strategies considering arbitrage trading in various markets. The PEMEL regulated the power offtake based on variable electricity prices, grid frequency divergences and TSO signals. Furthermore, a hydrogen price index was employed to assess the efficiency of the proposed models for hydrogen cost reduction.

It was concluded that, with the hypotheses adopted in this research, the installation of larger electrolysers only for FCR provision is marginally beneficial. Prioritising mFRR-Up over arbitrage trading resulted in high revenues but lower when compared to the aFRR-Up product. A relative analysis of the cost and revenue streams revealed that the TAP will rise in the aFRR-Up program compared to cases without or by considering other FAS types. Thus, consumers have to prioritise aFRR-Up provision over other grid services to improve investment profitability. It was understood that while concentrating on provisioning of FAS could be a less likely business case on its own due to the high degree of uncertainty, the stacked benefits from FAS and the hydrogen sale to different sectors improve the economic viability of hydrogen plants.

The outcomes also lead to the conclusion that hydrogen production in this concept not only relies on the price of electricity and transmission grid costs but also on the remuneration price and activation signals of FAS. Results showed that in addition to FAS revenues, expected higher hydrogen demand and efficiency of components and lower capital and operation costs in the coming years can reduce the break-even price of hydrogen.

The conducted research indicated that the operating costs are directly linked to the size of the electrolyser. Hence, optimal sizing of subcomponents and exemptions from tax and levies or other elements of grid costs are critical to reaching economic viability. The ratings of electrolysers were mainly calculated according to the maximum hydrogen demand from the mobility sector and FAS capacity. Moreover, sensitivity analyses indicated the decisive impact of hydrogen price variation in natural gas and industrial sectors on the size of subcomponents.

The methods explained in Chapters 4 and 5 can be used to determine optimal investment plans. Decision makers and investors can utilise the proposed methods and investigate how the provision of FAS and other factors would affect the sizing, design, operation of the components and, ultimately, the long-term economic performance of a hydrogen installation. This facilitates investment decisions in the long term. Moreover, $P2H_2$ facilities and grid operators could collaboratively profit from the suggested

methods to schedule the electrolyser to meet the hydrogen demand and provide various FAS types simultaneously. Therefore, the proposed models offer new opportunities for the proliferation of $P2H_2$ systems, further encouraging investment in such plants.

In Chapter 6, a security-constrained unit commitment problem was solved, considering consumer rationality in DRPs. While comprehensive models have been offered in literature regarding the dynamic electricity pricing, a wide range of customer viewpoints regarding the fluctuations of prices and incentives has remained unanswered, where their satisfaction and behaviour have not been addressed thoroughly. The main aim of Chapter 6 was to define an accurate model of DR considering customer behaviour and the effect of customer preferences on optimal power system operation. Chapter 6 further developed a pricing algorithm to find the optimal electricity prices and incentives to guarantee network reliability and comfort of customers, while minimising system operation costs in the presence of uncertainties. In the employed EDRP, a factor that shows the real value of the incentive payment perceived by the customers was used.

The electricity consumption was adjusted in response to designed incentives and hourly electricity prices to diminish the adverse effects of the outages in the power grid. Results validated the capability of the suggested strategy in the reduction of operating costs, customer payments, and peak load by optimal scheduling of generation and consumption units. The results of Chapter 6 also confirmed that consideration of different DRPs, various types of consumers and comfort constraints notably impact the power system reliability and daily operation costs.

It was shown that when individuals are in a situation where earnings and losses are possible, they prefer less risky options. If potential losses could be destructive or threaten customer lifestyles, they will naturally reject the choice of participation in DRPs that bring losses and discomfort. That is a reason for system operators to optimise the prices to avoid the customer losses at peak-price hours while they make sure that the system operation costs will be minimised. By limiting potential losses and maximising profits, current consumers will continue providing DR, and new clients might join the DRPs too.

Overall, the conducted examinations and simulations illustrated the positive impact of proposed optimisation methods to employ demand-side flexibility and improve the reliability of power systems, while consumers and investors can benefit economically from providing different demand-side response services.

7.2 Perspectives

This thesis presented strategies for the optimal operation and investment in $P2H_2$ facilities and responsive consumers in general, which can valuably contribute to expanding the flexibility of power systems in the transition toward net zero. During this work, several further research directions were identified, which can be analysed in future research:

In line with the work done in Chapters 4 and 5, future research might expand the flexibility provision with more efficient electrolysis technologies[1] or to examine flexibility beyond the borders of the HRSs. Given the plans for heavy electrification of industrial processes, the offered method can be, with modifications, employed to estimate the flexibility potential of other responsive loads.

During this doctoral research, the design and operation of coupled wind-hydrogen systems as a long-term storage option and to provide FAS were slightly touched upon but are still in progress. Exploring the opportunities for flexible offshore production and storage of renewable hydrogen from offshore wind and solar parks is another line of research. The intermittency and stochastic behaviour of wind production and the impact on the techno-economic feasibility of such plants could be a future topic.

Moreover, as mentioned before, this thesis mainly used deterministic and probabilistic methods to optimise the operation of $P2H_2$ systems. Hence, in future studies, it would be valuable to develop stochastic optimisation models to forecast the prices of energy and capacity markets and hydrogen demand in advance for the short-term operation of such facilities. In addition, a considerable part of this research was performed before energy prices became extremely high and volatile. This reminds us of the necessity of including sensitivity and risk analyses in future work.

While in Chapters 4 and 5 the implications of providing different FAS types for consumers were studied, the development of new ancillary services is to be included in future studies. An example is the opening of the inertia response market in Ireland and fast frequency reserve market in the Nordic area. This opening might create opportunities for specific consumers, such as electrolysers, and new business cases might appear.

Parameters like the response time of the electrolyser and the delay of TSO signals were not included in the presented models in Chapters 4 and 5. However, the inclusion of these parameters that could affect the provision of grid services at a shorter time scale could be the topic of future studies.

[1] An alkaline capillary-fed electrolysis cell demonstrates water electrolysis performance with a 98% energy efficiency, energy consumption of 40.4 kWh/kg hydrogen (vs. 47.5 kWh/kg in commercial electrolysis cells [1]

The possibility of considering the optimal participation of the $P2H_2$ systems or other fast responsive loads in all FAS types simultaneously is another subject worth investigating.

Chapter 6 explained a method to determine optimal scheduling plans of loads and generators such that network reliability and consumer comfort are guaranteed. In real applications, the stochastic nature of renewable energy production or energy consumption by consumers would affect the results, which should be modelled in future work. Besides, the CO_2 emissions and consumer payments minimisation by forming a multi-objective optimisation, considering the competition in the electricity and reserve markets, could be included in later studies.

While this thesis focused mainly on the balancing at the transmission level, the idea of local balancing is a potential subject for future works. With local balancing, power production and consumption are controlled locally by distribution system operators (DSOs). DSOs require accurate forecasts of generation and demand to balance the power. Then, novel machine learning algorithms should be developed, utilising knowledge of the local weather, the topology of the local grid and the load profiles of consumers.

References

[1] A. Hodges, A. L. Hoang, G. Tsekouras, K. Wagner, C. Lee, G. F. Swiegers, and G. G. Wallace. *A high-performance capillary-fed electrolysis cell promises more cost-competitive renewable hydrogen*. Nature communications, 13(1):1–11, 2022.

Author bibliography

[1] **A. Dadkhah**, D. Bozalakov, J. D. De Kooning and L. Vandevelde. *Techno-Economic Analysis and Optimal Operation of a Hydrogen Refueling Station Providing Frequency Ancillary Services*. IEEE Transactions on Industry Applications, vol. 58, no. 4, pp. 5171-5183, 2022.

[2] **A. Dadkhah**, N. Bayati, M. Shafie-khah, L. Vandevelde, and J. P. Catalão. *Optimal price-based and emergency demand response programs considering consumers preferences*. International Journal of Electrical Power & Energy Systems, 138, 107890, 2022.

[3] **A. Dadkhah**, D. Bozalakov, J. D. De Kooning and L. Vandevelde. *On the optimal planning of a hydrogen refuelling station participating in the electricity and balancing markets*. International Journal of Hydrogen Energy, 46(2), 1488-1500, 2021.

[4] **A. Dadkhah**, G. Van Eetvelde and L. Vandevelde. *Optimal Investment and Flexible Operation of Power-to-Hydrogen Systems Increasing Wind Power Utilisation*. In 2022 International Conference on Environmental and Electrical Engineering (EEEIC 2022).

[5] **A. Dadkhah**, D. Bozalakov, J. D. De Kooning and L. Vandevelde. *Optimal sizing and economic analysis of a hydrogen refuelling station providing frequency containment reserve*. In 2020 IEEE International Conference on Environment and Electrical Engineering and 2020 IEEE Industrial and Commercial Power Systems Europe (EEEIC/I&CPS Europe).

[6] **A. Dadkhah**, B. Vahidi, M. Shafie-khah and J.P. Catalão. *Power system flexibility improvement with a focus on demand response and wind power variability*. IET Renewable Power Generation, 14: 1095-1103, 2020.

[7] **A. Dadkhah**, and B. Vahidi. *On the network economic, technical and reliability characteristics improvement through demand response implementation considering consumers' behaviour*. IET Generation, Transmission & Distribution, 12(2), 431-440, 2018.

[8] A. Forooghi Nematollahi, **A. Dadkhah**, O. Asgari Gashteroodkhani, and B. Vahidi. *Optimal sizing and siting of DGs for loss reduction using an iterative-analytical method*. Journal of Renewable and Sustainable Energy, 8(5), 055301, 2016.

[9] N. Bayati, **A. Dadkhah**, S. H. H. Sadeghi, B. Vahidi, and A. E. Milani. *Considering variations of network topology in optimal relay coordination using time-current-voltage characteristic*. In 2017 IEEE International Conference on Environment and Electrical Engineering and 2017 IEEE Industrial and Commercial Power Systems Europe (EEEIC/I&CPS Europe).

[10] B. Vahidi, and **A. Dadkhah**. *New demand response platform with machine learning and data analytics*. In Demand Response Application in Smart Grids (pp. 113-137). Springer, Cham, 2020.

In the end, I would like to thank those who financially supported this thesis.

- the GREENPORTS project (Gas from REnewable Energy in PORTS) funded by VLAIO (Flemish Agency for Innovation and Entrepreneurship) - Grant agreement: HBC.2017.0687.
- the TRILATE project (TRILateral research for optimal Investments in Adequate cross-border infrastructure) funded by the Energy Transition Fund of the Belgian federal government, managed by the FPS Economy, SMEs, Self-employed and Energy.
- the BEOWIND project funded by the Energy Transition Fund of the Belgian federal government managed by the FPS Economy.
- the NorthWest Europe INTERREG project ITEG (Integrating Tidal Energy into the European Grid) led by the European Marine Energy Centre (EMEC) - [NWE 613].

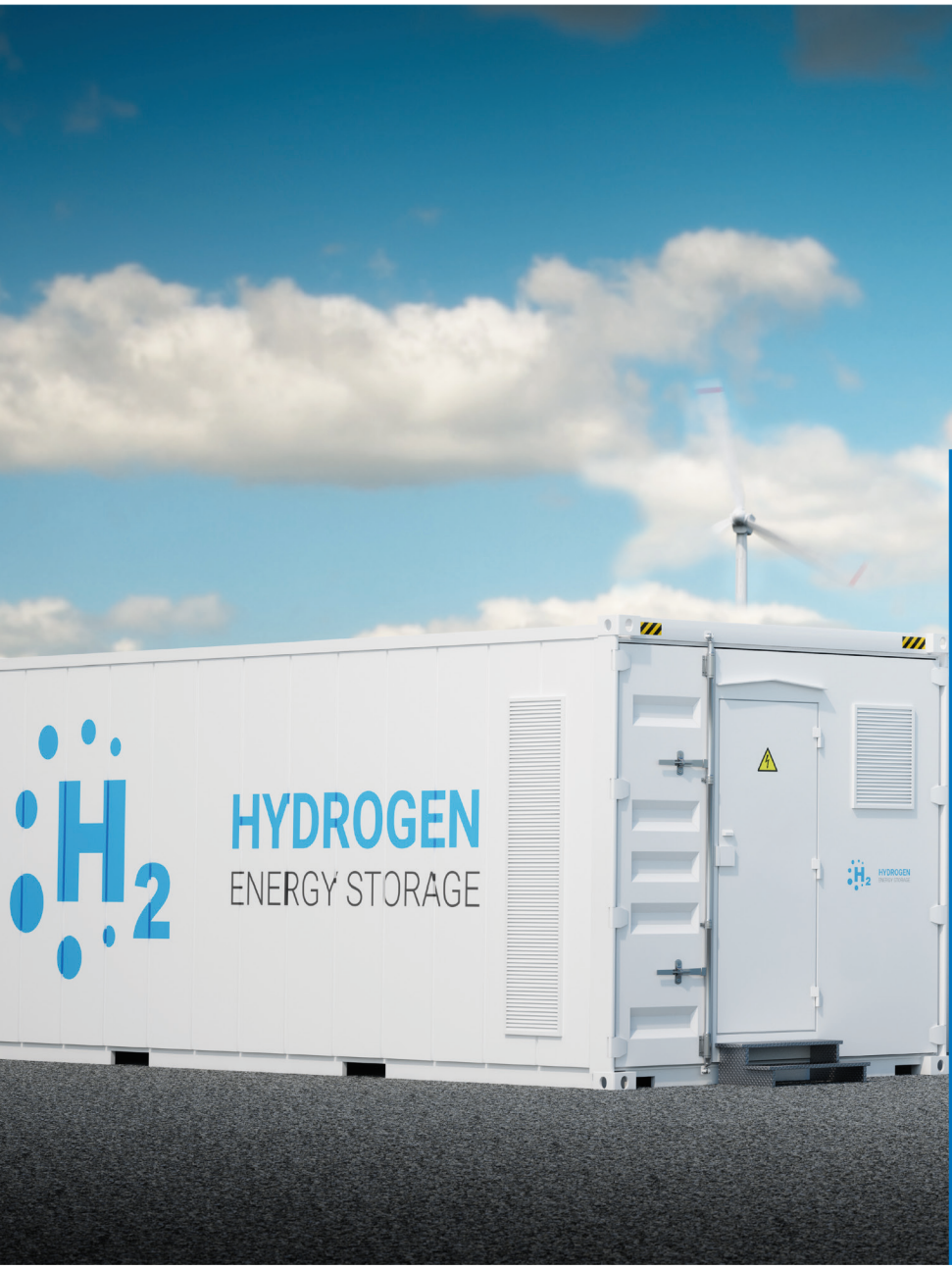

Towards net zero – flexible energy systems with a focus on hydrogen.